

FOR FURTHER TRAN ~~MIT~~

2  
B.S.

AFML-TR-77-109

AD A 054431

AU NO.             
DDC FILE COPY

# INFLUENCE OF CROSSLINKING ON THE MECHANICAL PROPERTIES OF HIGH $T_g$ POLYMERS

MATERIALS RESEARCH CENTER  
LEHIGH UNIVERSITY  
BETHLEHEM, PENNSYLVANIA 18015

JULY 1977

TECHNICAL REPORT AFML-TR-77-109  
Final Report for Period May 1975 - April 1977

Approved for public release; distribution unlimited.

DDC  
RECEIVED  
MAY 31 1978  
D

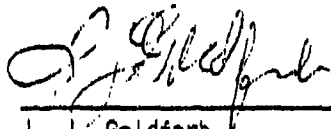
AIR FORCE MATERIALS LABORATORY  
AIR FORCE WRIGHT AERONAUTICAL LABORATORIES  
AIR FORCE SYSTEMS COMMAND  
WRIGHT-PATTERSON AIR FORCE BASE, OHIO 45433

## NOTICE

When Government drawings, specifications, or other data are used for any purpose other than in connection with a definitely related Government procurement operation, the United States Government thereby incurs no responsibility nor any obligation whatsoever; and the fact that the government may have formulated, furnished, or in any way supplied the said drawings, specifications, or other data, is not to be regarded by implication or otherwise as in any manner licensing the holder of any other person or corporation, or conveying any rights or permission to manufacture, use, or sell any patented invention that may in any way be related thereto.

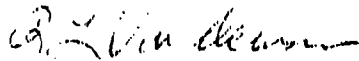
This report has been reviewed by the Information Office (OI) and is releasable to the National Technical Information Service (NTIS). At NTIS, it will be available to the general public, including foreign nations.

This technical report has been reviewed and is approved for publication.



I. J. Goldfarb  
Project Monitor

FOR THE COMMANDER



R. L. Van Deusen, Chief  
Polymer Branch  
Nonmetallic Materials Division

Copies of this report should not be returned unless return is required by security considerations, contractual obligations, or notice on a specific document.

SECURITY CLASSIFICATION OF THIS PAGE (When Data Entered)

REPORT DOCUMENTATION PAGE		READ INSTRUCTIONS BEFORE COMPLETING FORM
1. REPORT NUMBER (18) AFML TR-77-109 ✓	2. GOVT ACCESSION NO.	3. RECIPIENT'S CATALOG NUMBER
4. TITLE (and Subtitle) (6) INFLUENCE OF CROSSLINKING ON THE MECHANICAL PROPERTIES OF HIGH T <sub>g</sub> POLYMERS. 48-4033078	5. TYPE OF REPORT & PERIOD COVERED (9) Final Report for Period May 1975-Apr 1977	
6. AUTHOR(s) (10) John A. Manson, SooJaa L. Kim Leslie H. Sperling	7. PERFORMING ORG. REPORT NUMBER	
8. CONTRACT OR GRANT NUMBER(s) (15) F33615-75-C-5167 ✓	9. PROGRAM ELEMENT, PROJECT, TASK AREA & WORK UNIT NUMBERS (16) 23030503 (17) Q5 /	
10. PERFORMING ORGANIZATION NAME AND ADDRESS Materials Research Center ✓ Lehigh University Bethlehem, PA 18015	11. REPORT DATE (71) JUN 1977 12. NUMBER OF PAGES 145 pages (12) 146p	
13. CONTROLLING OFFICE NAME AND ADDRESS Air Force (MBP) Air Force Wright Aeronautical Laboratories Wright-Patterson AFB, Ohio 45433	14. SECURITY CLASS. (of this report) Unclassified	
15. DECLASSIFICATION/DOWNGRADING SCHEDULE		
16. DISTRIBUTION STATEMENT (of this Report) Approved for Public Release; Distribution Unlimited		
17. DISTRIBUTION STATEMENT (of the abstract entered in Block 20, if different from Report)		
18. SUPPLEMENTARY NOTES		
19. KEY WORDS (Continue on reverse side if necessary and identify by block number) Crosslinked networks, Decrosslinking, Density and Distribution of crosslinks, Epoxy resins, Fatigue, Fracture mechanics, Glass transition temperature, High-T <sub>g</sub> resins, Interpenetrating Polymer Networks, Labile crosslinks, Mechanical properties, Millar networks, Model networks, Swelling behavior, Viscoelastic behavior.		
20. ABSTRACT (Continue on reverse side if necessary and identify by block number) A study was conducted on the effects of crosslinking on the mechanical properties of high-T <sub>g</sub> polymers, with emphasis on the role of average crosslink density and on variations in the distribution of chain lengths between crosslinks. Two model systems were used: one based on the use of polystyrene/polystyrene interpenetrating polymer networks (Millar networks), and the other based on the use of bisphenol-A-type epoxy/methylene dianiline resins synthesized to provide controlled variations in network properties. With the Millar		

DD FORM 1 JAN 73 1473 EDITION OF 1 NOV 68 IS OBSOLETE

SECURITY CLASSIFICATION OF THIS PAGE (When Data Entered)

404 200

371

20. Networks, which were prepared by polymerizing a crosslinked polystyrene network within a precrosslinked polystyrene matrix, measurements of creep, swelling, and rubbery modulus showed that the properties at equal average crosslink density were dominated by the crosslink density of the first-formed network. Thus, when networks formed at different times can interpenetrate, the continuity or coherence of each plays a major role in determining behavior. Confirmation was provided by observation of phase separation (phases  $\sim 10\text{nm}$  in size) in the less continuous network. With the epoxy networks, viscoelastic and elastic response, stress-strain and impact behavior, fatigue crack propagation, and fracture toughness were determined primarily by the average crosslink density and not by its distribution, whether a given crosslink density was obtained by varying stoichiometry or by varying molecular weight of the epoxy. Only a few exceptions occurred and then only over a narrow range of distribution of crosslinks. All specimens exhibited heterogeneity at several levels ( $\sim 10\text{nm}$  and  $100\mu\text{m}$ ). A model was proposed to account for the morphologies and mechanical properties observed.

# FOREWORD

The Lehigh Project Co-Directors were Dr. John A. Manson, Professor of Chemistry and Director of the Polymer Laboratory, Materials Research Center, and Dr. Leslie H. Sperling, Associate Professor of Chemical Engineering, and Senior Staff member, the Polymer Laboratory. The Faculty Associates were: Dr. Richard W. Hertzberg, Professor of Metallurgy and Materials Science and Director of the Mechanical Behavior Laboratory, and Dr. John W. Vanderhoff, Professor of Chemistry and Associate Director - Coatings, Center for Surface and Coatings Research. Special advice on synthesis was provided by Professor N. D. Heidel, Professor of Chemistry. Also contributing to the project were Research Associate Dr. S. L. Kim, Visiting Scientist S. Yamoda, and Graduate Students Subodh C. Misra, Michael Skibo, Carol M. Vasold, and David S. Siegfried. Liaison with the Air Force Materials Laboratory was provided initially by Capt. A. J. Wereta, Jr., and during the second year, by Dr. Ivan Goldfarb.

ACCESSION NO.		
RTD	Write Section	<input checked="" type="checkbox"/>
ODS	Ref. Section	<input type="checkbox"/>
UNANNOUNCED		<input type="checkbox"/>
JUSTIFICATION.....		
BY .....		
DISTRIBUTION/AVAILABILITY CODE		
Dist.	AVAIL. and/or SPECIAL	
A		

# TABLE OF CONTENTS

SECTION	PAGE
SUMMARY	xi
A. General	xi
B. Model Networks	xi
C. Epoxy Networks	xiii
I INTRODUCTION	1
A. Statement of the Problem	1
B. Objective and Scope of the Problem	1
C. General Discussion	2
II TECHNICAL APPROACH	6
III SYNTHESIS OF MODEL NETWORKS	8
A. Introduction	8
B. Experimental Details, Results, and Discussion	10
IV PROPERTIES OF MODEL NETWORKS	11
A. Introduction	11
B. Experimental Details, Results, and Discussion	11
V SYNTHESIS OF EPOXY NETWORKS	27
A. Structure and Stoichiometry	28
B. Experimental Details, Results, and Discussion	32
VI CHARACTERIZATION OF EPOXY NETWORKS	38
A. Introduction	38
B. Experimental Details, Results, and Discussion	40
VII FRACTURE TOUGHNESS, FATIGUE CRACK PROPAGATION AND STRENGTH OF EPOXY NETWORKS	71
A. Introduction	71
B. Experimental Details, Results and Discussion	75
VIII MORPHOLOGY AND NETWORK MODELS	101
A. Introduction	101
B. Experimental Details, Results, and Discussion	102
IX CONCLUSIONS AND RECOMMENDATIONS	120
REFERENCES	125
APPENDIX	131

# LIST OF TABLES

TABLE		PAGE
1	Values of $M_c$ (Grams/Mole) for Millar IPNs and Controls	13
2	Characteristics of Epoxy Prepolymers	29
3	Compositions of Series A Epoxy Resins	34
4	Compositions of Series B (Blends) Epoxy Resins	35
5	Compositions of Series D (Versamid-cured) Epoxy Resins	36
6	Unblended (as-is) Epoxy Resins	36
7	Bimodal Distribution Epoxies	37
8	Swelling and Extraction of Series E Epoxies	43
9	Swelling and Extraction of Series F Epoxies (Bimodal Blends)	43
10	Residual Functional Groups in Series A Epoxies and Corrected $M_c$	44
11	Values of $M_c$ for Series A Epoxy Resins	46
12	Values of $M_c$ for Series E Epoxy Resins	48
13	Values of $M_c$ for Series F Epoxy Resins	48
14	Dynamic Mechanical Data of Series A Epoxy Resins (Variable Stoichiometry)	52
15	Characteristics of the $\beta$ Transition of Series A Epoxy Resins (Variable Stoichiometry)	52
16	Dynamic Mechanical Data of Series B Epoxy Resins (Blends)	57
17	Dynamic Mechanical Properties of Series E Epoxy Resins (Commercial Resins)	58
18	$T_g$ Data for Series E Epoxy Resins	60
19	Dynamic Mechanical Properties of Series F Epoxy Resins (Bimodal Blends)	62
20	$T_g$ Data for Series F Epoxy Resins	64
21	Creep Data for Epoxy Series A	66
22	Creep Data for Series E Epoxy Resins (Reduced to 129°C)	68
23	Creep Data for Series F Epoxy Resins (Reduced to 129°C)	68

TABLE		PAGE
24	Fracture Toughness and Fatigue Characteristics of Epoxy Resins (Series A, B, D)	77
25	Fracture Toughness and Fatigue Characteristics of Epoxy Resins (Series E and F)	80
26	Tensile Data for Series E Epoxy Resins	95
27	Impact Data for Series E and Series F Epoxy Resins	99
28	Tensile Data for Series F Epoxy Resins (Bimodal Blends)	99

## LIST OF ILLUSTRATIONS

FIGURE		PAGE
1	Schema showing typical variations in nature and composition of crosslinked polymer networks (after reference 2).	4
2	Schema for Millar-type IPN.	7
3	Creep data for polystyrene containing 2.2% DVB.	15
4	Experimental and theoretical shift factor, $a_T$ , for Millar IPN's.	16
5	Creep curves for Millar IPN's (% DVB in polymer I = 0.4).	17
6	Creep curves for Millar IPN's prepared for electron microscopy.	18
7	Creep curves for Millar IPN's (% DVB in polymers I and II = 0.4).	19
8	Creep curves for swollen Millar IPN's (% DVB in polymer I = 4).	20
9	Electron micrograph of thin section Millar IPN 25/75 (0.4/4% DVB, 1% isoprene in polymer II).	21
10	Electron micrograph of thin section IPN 72.2 PEAB/27.8 PMMA.	22
11	Schemata showing (a) effects of crosslinking stoichiometry on molecular structure, and (b) effects of crosslinking on modulus-temperature behavior.	30
12	Swelling data of series A epoxy resins as function of amine/epoxy ratio.	41
13	Swelling data as function of $M_c$ : closed circle, epoxy excess in series A; open circle, amine excess in series A; triangle, series E.	42
14	Swelling of Series E and Series F epoxies (bimodal blends) as a function of $M_c$ (theor.).	45
15	Correlation between $M_c$ from theoretical equation and $M_c$ from rubbery modulus: closed circle, epoxy excess in series A; open circle, amine excess in series A; triangle, series E and F.	47
16	Dynamic mechanical data for A-20 epoxy resin, $f = 110$ Hz.	50


FIGURE		PAGE
17	Dynamic mechanical properties of series A epoxy resins as functions of stoichiometry. Range of data also shown for series B,  .	53
18	Dynamic mechanical parameters at $T_g$ as function of $M_c$ : closed circle, epoxy excess in series A; open circle, amine excess in series A; triangle, series E.	54
19	Dynamic mechanical parameters at $\beta$ transition vs. amine/epoxy equivalent ratio, series A epoxy resins at 110 Hz.	55
20	Dynamic mechanical parameters at $\beta$ transition as function of $M_c$ : closed circle, epoxy excess in series A; open circle, amine excess in series A; triangle, series E.	56
21	$T_g$ as function of $M_c$ (theor.) for series E and F.	59
22	$T_g$ as function of wt % of Epon 825 in the resin for series E and F.	63
23	Creep compliance of A-10 epoxy resin.	65
24	Creep compliance behavior of series A epoxy resins. Data reduced to 150°C.	67
25	Creep data for series E and series F epoxy resins.	69
26	Fracture toughness, $K_{IC}$ , and FCP parameters $\Delta K^*$ ( $\Delta K$ at $da/dN = 3 \times 10^{-4}$ mm/cyc), and slope of the $da/dN$ curve as a function of the stress intensity factor range, $\Delta K$ , as function of stoichiometry; circles and triangles for series A, open corresponding to A-10A; shaded area for series B.	78
27	Fracture toughness, $K_{IC}$ , and FCP parameters $\Delta K^*$ ( $\Delta K$ at $da/dN = 3 \times 10^{-4}$ mm/cyc), and slope of the $da/dN$ curve as a function of the stress intensity factor range, $\Delta K$ , as function of $M_c$ : open circle, amine excess in series A; closed circle, epoxy excess; shaded area, series B; open triangle, series E; closed triangle, series F.	79
28	Typical FCP behavior as a function of $\Delta K$ . Specimen, A-18; $f=10$ Hz.	82
29	FCP behavior of series A epoxy resins; $f=10$ Hz.	83
30	FCP behavior of series B (broad distribution) epoxy resins: rate of crack growth per cycle as a function of $\Delta K$ ; $f=10$ Hz.	84
31	FCP behavior of series D (polyamide-cured) epoxy resins: only the first and last points shown; $f=10$ Hz.	85
32	FCP behavior of series E and series F epoxies; $f=10$ Hz.	86

FIGURE		PAGE
33	Correlation of $AK^{\frac{1}{2}}$ ( $AK$ at an arbitrary crack growth rate) and $K_{IC}$ in epoxy resins.	87
34	Typical FCP behavior of epoxy resin as function of $\Delta K$ : specimen A-20, $f=10$ Hz; circles observed during fatigue test and squares calculated from fracture surface striations.	88
35	Tensile parameters for series A epoxy resins as function of amine/epoxy ratio.	91
36	Tensile parameters as function of $M_C$ : closed circle, epoxy excess in series A; open circle, amine excess in series A; open triangle for series E; closed triangle, series F.	92
37	Tensile toughness, $T$ , of series A as function of $M_C$ : closed circle, epoxy excess and open circle, amine excess.	93
38	Tensile toughness, $T$ , of series A epoxy resins vs. amine/epoxy ratio.	94
39	Charpy Impact strength, $I$ , of series A epoxy resins as function of amine/epoxy ratio.	96
40	Charpy Impact strength, $I$ , as function of $M_C$ : closed circle, epoxy excess in series A; open circle, amine excess in series A; open triangle, series E; closed triangle for series F, squares are Bell's data (ref. 46).	97
41	Impact strength and $\beta$ -transition temperature for series E epoxy resins.	98
42	Scanning electron micrographs of epoxy (E-7) surface etched with aq. $Cr_2O_3$ for various periods of time: A= 2 hr, B=4 hr, C=7 hr, D=11 hr.	104
43	Scanning electron micrographs of series A epoxy resins (etched 7 hr in $Cr_2O_3$ ): A=A-7, B=A-8, C=A-10, D=A-11.	105
44	Scanning electron micrographs of series A epoxy resins (etched 7 hr in $Cr_2O_3$ ): A=A-14, B=A-16, C=A-18, D=A-20.	106
45	Electron micrographs of replicas made after etching samples of series A for 4 hr in aqueous $Cr_2O_3$ : A=A-7, B=A-8, C=A-11, D=A-14, E=A-16, F=A-20.	107
46	Scanning electron micrographs of series E epoxies etched with aqueous $Cr_2O_3$ for 7 hr: A=E-1, B=E-2, C=E-3, D=E-5, E=E-6, F=E-7.	108
47	Electron micrographs of 2-stage replicas of series E samples etched for 4 hr in aq. $Cr_2O_3$ . A=E-1, B=E-2, C=E-3, D=E-5, E=E-6, F=E-7.	109

FIGURE		PAGE
48	Electron micrograph of Epon 1001/MDA epoxy (E-5) etched for 7 hr in aq. $\text{Cr}_2\text{O}_3$ . A and B, cross-section area; C, surface; D, resin cast using an acetone solution of a fraction of Epon 1001.	110
49	Scanning electron micrographs of Epon 828/Versamid 40 epoxy (described in reference 49; contained glass beads).	112
50	Scanning electron micrographs of series F epoxies, etched 7 hr with aq. $\text{Cr}_2\text{O}_3$ and their counterparts in series E. A=E-2, B=F-1, C=E-5. Specimens F-1 and F-5 were blended to match E-2 and F-5, respectively.	113
51	Scanning electron micrograph of series F epoxies etched 7 hr in aq. $\text{Cr}_2\text{O}_3$ : A=F-2, B=F-3, C=F-4, D=E-3, specimen F-4 is the counterpart of specimen E-3.	114
52	Electron micrographs of 2-stage replicas of series F epoxies, etched 4 hr in aq. $\text{Cr}_2\text{O}_3$ : A=F-1, B=F-4, C=F-5.	115
53	Electron micrographs showing microgel particles from epoxies (using formulations for E-2 and E-5). A and B show gel particles etched out from cured epoxy by aq. $\text{Cr}_2\text{O}_3$ after 4 hr at 70°C. C and D show microgel isolated prior to gelation.	116
54	Proposed mechanism for morphology development.	118

## SUMMARY

### A. General

In order to gain more understanding of the effects of crosslinking on the mechanical properties of high-T<sub>g</sub> polymers, a fundamental study of the role of crosslink density, distribution of segment lengths between crosslinks, and network imperfections was begun. A dual approach was selected: (1) the preparation and study of novel model networks based on the use of (a) special graft-type polymers (Bamford networks) and (b) interpenetrating polymer networks (Millar-type IPN's), and (2) the preparation and study of epoxy/diamine networks. Although the model systems are not of interest per se as materials, they offer the possibility of easily varying network characteristics and, in some cases, morphology. Of the two models attempted, the Bamford approach proved to be impractical. However, the IPN system (based on polystyrene) proved to be facile and capable of modeling some aspects of the two-phase morphology now known to exist in many thermosetting high-T<sub>g</sub> polymers. The epoxy/diamine system was selected because resins of this type are of practical interest. Though the epoxy networks are inherently more limited in controlled network variation than the models, the epoxies also proved to be capable of demonstrating the effects of interest.

### B. Model Networks

Two model networks were investigated during the course of the present contract:

(1) The synthesis of AB crosslinked copolymers (Bamford networks) was attempted. The basic idea was to prepare an idealized crosslinked polystyrene that contained two independent  $M_c$ 's, and a controllable number of free chains and chains bound to the network at one end. A new monomer, the mixed anhydride of trichloroacetic acid and acrylic acid, was required.

(2) Millar interpenetrating polymer networks based on polystyrene/polystyrene were synthesized. The crosslink level of each network could be varied independently, to produce another model thermoset plastic with two  $M_c$  values.

Work was discontinued on the synthesis of the Bamford-type networks in June, 1976, after it was shown to be too difficult to purify the crude mixed anhydride required. An alternate model system was therefore sought to investigate the behavior of irregularly-formed polymer networks.

The new system selected was a polystyrene/polystyrene Millar interpenetrating polymer network. An IPN is synthesized by first

polymerizing a crosslinked polymer I network, then swelling in monomer II plus crosslinker and activator, and polymerizing monomer II in situ. When both polymers are identical, the product is designated a Millar IPN (named after the researcher who first described these materials). In the present study, the crosslinker (divinyl benzene) level of the two networks was varied independently, with emphasis on crosslinker levels of 0%, 0.4%, and 4.0%. Single polystyrene networks were made for comparison.

The creep behavior of the materials was investigated in the range of 60°C to 120°C, thus covering the range from glassy behavior through the glass-rubber transition. Master curves were prepared and the shift factors compared with each other and with values predicted from the WLF (Williams-Landel-Ferry) equation. In each case, the Millar IPN's were found to creep in a manner much more like the polymer I single network than the single network having the identical average overall crosslink level.

Swelling studies on the several Millar IPN's and single networks were carried out and analyzed via the Flory-Rehner equation to yield  $M_c$ , the average crosslink density. In each case again, the swelling behavior was closer to the polymer I behavior than to the overall-average. The same was true for the rubbery-plateau modulus,  $E_r$ , analyzed via the theory of rubber elasticity to also yield  $M_c$ .

The inference was drawn that the behavior could be explained by assuming that network I was more continuous in space than network II. While this is well-established for IPN's where the two polymers differ, this was an unexpected finding here, but a finding probably relevant to the gelation of a thermosetting system. Indeed such a model was proposed speculatively many years ago by Bobalek.

On another IPN research program, an equation had been derived by Donatelli, et al. to determine the phase domain size in IPN's as a function of the weight fraction of each polymer, the crosslink density of network I, and the interfacial tension between the two polymers (the latter being zero for a Millar IPN). Use of the Donatelli equation led to a prediction of domain sizes of 60-100Å for polymer II.

To verify this prediction, special samples of the polystyrene/polystyrene Millar IPN's were prepared, with one component containing a trace of isoprene, which was subsequently stained with osmium tetroxide to develop staining suitable for electron microscopy using 300Å thick specimens. The results confirmed predictions: domains of slightly less than 100Å were observed, with polymer I tending to be more continuous than polymer II.

The value of the above experiment lies in its probable application to other networks. It has long been known that certain single networks may such as epoxies and polyesters may develop greater or lesser domain formation during polymerization (curing). The systematic finding of segregation in the above experiment suggests that perhaps in many single networks also, the earlier polymerized monomer or prepolymer may form a more continuous structure than the latter polymerized monomer.

### C. Epoxy Networks

Several series of bisphenol-A-based epoxy resins were prepared using methylene dianiline as curing agent. Essentially complete curing was attained, as shown by measurements of dynamic mechanical response. In series A, the average molecular weight between crosslinks,  $M_c$ , was varied by altering the stoichiometry, with amine excess varying from -30 percent to +100 percent. In series B,  $M_c$  was held constant, while the distribution of  $M_c$  was varied by blending epoxy prepolymers having different molecular weights. In series C,  $M_c$  was again held constant, but the amine content was varied. In series D, several resins were prepared using polyamide curing agents. In series E,  $M_c$  was varied at 1:1 stoichiometry by use of epoxy prepolymers having different molecular weights.

Characterization of the following properties (not all resins) was completed:  $M_c$ , by swelling and measurements of rubbery modulus; the state of cure, by differential scanning calorimetry (DSC); chemical analysis and dynamic mechanical spectroscopy (DMS); viscoelastic response per se by DMS; stress-strain and impact response; creep; fracture toughness and fatigue crack propagation (FCP) behavior; and morphology, by electron microscopy.

A precise baseline of viscoelastic behavior, stress-strain and impact response, fracture toughness, and FCP response has been established for series A (varying stoichiometry) and a similar baseline of viscoelastic behavior for series E (varying molecular weight of the epoxy). These baselines serve as standards against which the effects of other network variations may be compared with confidence.

As expected, an increase in the degree of crosslinking (or a decrease in  $M_c$ ) causes an increase in  $T_g$  ( $T_g$ ),  $T_g$  (the temperature of the major low-lying transition), the breadth of the transitions, the rubbery modulus, and the swelling ratio. However, absolute values of  $T_g$  were higher than expected based on the experiences of others with the same system. Increased crosslinking also caused a decrease in the magnitude of  $\tan \delta_{max}$  near the  $T_g$ , the extent of creep, and the slope of the modulus-temperature curve at  $T_g$ . In most cases, the dependence of viscoelastic parameters on  $M_c$  was similar for specimens having an excess or deficit of amine; the one exception was the transition slope, which varied differently depending on whether amine or epoxy was in excess. Creep and  $T_g$  were found to be most sensitive to crosslink density.

One apparently new quantitative observation was made: that the dependence of a given viscoelastic parameter on  $M_c$  is essentially the same whether a given value of  $M_c$  was attained by varying the stoichiometry or by varying the molecular weight of the prepolymer. This fact should facilitate the comparison of effects of other network variations.

Increasing the amine/epoxy (A/E) ratio increased the fracture toughness ( $K_{IC}$ ), the stress intensity factor required to drive a crack ( $K_{IC}$ ), and after passing through a minimum, Young's modulus and the tensile strength.

However, increasing the A/E ratio decreased the impact strength and tensile toughness. Increasing the molecular weight of the epoxy prepolymer also increased  $K_{IC}$  and  $\Delta K_{IC}$ , but decreased impact strength and decreased tensile strength.

Effects of the distribution of segment lengths between crosslinks were negligible not only in the glassy and rubbery states, as expected, but also in the glass-to-rubber transition region. However, anomalies were noted in one especially broad (bimodal) distribution, which showed deviations in most properties from those for the same average  $M_c$ .

Electron microscopy confirmed the existence of microgel particles, even before the gel point, and indicated that aggregates were probably formed, as well as inclusions of secondary cured material and, in the case of high-molecular-weight epoxies, shells of highly crosslinked materials. Based on these findings, and on estimates of critical flaw sizes from fracture and tensile tests, a tentative model was proposed to explain as much of the observed behavior as possible. The continuity of the phases and the strength of bonding between the aggregates or microgel particles was emphasized, and a strong analogy noted with respect to interpenetrating polymer networks.

## SECTION I

### INTRODUCTION

#### A. Statement of the Problem

Crosslinked polymer networks comprise some of the oldest and most useful polymers in modern technology. Because of their good dimensional stability, resistance to viscous flow at elevated temperatures, and resistance to water and solvents, resins based on such materials as epoxies, phenolics, polyesters, and aminoplasts find many applications, for example as components for mechanical and electrical uses, as composite matrices, and as protective coatings. Similarly, cured elastomers fill many common engineering needs.

Although such crosslinked or "thermoset" networks can often be made easily, with relatively little technical expertise, knowledge of structure-property relationships is in a much less satisfactory state than with thermoplastics (1-3).

Reasons include inherent complexity of the chemistry involved, sensitivity to processing conditions (often poorly controlled), intractability and difficulty of characterization, and a frequent lack of attention because many ordinary service demands can be met without sophisticated technical knowledge. However, as technology moves towards more and more demanding technical specifications, as in the case of aerospace materials, and towards more precise and demanding balances between costs, benefits, and materials conservation, much more must be learned about these materials. At present, the engineer would still like more information (in comparison to other materials) to use as a basis for materials selection or component design.

Thus, relatively little is known about such basic parameters as the degree and distribution of crosslinking\* as a function of composition, morphology and processing conditions, on the one hand, and as related to mechanical behavior such as creep, stress-strain behavior, and fracture, on the other.

#### B. Objective and Scope of the Program

##### a. Objective:

The principal objective of this program is to determine the influence of crosslinking and network structure, in particular variations in the distribution of chain lengths between crosslinks, on the mechanical properties

---

\* It should be noted that variations in crosslink distribution may occur both on molecular and microscopic scales, the former being the subject of this report, but also relevant to the latter.

of polymers exhibiting high glass transition temperatures,  $T_g$ 's, above the temperature of use.

b. Scope:

The scope of the program includes the study of both model and practical high- $T_g$  resins, as follows:

(1) Development of syntheses for, and characterization of, model crosslinked systems which permit control of the degree and distribution of crosslinks.

(2) Synthesis and characterization of high- $T_g$  epoxy resins having controlled degrees and distributions of crosslinks.

(3) Characterization of viscoelastic behavior, including stress-strain response at high and low rates of loading, and creep or stress relaxation to reflect both short-term and long-term response.

(4) Determination of static and cyclic (fatigue) fracture behavior.

(5) Determination of typical morphologies by optical, electron and scanning electron microscopy.

(6) Correlation of fundamental properties, especially composition and degree and distribution of crosslinking, with engineering behavior under static and cyclic loading.

c. General Discussion:

As discussed in section A, the increasing use of crosslinked polymers for critical and demanding engineering applications requires much better fundamental knowledge about the molecular networks concerned, and the relationships between the network characteristics, synthesis or processing, and mechanical and other properties. A major reason for the deficiency in our knowledge is the complexity and variety of network structures which may be encountered (1,2). This complexity leads to several difficulties in experimental studies of the type concerned in this discussion.

First, it is difficult to characterize important characteristics of crosslink density (or  $M_c$ , the average molecular weight between crosslinks), the distribution in the length of chains between crosslinks, and the amount of material not incorporated in the network. Second, such characteristics are sensitive to process variables such as stoichiometry, temperature, and additives (2,5-26). A third problem is the tendency for the curing of many systems such as epoxy resins to be often complex with respect to both a multiplicity of simultaneous reactions and to morphology (2,7-9,15,24,26). From the simplest chemical point of view, an ideal polymeric network may be conceived of as a three-dimensional system of connected chains forming

a single macroscopic molecule (Figs. 1a, 1b). A "single molecule" is formed, because a Maxwell's demon may traverse the entire system, stepping only upon regular covalent bonds. Clearly, the behavior must depend on the tightness of the network with such a model; a network such as shown in Fig. 1a would exhibit less swelling than the network in Fig. 1b, which has a large  $M_c$ . Even with such models for an "ideal" homogeneous unimolecular network, however, a problem arises, for in many real cases (Figs. 1c, 1d) the lengths of chains between crosslinks may vary depending on the structure of the monomers or prepolymers, or on the vagaries of reaction kinetics. Of particular interest to this study is the effect of a distribution in  $M_c$ . (Such a distribution will occur in a homogeneous system; in a heterogeneous system, several such distributions may exist as well as variations in  $M_c$  itself in the various phases.)

Furthermore, as shown in Figs. 1e to 1h, a real polymer network is usually quite different from the ideal in structure. Not only do loops and dangling chain ends detract from the effectiveness of the structure, but shorter chains, either linear or branched, may exist without direct chemical connection to the network. Also in some cases reactive diluents such as styrene oxide may be added reacting at one end of the molecule and leaving the other dangling. Such entities largely serve to dilute the network, and tend to adversely affect physical and mechanical properties (1).

Finally, the topology and morphology of the networks may vary still more from the picture presented (2). Considerable evidence suggests that at least in some cases composition may be quite heterogeneous, even to the point that distinct phases may coexist, especially in the neighborhood of interfaces (1,8,9,13,22-26). Indeed, in such cases another model might be an inverted version of, for example, Fig. 1g, with highly branched or cross-linked domains embedded in a lower molecular weight matrix; Fig. 1h illustrates such a domain model, as well as the general case of compositional heterogeneity (noting that phase boundaries need not be sharp). Variations may also exist if one of the multifunctional reactants has itself a distribution of molecular weight between its functional groups (Fig. 1); such variations are characteristic of epoxy resins.

Typical methods for study of networks have been directed primarily at determining an average value for  $M_c$ , and have been mainly based on stoichiometric predictions, swelling, elastic moduli, creep, mechanical damping, and glass transition behavior (1,2; see also section B.b). Thus, classical theories developed by Flory (27, chapter IX) and others (1,2) have served to predict gelation and crosslinking in a statistical way, albeit to an approximation which may or may not be a good one (2). In the case of vulcanized rubbers, which exhibit high values of  $M_c$  (say, 5000), much understanding of elastomeric networks has already been achieved. While our knowledge remains incomplete, the theory of rubber elasticity (1, chapter XI), the Flory-Rehner swelling theory (1, chapter IX), and the theory of viscoelasticity (28) provide guideposts for determining not only chemical properties such as crosslink density, but also a practical basis

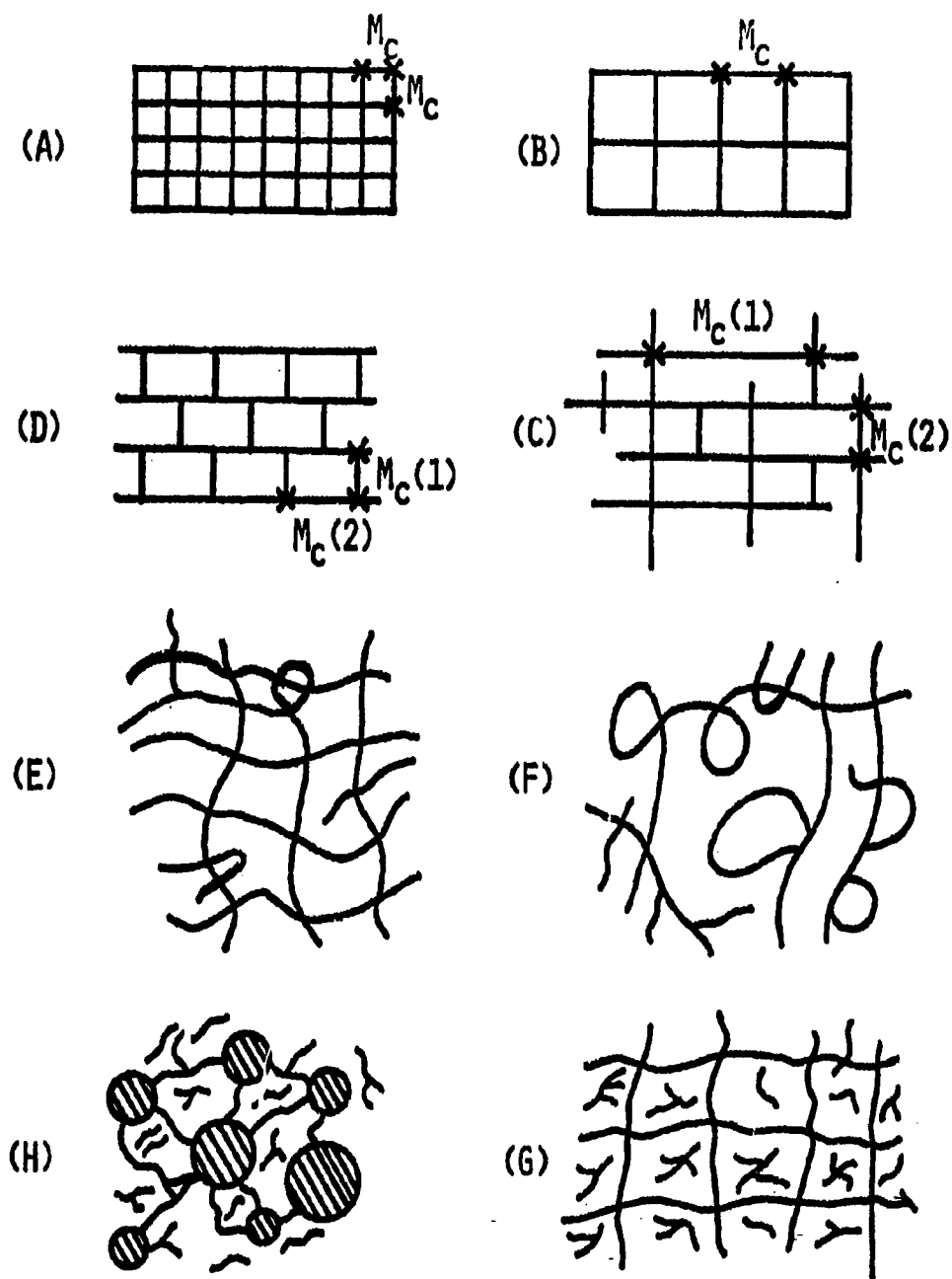


Figure 1. Schema showing typical variations in nature and composition of crosslinked polymer networks (after reference 2).

for estimating modulus, creep, stress-strain behavior and fracture (29-36). Treatment of the distribution of crosslinks has often been considered as one of the unsolved problems of polymer science (37). Although it has been predicted on theoretical grounds that the rubbery modulus should be independent of the distribution of  $M_c$  (38), experimental tests such as those based on tagging crosslinks with heavy metal atoms (39, 40) have not been used to confirm the prediction.

At room temperature, all such elastomers, of course, are above their glass transition temperature,  $T_g$ . If the crosslinked polymer is below its glass transition temperature, its molecular chains are incapable of long range coordinated motion, and the material becomes stiff and glassy. Such "thermoset" resins are typified by a variety of commercial materials, including phenolformaldehyde resins, melamine resins, crosslinked polyesters, and epoxy resins. Unfortunately, with materials of this type, which exhibit high degrees of crosslinking and great chemical complexity ( $M_c \ll 5,000$ ,  $\sim 300$  for some common epoxies), equations useful for elastomers tend to fail and require empirical modification (2), and in addition many characterization parameters in the glassy state are insensitive to the nature of the crosslinking. Moreover, as pointed out cogently by Nielsen (1,2), there is surprisingly little fundamental study of mechanical behavior using materials characterized to the limits of the state-of-the-art. To be sure, there are exceptions, for example, recent studies of epoxy behavior by a number of authors (6, 7, 14-19, 46, 47) but studies correlating fundamental and engineering behavior are not as common as might be supposed. In any case, model systems based on anionic polymerization (41) or on Millar-type IPN's (42-45) should provide valid approaches to the question of how distribution in  $M_c$  affects behavior in the glassy state and glass-rubber transition region.

Another difficulty with gelling or thermosetting systems is that, as pointed out long ago by Nielsen (8) and others (2), and more recently by Cilliham (5), the temperature of cure plays a role far beyond that of simply altering reaction rates in a chemical sense. As curing proceeds at a given nominal temperature, the network develops and its  $T_g$  increases. However, when the  $T_g$  of the network reaches ambient temperature (which may exceed the nominal temperature due to adiabatic self-heating), the rate of further crosslinking is drastically reduced due to slowing of reactant diffusion by the stiffening of the network. Thus, if the specimen is heated to above its curing temperature, as might well be the case in a modulus-temperature study, additional curing may occur during the test itself. Information about the network deduced from such tests is relevant only to the material subjected to the additional thermal history of the test, not to the original specimen as cured. Clearly, the curing temperature must be higher than the maximum test temperature if one is to achieve a network which will be stable during testing.

In summary, because of the importance of thermoset resins to present and future technology, we need much better experimental and theoretical understanding of the relationships between processing, the network formed, and its behavior. At present, detailed empirical or semi-empirical studies are relatively few in number, especially with respect to fracture behavior.

## SECTION II

### TECHNICAL APPROACH

From the standpoint of relevance to the engineering applications, an epoxy resin system would be of considerable interest. Although the chemistry is complex, the systems are easily adaptable to specimen preparation, and an increasing number of quantitative studies relating at least average or relative network properties such as  $M_c$  to stoichiometry and curing conditions have appeared (5-23, 46-50). In several studies by others and this group (7, 49, 50), it has been possible to demonstrate that full curing can be effectively obtained using certain cure histories. Also, at least some qualitative evidence was available relating viscoelastic parameters such as damping to the breadth of the presumed distribution of crosslinks (2), and some evidence was available on stress-strain behavior (7, 46), fracture (32, 33), and impact strength (46), the latter as a function of  $M_c$ . Disadvantages include difficulty in precisely controlling the distribution and nature of crosslinks (due to the fact that commercial resins usually exhibit a distribution of molecular weight) and in directly measuring the crosslink distribution. Nevertheless, it seemed reasonable to conclude that a thorough characterization of viscoelastic behavior in blends of epoxy resin should enable correlation of the distribution of  $M_c$  and other network variables with ultimate behavior under static and cyclic loading. Existing studies were of insufficient scope to permit such a correlation.

To complement this study, and in a sense to calibrate it, it seemed desirable to also study a still more definable model system. For this purpose, a novel network system developed by Bamford and others was first selected (for a review, see reference 4). This system had several advantages but could not, in fact, be adapted to serve this program within the time available (51). Because of these difficulties, another model system was selected based on Miller-type (42-45) interpenetrating networks (IPN's). To prepare these, crosslinked polystyrene ( $M_c=a$ ) is swollen with a styrene/crosslinking-agent mixture (to yield  $M_c=b$ ), and the monomer polymerized (Fig. 2). Thus, for a given average  $M_c$ , the distribution can be varied widely by varying  $a$  and  $b$ . In addition, it was thought that, by analogy with other IPN's (52), the behavior of the model might reflect the nature of the network morphology, which in turn might be expected to reflect the sequential nature of the network formation. Finally, the synthetic techniques are readily adaptable to making laboratory specimens for mechanical studies.

In short, two complementary candidate systems were selected: one a potentially good, though not perfect, approximation to an ideal network model but of academic interest as a material, and the other a less good approximation to an ideal model, but a system with existing engineering application. Thus, the two approaches should be considered as a dual model system: a primary, well-definable model coupled with a model which is less easily defined, but of greater technical interest per se. The primary model should serve to illuminate and calibrate the secondary model, the epoxy system; the two should be considered together.

Specific discussions of each system follow in sections III and IV.

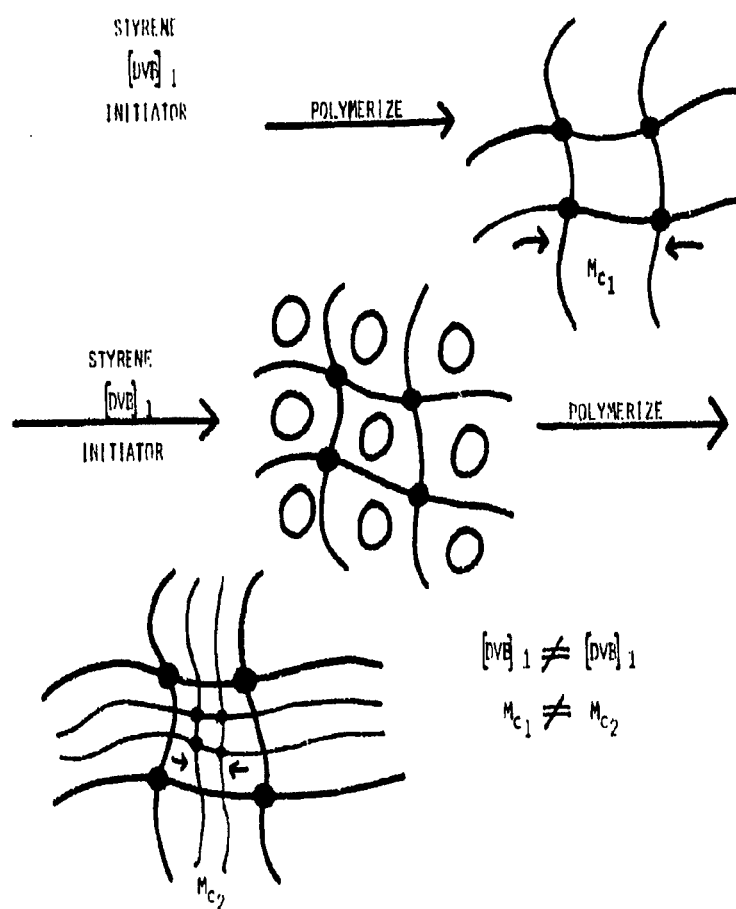


Figure 2. Schema for Millar-type IPN.

## SECTION III

### SYNTHESIS OF MODEL NETWORKS

#### A. Introduction

The principal aim of this research is to show how the mechanical behavior of glassy networks depend upon the distribution of  $M_c$  values and how free or dangling chains alter behavior. Polystyrene, with a glass transition temperature,  $T_g$ , of +100°C was selected as the model network, because its glass temperature is above room temperature, and its general physical behavior is well known.

The objective, then, was to prepare networks with two distributions of  $M_c$  through the use of the Millar synthesis (42-45).

##### a. Millar IPN's:

As mentioned previously, this class of IPN's is a special case in which each network is the same chemically. The following steps are involved:

- (1) preparation of polymer I network (in this case polystyrene crosslinked with divinylbenzene, DVB),
- (2) swelling of a styrene/DVB/monomer-II mixture into polymer I, and
- (3) polymerization of the imbibed monomer II to give polymer II.

Thus the network of polymer II is synthesized within the existing network of polymer I. The crosslink density of each network can be varied easily by varying the concentration of DVB, thus making it possible to synthesize a wide variety of crosslink distributions.

#### B. Experimental Details, Results, and Discussion

##### a. Synthesis:

Millar IPN's in which the two interpenetrating networks are both crosslinked polystyrene (PS) were synthesized along with single PS networks and linear PS as controls. All single networks and polymer I networks were synthesized by thermal polymerization using di-lauroyl peroxide as the free-radical initiator at 60°C. The initiator concentration was 0.4% by weight based on monomer volume. Divinylbenzene (DVB) (which is an isomeric mixture containing 55% p-DVB) was used as the crosslinking agent.

Monomer mixtures were prepolymerized in an oven at 60°C for various lengths of time (depending upon the DVB concentration) until a significant increase in viscosity was noted (corresponding to about 10% conversion).

By prepolymerization, shrinkage was minimized, and a smoother and more uniform product was produced. The prepolymer syrup was transferred to a mold formed by a gasket of ethylene-propylene rubber between two glass plates held together by clamps (10mm x 15mm x 2mm). Polymerization was continued in the oven for 3 or 4 days, at which time the polymer sheets were removed and heated for 24 hours at 110°C in a vacuum oven to remove any unreacted monomer. Weight losses were usually about one percent, and never more than two percent, indicating that polymerization was essentially complete.

To make the Millar IPN, additional monomer together with cross-linker, and initiator (monomer mixture II) was introduced by swelling the polymer I network so that it contained the desired amount of monomer mixture II. Specimens were then allowed to equilibrate overnight so that diffusion of the monomer mixture would occur and distribute monomer II uniformly throughout polymer I. The polymer II network was made by either photopolymerization using 0.4% benzoin as initiator or by thermal polymerization using 0.4% di-lauroyl peroxide. In the earlier experiments, photopolymerization at room temperature was employed using UV light to activate the benzoin initiator. To show that the mode of polymerization of polymer II does not affect the properties of Millar IPN's, thermal polymerization of polymer II was also carried out. Creep and swelling experiments confirmed that there are essentially no physical differences between the Millar IPN's polymerized thermally and those polymerized photochemically. Polymer II was enclosed between glass plates and a gasket and polymerized for 3 to 4 days, removed from the mold, and heated under vacuum at 110°C for 24 hours to remove unreacted monomer. Polymerization was virtually complete, as indicated by the occurrence of only small weight losses (one or two percent).

b. Specific Compositions:

Millar IPN's were synthesized in which polymer I contained 0.4% DVB and polymer II contained 4% DVB in the following weight proportions: 75/25, 50/50, and 25/75. Polymer I was thermally polymerized and polymer II was photopolymerized. A single PS network containing 2.2% DVB was synthesized to use as a comparison for the 50/50 Millar IPN. Hence, the 50/50 IPN and the 2.2% DVB network both contain the same average amount of crosslinking agent.

Thus, several IPN's were also synthesized using a polymer I containing 0.4% DVB, and 4% DVB in polymer II. Another set of Millar IPN's with polymer I containing 0.4% DVB and polymer II containing 4% DVB containing 1% isoprene (for electron microscopy) were synthesized by thermally polymerizing both networks.

For experiments with preswelling, polymer I was polymerized at 60°C in the presence of 50% by volume of toluene. When 0.4% DVB was used, no gelation occurred, presumably due to a reduction of the Tromsdorff effect.

Preswollen networks containing 4% DVB and 50% by volume of toluene, however, were synthesized. One such sample was completely deswollen (50%). A preswollen network containing 4% DVB was partially deswollen and the remaining toluene exchanged in monomer mixture II containing 0.4% DVB to make a 50/50 Millar IPN.

Attempts to make Inverse Millar IPN's where polymer I contains 4% DVB were unsuccessful. Various approaches were used. A 4% DVB network sample is too highly crosslinked to imbibe more than about 20% monomer solution at room temperature without breaking up. In order to swell the 4% DVB network, specimens were heated to above their  $T_g$  and immersed in hot toluene. Then the cooled, swollen samples were placed in monomer solutions to allow liquid exchange to occur. Upon completion of polymerization, samples were removed and found to have broken up into small pieces. The weight percent of polymer II containing 0.4% DVB in these specimens was 50% and less. Another approach involved swelling 4% DVB network specimens at room temperature with monomer solution for short periods of time so as to add 10-25% monomer II. Even at this ratio of polymer I to polymer II, the Millar IPN usually broke up upon polymerizing. Only a few specimens containing a very small amount of polymer II (10% or less) survived the polymerization of polymer II without breaking up, and even these were of inferior quality being very soft after polymerizing for up to 7 days. When a 2.2% DVB network was swollen with 50% of a 2.2% DVB monomer solution, it too broke up upon polymerization.

#### c. Conclusions

The synthesis of the Millar-type IPN's in which the first polymer synthesized is the less crosslinked one proceeded smoothly by either photochemical or thermal techniques, yielding cast specimens ready for mechanical characterizations. In fact, the technique is one of the most facile possible and presents no problems of any kind. On the other hand, the technique is not yet adaptable to making the reverse type, in which the first-formed polymer is the more highly crosslinked one.

## SECTION IV

### PROPERTIES OF MODEL NETWORKS

#### A. Introduction

The physical and mechanical behavior of polymer networks depends upon the crosslink density, the distribution of molecular weights of chain segments between crosslinks,  $M_c$ , the number of free or dangling chains, and the temperature. Three general temperature regions have been identified: (1) above the glass-rubber transition region, where the material behaves like an elastomer, (2) within the glass-rubber transition region, where the material is viscoelastic, and (3) below the glass-rubber transition region, where more or less glassy behavior predominates. The experiments performed under this contract are primarily directed towards region (3), with some effort placed in region (2) to show the changes in behavior that may be expected as the polymer chains gain mobility. Region (1) is of interest only in the analytical determination of crosslink density (see section a, below).

Properties of particular interest include creep or stress relaxation (to determine long-term behavior), stress-strain response, and fracture characteristics. Progress to date is discussed below.

#### B. Experimental Details, Results, and Discussion

##### a. Experimental Methods

$M_c$ : While absolute values of crosslinking cannot generally be obtained with densely crosslinked systems such as epoxy resins (2), approximate values in more "open" systems can be estimated in several ways, the most common being by swelling and by measurement of the creep compliance in the rubbery state.

Thus values of  $M_c$ , the average molecular weight between crosslink sites, were obtained by swelling samples in toluene and using the Flory-Rehner equation (27, 53):

$$\frac{1}{M_c} = \frac{\ln(1 - v_2) + v_2 + \chi_{12}v_2^2}{\rho V_0 (v_2^{1/3} - v_2/2)} \quad (1)$$

where  $v_2$  represents the volume fraction of polymer in the sample at equilibrium,  $V_0$  is the solvent molar volume, of density  $\rho$  (1.08g/cm<sup>3</sup>) and  $\chi_{12}$  the polymer-solvent interaction parameter was taken as 0.44. In each case volumes were assumed to be additive. The soluble fraction was small in each case, ranging from 3% (4% DVB) to 5% (0.4% DVB) to 3%-5% (IPNs).

In addition, values of  $M_c$  were estimated from the equilibrium shear modulus,  $G(\infty)$  or  $1/J(\infty)$ , where  $J(\infty)$  is the indicated limiting value of  $J(t)$ , by means of the theory (24) of rubber elasticity, to give  $M_c$  ( $1/J(\infty)$ ):

$$M_c (G(\infty)) = M_c (1/J(\infty)) = \rho RT J(\infty) \quad (2)$$

where  $\rho$  is the density,  $R$  the gas constant, and  $T$  the absolute temperature (in this case,  $120^\circ\text{C}$ ). Finally, the theoretical value of  $M_c$  was calculated from the molar ratio of DVB to styrene.

Creep: Studies of creep as a function of time and temperature were carried out using a Gehman Torsional Stiffness Tester (54). Creep experiments covered the entire range of viscoelastic behavior from the glassy region at  $60^\circ\text{C}$  to the rubbery region at  $120^\circ\text{C}$ . Compliance readings were taken at various intervals in time from 10 seconds to 1000 seconds. The shear creep compliance,  $J(t)$ , was calculated from the angle of twist of the specimen induced by the torsion wire as indicated by the apparatus.

Master curves were obtained by shifting data obtained at various temperatures with respect to a reference temperature (28), assuming that all relaxation mechanisms had the same temperature dependence. This assumption was probably justified because the materials under investigation differed only in the amount of crosslinker present in the individual networks. Theoretical shift facts were also calculated from the Williams-Landel-Ferry (WLF) equation

$$\log a_T = \frac{17.44(T-T_g)}{51.6 + (T-T_g)} \quad (3)$$

where temperatures are in  $^\circ\text{K}$ .

Each curve of reduced compliance was shifted with respect to the curve at  $100^\circ\text{C}$  (the reference temperature which is also the glass transition temperature) until all fit together to form a smooth master curve. Master curves for various materials could then easily be compared.

Electron Microscopy: Specimens (2mm x 2mm x 20mm) were cut from the IPNs and one end of each sample was trimmed to a truncated pyramid with sides approximately 0.1mm in size. The specimens were exposed to osmium tetroxide vapor for about two weeks in order to selectively stain the isoprene-mer portion of the PS polymer II phase. A Porter-Blum MT-2 ultramicrotome equipped with a diamond knife was used to obtain ultrathin sections about 300Å thick. Transmission electron micrographs were taken by direct observation with a Phillips 300 transmission electron microscope.

Results of the various measurements are summarized below.

### 1. Crosslink Density

In Table I, results of the two methods used are compared with the theoretical values for  $M_c^*$  calculated from the stoichiometry. Note that a finite value of  $M_c$  is obtained for linear PS due to the existence of elastically effective physical entanglements in the rubbery plateau region. Thus in general,  $M_c(1/J(\infty))$  tends to be smaller than  $M_c(\text{theor.})$  due to the contribution of the entanglements to the effective crosslink density. From Table I, it may be seen that the  $M_c(1/J(\infty))$  values for the 50/50 Millar IPNs are significantly larger than expected when compared to the  $M_c(1/J(\infty))$  for the 2.2% DVB single network. Generally,  $M_c(E)$  values for the Millar IPNs lie somewhere in between the experimental values for a 0.4% DVB network and that for a 2.2% DVB network. It seems that the first network formed dominates the crosslink density of the IPN.

Swelling data also support the idea of greater contribution of the 0.4% DVB Polymer I network, although not as dramatically as do the  $M_c(1/J(\infty))$  values.  $M_c$  values calculated from the weight gain of specimens after attaining equilibrium swelling in toluene tend to be higher than expected based on overall DVB content (that is, they tend to swell more than expected). The swelling of polymer networks in a good solvent at room temperature for the time needed to attain equilibrium swelling allows all regions of various crosslink densities to swell to the maximum degree. Therefore, in the Millar IPNs, the  $M_c$  (weight gain) values measured by swelling tests may not reflect the greater contribution of Polymer I domains to the same extent as do the  $M_c(1/J(\infty))$  values (see below).

Table I. Values of  $M_c^a$  for Millar IPNs and Controls

Specimen	Swelling Data $M_c$ (Weight Gain)	$M_c(1/J(\infty))$ at 120°C	$M_c$ (Theory)
<u>Control</u>			
Linear PS	$\infty$	$1.0 \times 10^4$	$\infty$
0.4% DVB	$3.0 \times 10^4$	$6.9 \times 10^3$	$2.9 \times 10^4$
2.2% DVB	$6.5 \times 10^3$	$2.3 \times 10^3$	$5.4 \times 10^3$
4% DVB	$3.1 \times 10^3$	$2.0 \times 10^3$	$2.9 \times 10^3$
<u>Millar IPNs</u> (0.4/4% DVB)			
75/25	$1.7 \times 10^4$	$4.9 \times 10^3$	$9.1 \times 10^3$
50/50	$8.6 \times 10^3$	$4.4 \times 10^3$	$5.4 \times 10^3$
25/75	$5.0 \times 10^3$	$4.7 \times 10^3$	$3.8 \times 10^3$
55/45	$7.1 \times 10^3$	$4.5 \times 10^3$	$5.6 \times 10^3$
25/75	$3.5 \times 10^3$	$4.0 \times 10^3$	$3.8 \times 10^3$

<sup>a</sup>It should be remembered that  $M_c$  is inversely proportional to crosslink density.

## 2. Creep Behavior

Typical creep data are shown in Figure 3. The shift factors,  $a_T$ , were calculated and compared graphically to those obtained from the WLF equation (eq. 1) in Figure 4. As can be seen from the plot, agreement with the WLF shift factors is quite good in the region near and just above the  $T_g$ , 100°C. According to empirical evidence, the WLF equation is only valid between  $T_g$  and  $T_g + 100^\circ\text{C}$  for linear polymers and may not necessarily hold for crosslinked polymers. Figure 5 shows the master curves that resulted from creep experiments performed on the Millar IPNs. All three polymers creep more than the 2.2% DVB single network and have rubbery plateau regions lower than those found for the single network. Differences among the three Millar IPNs are not as great; the 50/50 and 25/75 systems being very similar and creeping somewhat less than the 75/25 specimen. Two IPNs in the weight ratios of 25/75 and 55/45 and their master curves are presented in Figure 6 along with the master curves for 0.4% DVB and 2.2% DVB networks. The creep behavior of the 55/45 Millar IPN is very similar to that of the 0.4% DVB network and it creeps significantly faster than the 2.2% DVB network. Only in the rubbery plateau region does it have a lower compliance than the 0.4% DVB network. The 25/75 master curve is very similar in shape to the 2.2% DVB curve up until the rubbery region is reached. Although it has the highest DVB content of all 4 specimens (3.1% DVB), its rubbery plateau lies between that for the 0.4% DVB network and the 2.2% DVB network.

The data presented in Figures 5 and 6 support the notion that more continuous Polymer I domains and less continuous\* Polymer II domains exist in the Millar IPNs. A more continuous Polymer I would be consistent with the creep data showing more creep in the 50/50 Millar IPN than in its corresponding equivalent 2.2% DVB single network. We also see that the 55/45 IPN creeps in a manner much closer to that of the 0.4% DVB network than the 2.2% DVB network. Thus, Polymer I dominates the creep behavior and rubbery compliances of the Millar IPNs.

Additional Millar IPNs were synthesized with Polymer I containing 0.4% DVB. Master curves for Millar IPNs containing 0.4% DVB in Polymers I are presented in Figure 7. These were made to investigate the influence of stretching the Polymer I network on the creep behavior while maintaining the same overall DVB concentration. The creep response is almost identical to that of the 0.4% DVB single network. Only in the rubbery region do differences occur; the Millar IPN has a somewhat lower rubbery plateau than expected. A 55/45 Semi-I\*\* Millar IPN with Polymer I containing 0.4% DVB and Polymer II containing linear PS creeps in a manner in between that of the linear PS and the 0.4% DVB network. Apparently, in this case, the linear polymer and the 0.4% DVB network control the creep to the same extent. The Polymer I domain may not be as continuous in the Semi-I IPN.

---

\*The "more continuous" referring to the dominant matrix.

\*\*A Semi-I IPN is one in which Polymer II is not crosslinked, but Polymer I is.

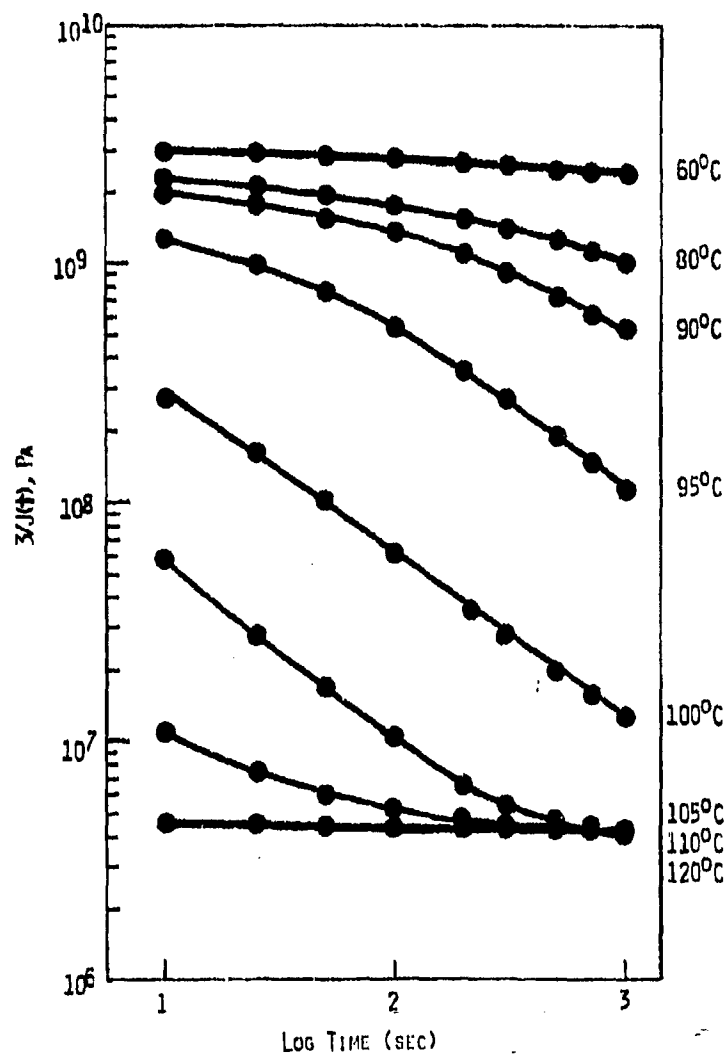


Figure 3. Creep data for polystyrene containing 2.2% DVB.

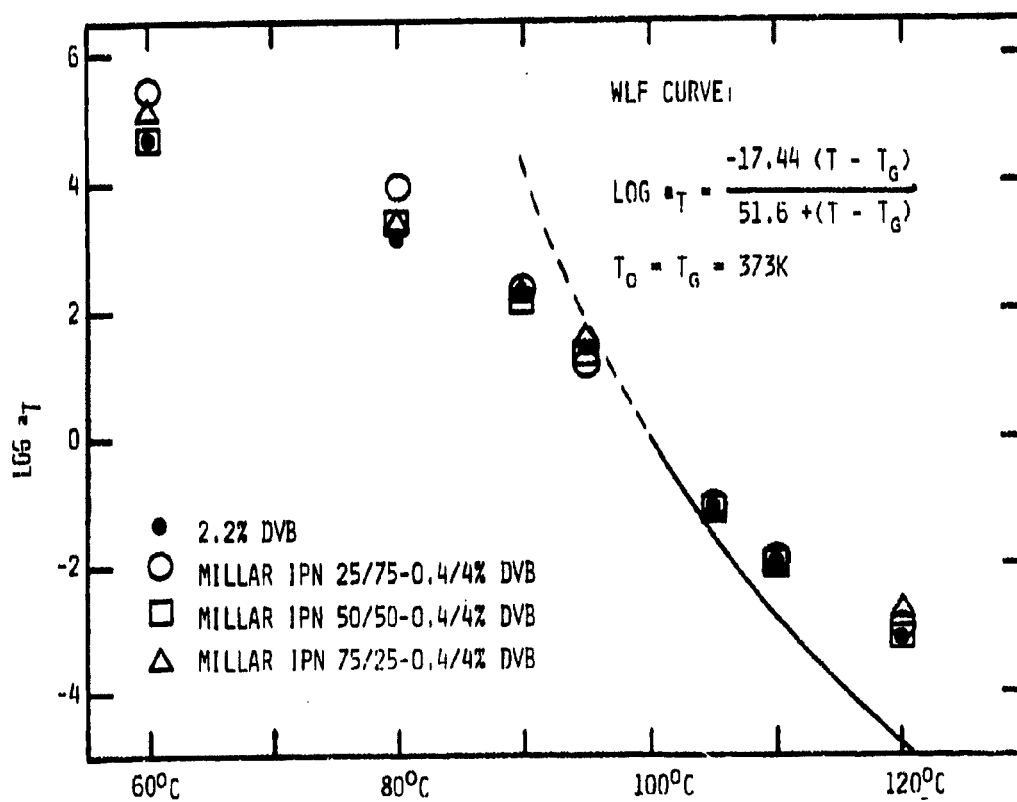


Figure 4. Experimental and theoretical shift factor,  $a_T$ , for Millar IPN's.

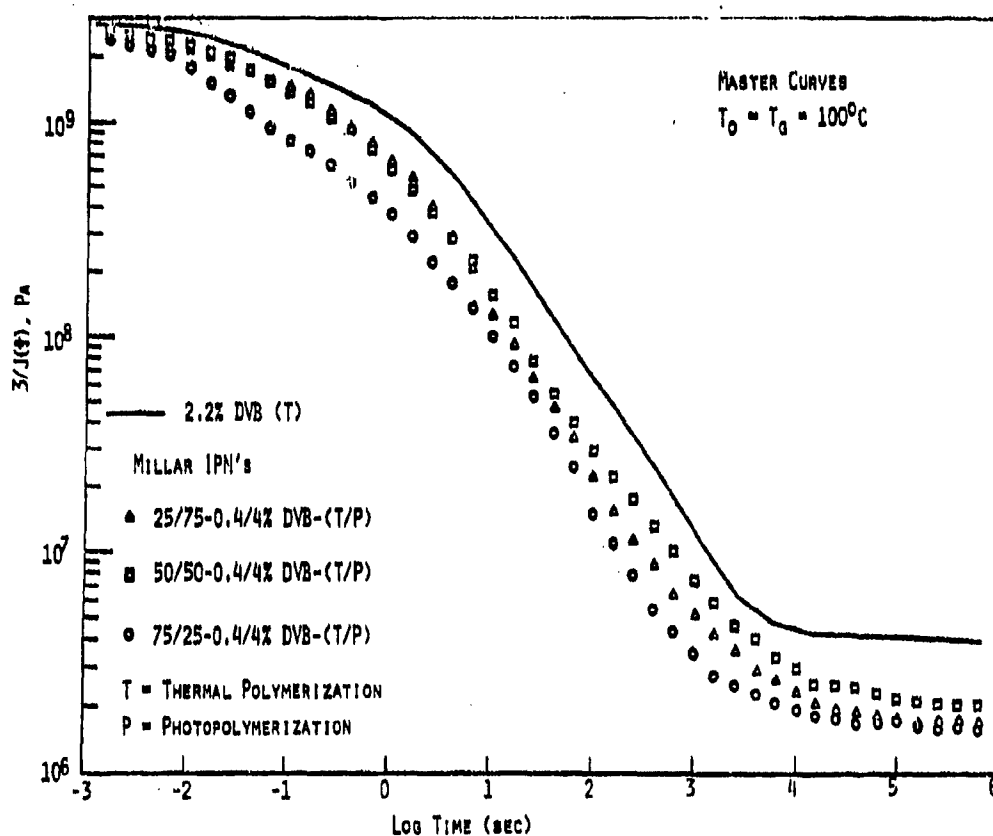


Figure 5. Creep Curves for Millar IPNs (% DVB in Polymer I = 0.4)

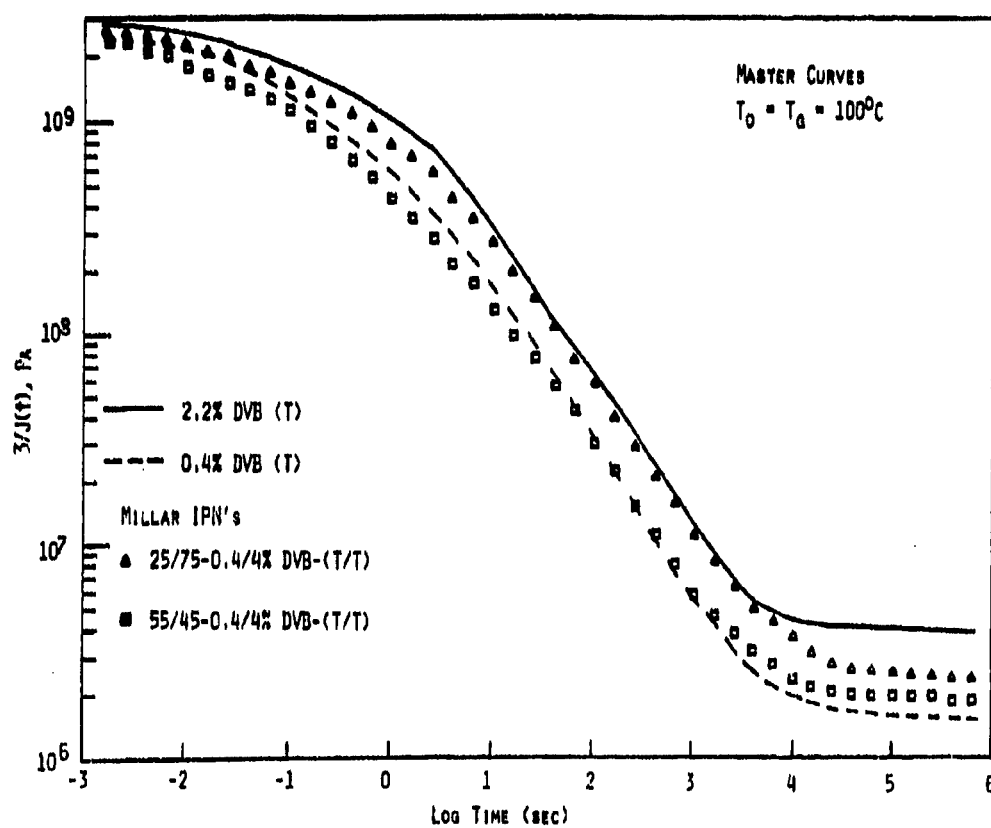


Figure 6. Creep curves for Millar IPNs prepared for electron microscopy.

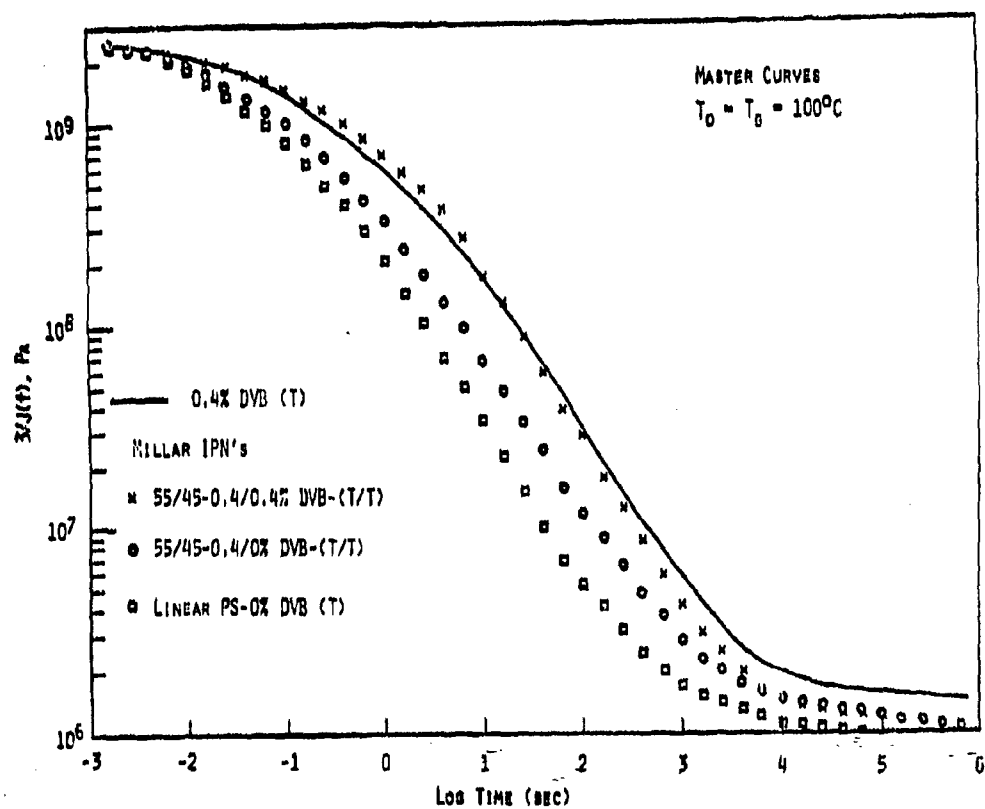


Figure 7. Creep curves for Millar IPNs (% DVB in polymers I and II = 0.4).

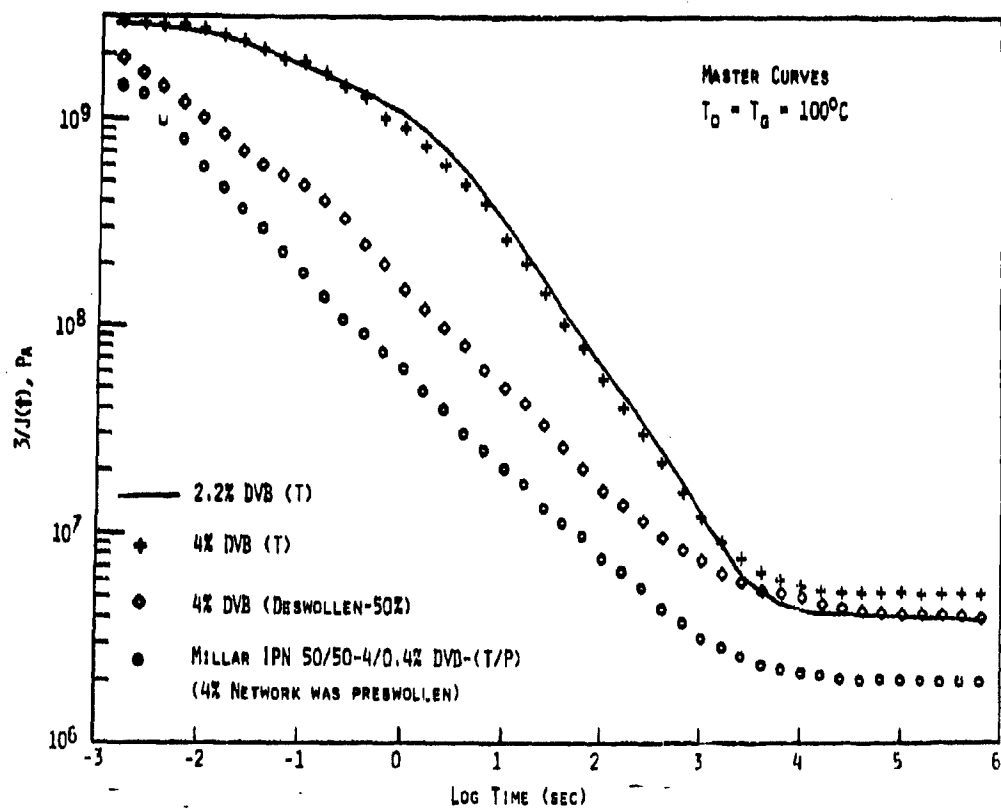


Figure 8. Creep curves for swollen Millar IPNs (% DVB in Polymer I = 4).

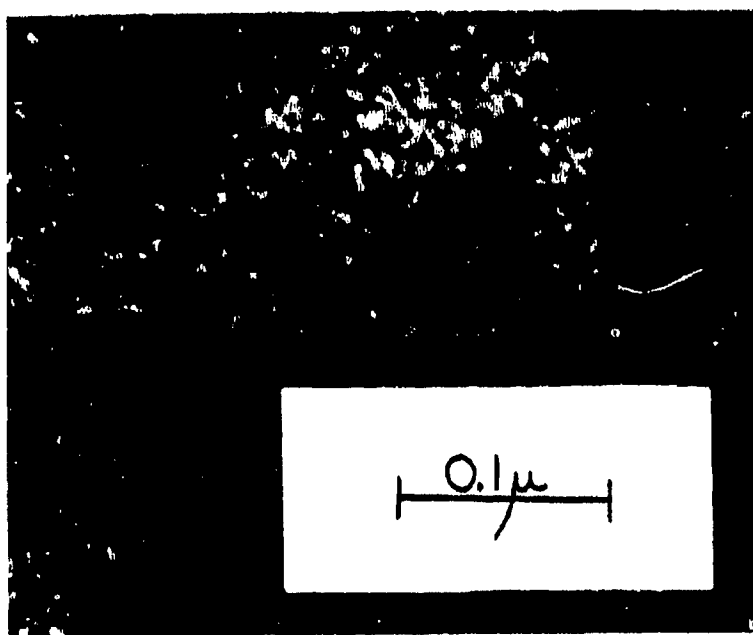


Figure 9. Electron micrograph of thin section Millar IPN 25/75 (0.4/4% DVB, 1% Isoprene in polymer 1D).



Figure 10. Electron micrograph of thin section IPN 72.2-PEAB/27.8 PMMA.

In order to further investigate the effect of preswelling in the creep behavior, it was decided to preswell Polymer I by forming the network in the presence of a diluent (toluene). The toluene could then be exchanged directly for monomer mix 2 so that Polymer I remains in a highly relaxed state. The properties of preswollen polymer networks have been previously studied by Shen and Tobolsky (55, 56). They studied the effects of diluents on the rubber elasticity of both lightly and highly crosslinked preswollen polymer networks and the corresponding deswollen networks. Creep response (Figure 8) for the deswollen 4% DVB network was faster than for a 4% DVB network, but the rubbery compliance was only slightly increased. Creep response for the 50/50 Millar IPN was even greater and the rubbery compliance was significantly above that for the 2.2% DVB network. Shen and Tobolsky (55, 56) postulated that when polymerization occurs in the presence of diluent, effective intermolecular chemical crosslinks may be decreased by the formation of intramolecular loops. Also, network interpenetration and trapped chain entanglements become less significant at higher diluent concentrations. These phenomena would explain why the preswollen specimens crept more rapidly and had higher rubbery compliances than the corresponding single networks. Another factor to consider in the deswollen 4% DVB network is that the network may have collapsed upon itself, and distances between crosslink points have been reduced by a factor  $3/2$ . The faster creep of the deswollen material may be in part a response to the internal stresses which developed in going from the relaxed, preswollen state to the deswollen state.

As mentioned above, the study of Millar IPNs was undertaken originally as a model system for non-uniform plastic networks. Creep data and to a lesser extent swelling data obtained so far are consistent with the occurrence of segregation: the first polymerized network appears to exhibit greater continuity than the second polymerized network. Reflection suggests that this might be arising because of random fluctuations in the crosslinking of Polymer I. Monomer 2 would tend to be located in the small regions of space with accidentally lower degrees of crosslinking, because the elastic compressive pressure would be lower. The greater this segregation effect is, the more control Polymer I will exert on viscoelastic creep response and swelling behavior.

### 3. Morphology

Creep experiments proved to be very interesting, but direct observation on the molecular level was needed to lend support to the above-stated notion of a more continuous Polymer I. In order to elucidate the Millar IPN morphology, a small amount of isoprene (about one percent) was incorporated in Polymer II for Millar IPNs in which Polymer I contained 0.4% DVB and Polymer II contained 4% DVB (isoprene tends to form a random copolymer with styrene).

It was decided to first predict the domain sizes of the less continuous phase using an equation developed by Donatelli et al. (57) and given in Appendix A. For the case of polystyrene Millar IPNs, the interfacial energy,  $\gamma$ , between Polymers I and II is expected to be zero. The Donatelli equation thus reduces to:

$$D_2^2 = \frac{C^2 K^2 (1 - W_2)}{v_1^2} \quad (4)$$

For a 50/50 polystyrene Millar IPN with 0.4% DVB in Polymer I and 4% DVB in Polymer II, we have:

$$K = 0.7 \text{ \AA} \quad [\text{from the Polymer Handbook (58)}]$$

$$W_2 = 0.5$$

$$v^2 = 3.39 \times 10^{-5} \text{ moles/g}$$

$$D_2 = \pm 85 \text{ \AA}, \text{ or zero}^*$$

For 25/75 and 75/25 Millar IPNs, we obtain  $D_2$  values of 60 \AA and 100 \AA, respectively. These predictions were then tested with a Millar IPN containing 25% Polymer I with 0.4% DVB and 75% Polymer II with 4% DVB and 1% Isoprene. Electron microscopy revealed a fine structure with phase domain diameters for Polymer II of from 50 to 100 \AA (Figure 9). This agrees very well indeed with the prediction of 60 \AA using the Donatelli equation Polymer II. In addition, although Polymer I is the minor component (25%) it appears to be the more continuous one. Hence, it is apparent that even when an IPN is synthesized with chemically identical components which should be completely compatible on a molecular level, a discontinuous Polymer II fine structure is detectable. Thus, the electron microscopy confirms the deduction (from creep behavior) that Polymer II within the more continuous Polymer I.

Previous work by Huelck, Thomas, and Sperling (52) showed that the network synthesized first controls the morphology of the IPNs and is an electron micrograph of an IPN containing 72.2% poly(ethyl acrylate) with 1% butadiene as Polymer I and 27.8% poly(methyl methacrylate) as Polymer II. Poly(ethyl acrylate) and poly(methyl methacrylate) are isomeric, each having the same molecular weight and very similar structures. The interfacial energy,  $\gamma$ , should be close to zero. As before, the micrograph (Figure 10) shows a fine structure with a more continuous Polymer I phase and a dispersed Polymer II phase with domains less than 100 \AA in size. The morphology seen here is similar to that found in the 25/75 Millar IPN.

An interesting question arises. Do these polymers represent the ultimate in compatibility of an IPN on a molecular level? Because both

---

\*Zero is obtained from the third root in the cubic equation when  $\gamma=0$

polymer networks are chemically identical in a Millar IPN (excluding variations in crosslinker level and addition of small amounts of isoprene), it is believed that these micrographs indicate the most compatible IPN possible. The Donatelli equation suggests that the Polymer II domains arise due to the physical restraints and the accidental inhomogeneities of polymer network I.

Consideration of the molecular processes which can lead to a greater and lesser phase continuity in Millar IPNs suggests that random crosslink variations in network I are important.

#### 4. Relevance to Other Systems

There is a striking analogy between the Millar IPNs and the multi-phase aspect of crosslinked resins such as epoxies (2, 9, 13, 15, 22-26) in which heterogeneities with sizes the order of  $\sim 100\text{\AA}$  have been observed. The question of network dominance must also play a role in, for example, epoxies, for at gelation, a continuous network is formed within which subsequent curing takes place.

#### 5. Conclusions

Let us begin by reviewing the evidence. Creep master curves for polystyrene/polystyrene Millar IPN's in the glassy and glass-rubber transition ranges indicated that the behavior was closer to that of polymer I than the overall composition would otherwise suggest. When compared with the creep behavior of single networks of (a) polymer I composition, (b) the statistical average of the two networks, and (c) polymer II composition, the creep master curve of the Millar IPN always fell between (a) and (b). The fact that network I dominated the mechanical creep behavior could be explained by assuming that polymer network I tended to be more continuous in space than network 2. Previous work with IPN's of two different polymers has clearly established the greater continuity of network I, but there was no a priori reason for assuming that the same was true for the Millar IPN case.

Before proceeding, two difficulties in the obtaining of the data require discussion. First, all of the data presented had the lower crosslinked network (0.4% DVB) as polymer I, and the higher crosslinked network (4.0% DVB) as polymer II. All attempts to synthesize the reverse Millar IPN with the 4.0% DVB network as polymer I failed. The reasons were the limited swellability of densely crosslinked networks, and their mechanical instability in the face of swelling pressures. Swelling network I in the presence of toluene, exchanging the toluene for styrene-DVB combinations, followed by polymerization yielded a far different product, probably due to the increased level of intra molecular crosslinking when the polymer molecules were artificially separated.

The second problem relates to the variation in the data between one master curve and another, both of nominally identical materials, with the creep data being taken as identically as possible. An estimate from the duplicates obtained (data not shown), indicates a standard deviation of about a half an order of magnitude on the time scale. Since the total variation of all of the data was about two orders of magnitude on the time scale, serious attention must be given to the possibility of the accidental nature of the data. First of all, the 25/75, 50/50, and 75/25 data each fell in the order expected, and all of them crept faster than the 2.2% DVB single network. Polymerization via U. V. light and through thermal chemistry yielded products that were substantially identical. The data were further supported by swelling studies and modulus in the rubbery range. Both of these experiments indicated that the Millar IPN behavior tended to be dominated by the crosslink level of network 1.

With the above experiments in hand, the Donatelli equation was applied, in an effort to estimate the domain sizes of network 2. Values of about 60-100 Å were calculated, depending on overall composition.

Actual transmission electron micrographs of osmium tetroxide stained samples substantiated the above presumptions: polymer network 2 appears to be less continuous, with phase domains somewhat smaller than 100Å. The experiment had some problems, however. For most was that ultramicrotome sections of under 300Å were required, to detect and study domains of less than 100Å. (Standard cutting thicknesses are rarely less than 600Å.) Also, to be sure that the phase domains were not caused by the different composition of polymer II the isoprene level was held to 1%, resulting in very light staining.

Overall, however, all of the evidence to date supports the notion that the first formed network in a Millar IPN tends to be more continuous than network 2. This finding has enormous implications for the synthesis of many types of thermoset plastics, which may behave in a similar manner. For example, do the first portions of material reaching the gelation stage maintain greater continuity than that which accidentally is polymerized later in time?

## SECTION V

### SYNTHESIS OF EPOXY NETWORKS

A number of epoxy systems have been intensively studied over the last few years (5-26,46-48), most based on bisphenol-A derivatives. Variations have included the nature of the epoxy resin or curing agent (10,11), the length between functional groups, which will help define  $M_c$  (11), temperature (5), and the introduction of reactive diluents, which may dilute the network and also alter the state of cure (7). Both amines and polyamides have been used; in the latter case (49,50), the  $M_c$  can be varied by changing the amide equivalent content.

For this study, one system considered for selection was the epoxy-amine-diluent system used by Whiting and Kline (7); (Epon 828-diethylene-triamine-styrene oxide). The system has been characterized thoroughly in terms of % reaction of the epoxy groups, and concentrations of both -OH and -CH<sub>2</sub>-O- groups followed as a function of amine and diluent (styrene oxide) contents. A wide variety of degrees of cure are obtainable, and also variations in  $M_c$  as a function of stoichiometry. Moreover, values of yield strength, ultimate tensile strengths and fracture energy have been obtained and related to process parameters. A similar system (Epon 828/methylene dianiline (MDA)) was also studied extensively by Bell et al. (6,46-48), who critically analyzed the stoichiometric aspects of curing and also determined the effects of  $M_c$  in other amine-cured resins (by changing the molecular weight of the amine curing agent) on tensile and impact strength.

Bell (47) also showed that the presence or absence of an exotherm had no effect on the curing reaction, that nearly complete curing could be achieved in this system, and that predicted values of  $M_c$  agreed well with values estimated by experiment. Later, Selby and Miller (17) studied the Epon 828/MDA system extensively, with emphasis on the effect of stoichiometry on fracture toughness. Since this combination of studies provided excellent background in fracture behavior as well as other properties, the Epon 828-MDA system was selected as a standard of reference for this study.

At the time this program was begun, another advantage of this system appeared to be the absence of gross heterogeneity of the type reported for other systems (2,8,22,23). Selby and Miller (17) found craters and hillocks (of the order of  $\mu m$  in size) on etched surfaces, but small-angle X-ray studies revealed no evidence for a two-phase structure in the 50Å to 100Å size range, and no relationship between the large morphological features and fracture behavior was observed. However, since then increasing evidence has been produced by Selby et. al. (17,26) Morgan and O'Neal (24), and Racich and Kautsky (25) confirming the existence of heterogeneities of various sizes. In fact, as will be discussed

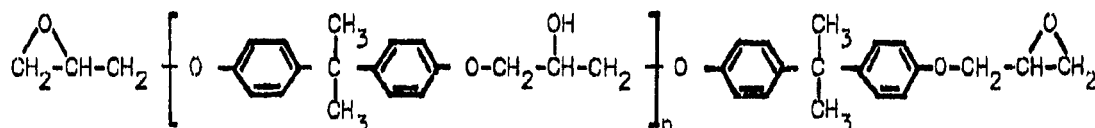
In section VIII, a complex morphology exists for the resins described herein. Thus, even with carefully prepared epoxy specimens, inhomogeneities exist, presumably reflecting non-optimum cosolubility of reactants or curing (59). In any case, with careful techniques, it should be possible to prepare resins which are reproducible in their morphology and properties, and to use these as standards of reference.

For initial study, several series of epoxies were prepared based on the Epon 828-MDA reference resin. Systems include blends to achieve equal equivalent weights but different distributions of molecular weight (and  $M_c$ ), and also homopolymers of varying molecular weight to provide additional standards for comparison. Characteristics of those and related resins are described in sections A-a and A-b, and procedures and results in section B.

#### A. Structure and Stoichiometry

##### a. Structure of Epoxies:

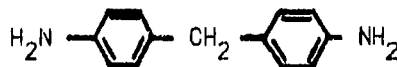
The epoxy prepolymers used in this study all have the following general structure:



where n varies from 0 to 24.

As supplied commercially, a distribution of composition usually exists. Indeed, it is possible to obtain only two prepolymers which have relatively narrow distributions of molecular weight and hence equivalent weight: Epon 825 (Shell Chemical Company) and Epi-Res 509 (Celanese Coatings Company). As will be described later, this fact along with requirements of curing restricts the control over heterogeneity in molecular weight  $M$  (and hence in  $M_c$ ) which can be achieved in blends.

The curing agents are available in several forms and purities, the essential component being methylene dianiline (MDA), also called p,p'-diaminophenyl methane (DDM):



The nominal characteristics (as supplied by the manufacturers) of the epoxy prepolymers are given in Table 2.

Table 2. Characteristics of Epoxy Prepolymers.

Prepolymer	Equivalent wt, g/eq	Composition, wt%		
		n=0	n=1	n=2-8
Epon 825	176	100	-	-
Epon 828	190	75	25	-
Epirez 520-C <sup>a</sup>	475	-	-	-
Epon 1001 <sup>a</sup>	500	11	16	72
Epirez 522-C <sup>a</sup>	600	-	-	-
Epon 1002 <sup>a</sup>	650	-	-	-
Epon 1004 <sup>a</sup>	938	-	-	-

<sup>a</sup> Solid at room temperature.

Confirmation of the distributions will require the use of gel permeation chromatography; this characterization was accomplished on the materials used in this study.

#### b. Stoichiometry and $M_c$ :

For estimation of  $M_c$ , the calculations of Bell (47) may be employed. Bell developed equations for  $M_c$  based on the stoichiometry of the curing reaction and the amount of primary amine and epoxy groups remaining in the polymer at a given time. Since calculated values were shown to agree well with values estimated from measurements of swelling and the polymer solvent-interaction term  $\chi$  (equation 1), the calculations seemed reasonable.

With curing conditions used in Bell's and this study, several idealized structures may be expected, depending on the stoichiometry (Fig. 11). In principle, the epoxy prepolymer is difunctional and the amine tetrafunctional so that under conditions of equivalence of functional groups, the following reaction will occur:

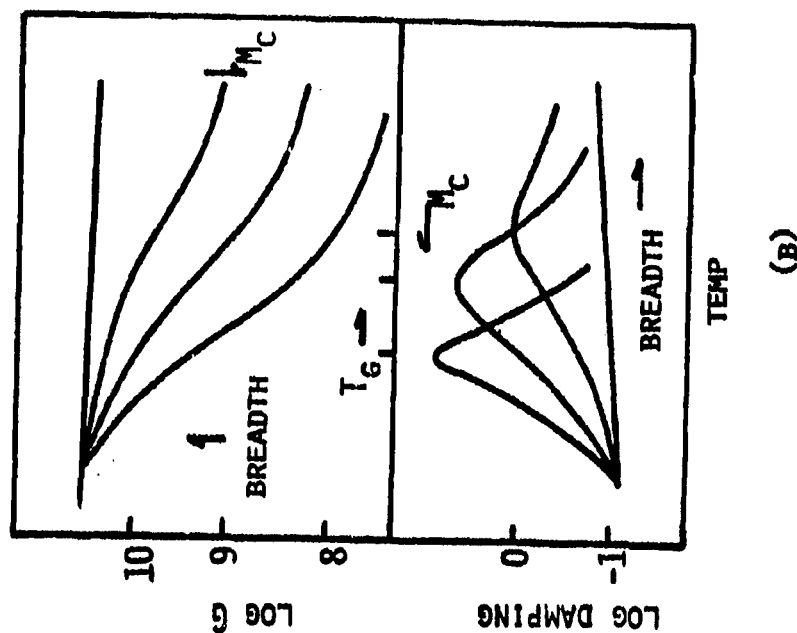
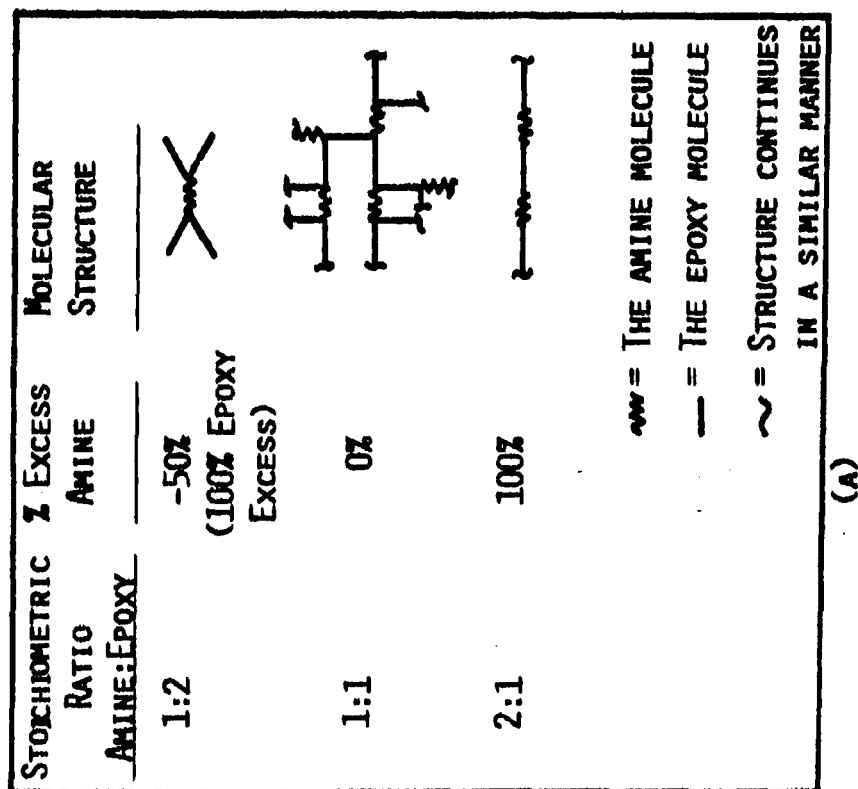
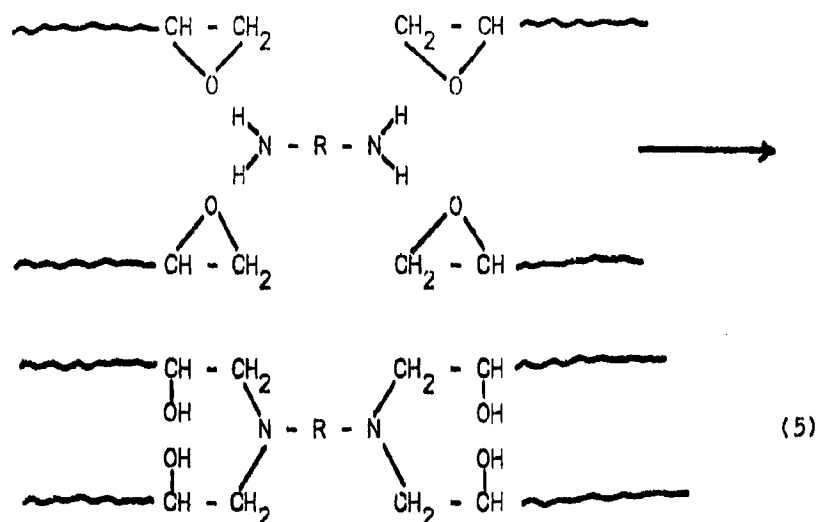


FIGURE 11. SCHEMATA SHOWING (A) EFFECTS OF CROSSLINKING STOICHIOMETRY ON MOLECULAR STRUCTURE, AND (B) EFFECTS OF CROSSLINKING ON MODULUS-TEMPERATURE BEHAVIOR.



At other stoichiometries, structures can be readily visualized by reference to Bell's paper.

Thus, with an amine/epoxy ratio of 2:1 (Fig. 11) enough primary amine groups are present to theoretically reaction with all epoxy groups and yield linear chains. In fact, as shown by Bell (47), however, some primary amine groups may remain after secondary groups have reacted, thus yielding some crosslinks. In this case, the effective  $M_c$  is given by (48)

$$M_c = \frac{aM_A + bM_B - (X+E)\{aM_A + bM_B\}/[3/2(2a-Y) + (X+2)]}{3/2(2a-X - Y) - (3/2(X+E))} \quad (6)$$

where:  $a$  and  $b$  are the number of moles of amine and epoxy, respectively;  $M_A$  and  $M_B$  are the molecular weights of the amine and epoxy, respectively; and  $X$  and  $Y$  are the numbers of unreacted primary and secondary amine groups, respectively. Since the concentration of unreacted epoxy groups,  $E$ , is equal to  $2b-4a+2X+Y$ , analysis of  $X$  and  $E$  gives  $Y$  (48). After analysis, Bell was then able to estimate  $M_c$ . From his tabulated data, a value of about 1500 may be estimated.

If, on the other hand, the structure were in fact linear, and conversion complete,  $M_c$  would in effect become the number average molecular weight  $M_n$  as given by

$$M_n = \frac{aM_A + bM_B}{a - b} \quad (7)$$

Using this equation, one would have a value for  $M_n$  of  $\infty$ . In reality, conversion of precisely all the functional groups is not complete; even a minuscule decrease from 100 percent conversion will yield finite molecular

weights. Hence the significance of calculated values for  $M_C$  or  $M_n$  is questionable unless very accurate analytical data on the concentration of residual functional groups is available.

For the case of equal stoichiometry, when  $b=2a$  (Fig. 11),  $M_C$  is given by

$$M_C = (aM_A + bM_B)/3(b-a) \quad (8)$$

when the amine is slightly in excess, equation 6 may be used as well.

When epoxy is up to about 20 percent in excess,  $M_C$  is given by

$$M_C = [aM_A - (b - 4a)M_B]/[3a - 3/2(2b - 4a)] \quad (9)$$

which allows for the presence of not more than one dangling end per branch point. The idealized structure will consist of an amine molecule with epoxy branches.

## B. Experimental Details, Results, and Discussion

As mentioned above, several series of unblended and blended epoxies were prepared. General procedures described by Bell (47) and Manson and Chiu (49,50) were followed for systems using liquid epoxies, depending on the system; variations were necessary in the case of solid epoxies. Resins were prepared in two thicknesses: 0.25 in. (6.35 mm) for fracture studies, and 0.020 in. (0.51 mm) for measurement of dynamic mechanical and other properties. Materials, procedures, and general results are discussed below.

### a. Materials:

The epoxy resins used were all diglycidyl ethers of bisphenol-A oligomers: Epon series 825, 828, 1001, and 1004 (Shell Chemical Company); and Epirez series 520-C and 522-C (Celanese Coatings Company). Of these prepolymers, Epon 1001 and 1004, and Epirez 520-C and 522-C were solids at room temperature. The curing agent used in most syntheses was methylene dianiline (MDA), obtained in the form of Torox (Shell Chemical Company) and 99%-pure MDA (Aldrich Chemical Company). In a few cases, the following polyamides were used as curing agents: Versamids 115 and 140 (General Mills Chemicals, Inc.). In the latter case, phenylglycidyl ether (Shell Chemical Company) was used as a reactive diluent. All resins of a given type were taken from a given batch; equivalent weights were used as supplied by the manufacturers.

### b. Preparation and Curing:

The various procedures for preparation and curing are summarized below. Compositions are given in following sections:

1. The general procedure for systems using liquid epoxy prepolymers with MDA as the curing agent was similar to that used by Bell (47). Following prior heating to 60°C, the resin and curing agent were evacuated for 5-15 min to remove bubbles, mixed, cast, and cured as follows: 45 min in a circulating oven at 60°C; 30 min at 80°C, and 2.5 hrs at 150°C; slow cooling to room temperature. The mold assemblies comprised clamped 5-in by 5-in glass plates separated by 0.02-in (0.51 mm) or 0.25-in (6.35 mm) ethylene-propylene copolymer or teflon spacers. Both Mold Release 223 (Ram Chemical Company) and Epoxy ParFilm (Price Driscoll Company) were used successfully as mold release agents; sheets of Mylar were also effective. With care, clear, yellowish to brown specimens were obtained from which bubble-free sections could be cut.

The cure cycle used was reported by Bell to give essentially complete curing (47) - a conclusion supported by data presented in section VI. Somewhat higher temperatures were used by Selby and Miller (17), but the effect of curing temperature as a variable was not examined in this study beyond completion of a few exploratory castings which did not yield consistent results.

In order to check on the efficacy of mixing (in case the multi-phase morphologies noted were due to poor mixing), some castings were made from solution in acetone.

2. Solid epoxy resins were first melted and then evacuated to remove any air bubbles. The curing agent was mixed in under vacuum, using a magnetic stirrer in order to avoid air entrapment. Thick and thin films were cast and cured using the following curing cycle; 1.5 hrs at 100°C and 2.5 hrs at 150°C. Later the samples were cooled slowly to room temperature.

3. For Versamid-cured systems the procedure developed by Manson and Chiu (49,50) was followed. First 6 percent by weight (based on the total mix) of phenyl glycidyl ether was mixed with the epoxy prior to addition of the polyamide in order to reduce viscosity and thus facilitate mixing and removal of bubbles. The epoxy resin was heated to 40°C, and evacuated in a vacuum oven to remove absorbed air and moisture. After the curing agent is heated to 40°C and added to the resin, the total mixture then evacuated for about 5 min. Sheets of samples were formed by use of the mold assemblies described in section b-1.

Details follow for the various series made.

c. Series A (varied stoichiometry):

This series (with MDA as curing agent) was prepared to provide a standard for comparison with other specimens prepared in this study and with the literature. Table 3 gives the compositions, on the basis of equivalent weights (based in turn on specifications supplied by the

manufacturer). Theoretical values of  $M_c$ , as calculated by equations 6 to 9, are given in Table 3, along with compositions.

Table 3. Compositions of Series A Epoxy Resins.

<u>Designation</u>	<u>Amine/Epoxy Ratio<sup>a</sup></u>	<u><math>M_c</math> (theoretical)<sup>b</sup></u>
A-7	0.7 : 1	1523
A-8	0.8 : 1	526
A-9	0.9 : 1	383
A-10	1.0 : 1	326
A-10A	1.0 : 1	326
A-11	1.1 : 1	370
A-12	1.2 : 1	415
A-14	1.4 : 1	597
A-16	1.6 : 1	924
A-18	1.8 : 1	1922
A-20	2.0 : 1	$\infty$ (Linear)
A-22	2.2 : 1	---

<sup>a</sup> All are based on the use of Shell Tonox curing agent, except for the A-10A case, for which 99% MDA was used.

<sup>b</sup> For reasons discussed by Bell (47) actual  $M_c$  values for specimens A-16 to A-20 may be in error. In any case, the error will not affect any trends observed in properties as a function of stoichiometry.

Thus this series provides resins covering a wide range in composition, ranging in amine excess from -30 percent to +100 percent.

d. Series B (blends at equal  $M_c$ ):

For this series, various resins were blended to achieve an epoxy equivalent weight of 190 g/eq (equivalent to that of Epon 828, and to a value for of 326). Stoichiometric amounts of MDA were used in all cases. Details are given in Table 4, which also includes data on the blending resins themselves. As may be seen, the breadth of the distribution of  $M_c$  achieved was necessarily limited.

Table 4. Compositions of Series B (Blends) Epoxy Resins.

Designation	wt % of					wt %		
	Epirez 522-C	Epon 1001	Epirez 502-C	Epon 828	Epon 825	n=0	n=1	n=2-8
B-1	-	11.4	-	-	88.6	89.9	1.8	8.3
B-2	-	10.3	-	9.6	80.1	88.4	4.1	7.5
B-3	10.0	-	-	-	90.0	-	-	-
B-4	-	-	11.8	-	88.2	-	-	-
B-5 <sup>a</sup>	-	-	-	100	-	75	25	-
B-6	-	5.7	-	50.0	44.3	82.4	13.4	4.2
B-7	-	2.3	-	80.0	17.7	-	-	-

<sup>a</sup>Control resin.

e. Series C (equal  $M_c$  but different stoichiometry):

In order to determine whether or not behavior at a given  $M_c$  depends on whether or not stoichiometry is 1:1, series C was made (51). However, since series A proved to be adequate for this purpose, no further work was done with series C.

f. Series D (Versamid Resins):

Details of these resins are given in the previous report (51). As mentioned, no work was done with this series during this report period. Several resins were prepared from Epon 828 using polyamide curing agent, Versamids 115 and 140. It seemed undesirable to examine effects of distribution in  $M_c$  using Versamid-based resins, which are softer, tougher, and typical of adhesives and coatings rather than rigid, high-T<sub>g</sub> resins. However, in view of considerable experience at Lehigh with such resins (49-51), and because such resins were expected to be easier to handle than the brittle MDA-cured ones, several specimens were cured (51). During this report period, resins based on stoichiometric ratios of Versamid-140 and Epon 825 and 828 were used.

Compositions are given in Table 5.

Table 5. Compositions of Series D (Versamid-cured) Epoxy Resins.

Designation	Relative Amine/Epoxy Proportions				
	Epon 825	Epon 828	Epon 1001	V-115 <sup>a</sup>	V-140 <sup>a</sup>
D-1	-	-	1.0	1.0	-
D-2	-	1.0	-	-	1.0
D-3	1.0	-	-	-	1.0

<sup>a</sup> Amine equivalent weights are: V-115 and V-140, 238 and 385 g/eq, respectively.

g. Series E (Unblended Resins, equal Stoichiometry):

To provide a baseline for examining the effects of  $M_c$  at constant stoichiometry, resins based on the following prepolymers were synthesized using stoichiometric amounts of MDA as curing agent: Epon 825, 828, 834, 1001, 1002, and 1004 (see Table 6).

Table 6. Composition of Series E (Unblended, as-is) Epoxy Resins.

Designation	Epon Prepolymer	Epoxy Equivalent	Theoretical $M_c$
E-1	825	176	308
E-2	828	190	326
E-3	834	271	430
E-4 <sup>a</sup>	834	271	493
E-5	1001	500	740
E-6	1002	680	980
E-7	1004	998	1400

<sup>a</sup> Inadvertent deviation from precise stoichiometry.

Of these, Epon 825 has a narrow distribution of molecular weight, while the others have fairly broad distributions. Also E-4 contained a slight excess of amine (amine/epoxy ratio  $\sim 1.1$ ).

b. Series F (Bimodal-distribution Blends):

In order to broaden the distribution of  $M_c$  beyond the range characteristic of Series B, it was necessary to move to values of  $M_c$  which differed from the value of 326 (Epon 828). It was possible to vary the distribution of  $M_c$  by making resins which had the same average  $M_c$  values as Epon 828, Epon 834, and Epon 1001. This was done by blending a Epon 825 (narrow distribution of molecular weight) with Epon 1004. Distributions of  $M_c$  may be expected to be essentially bimodal, with little overlap. Details are given in Table 7.

Table 7. Bimodal Distribution Epoxies.

Sample Designation	Epoxy Equivalent	$M_c$	wt % Epon 825 In Blend <sup>a</sup>
F-1	190	326	91.0
F-2	255	413	61.9
F-3	260.5	419	60.0
F-4	271	430	56.9
F-5	500	740	20.2

<sup>a</sup>Blend with Epon 1004. F-1, F-4, and F-5 are equivalents of Epons 828, 834, and 1001, respectively.

1. Discussion

Using the techniques described, it was possible to prepare specimens suitable for testing, albeit with considerable difficulty in the case of the solid epoxies. Reproducibility of casts appears to be reasonable (see section VI).

With respect to the blends, it is clear that there are limits on the number of blends that can be prepared from resins which themselves have a distribution.

## SECTION VI

### GENERAL CHARACTERIZATION OF EPOXY NETWORKS

#### A. Introduction

A principal aim in the epoxy portion of the program is to study effects of network structure on ultimate properties such as strength, toughness, and fatigue resistance, as well as on behavior at small-deformation such as creep or stress relaxation. Adequate correlation requires thorough characterization of the polymers concerned - an ideal procedure all-too-often unrealized in practice.

Some studies in the literature have been concerned with several aspects of behavior, for example, tensile strength as a function of  $M_c$  (7,46) in epoxies rather well characterized in terms of dynamic mechanical behavior. Other studies, for example of fracture toughness and fatigue have not included such characterization, and sometimes the epoxies themselves are not specified (60-63). It was therefore decided to establish a standard series of well-characterized polymers against which specimens having varying distributions of  $M_c$  and other network characteristics could be compared.

Parameters of particular interest are the crosslink density as expressed by  $M_c$ , which also reflects the degree of cure, and the viscoelastic behavior, which reflects the segmental mobility and energy dissipation characteristics. In particular, viscoelastic response is often sensitive to differences in network structure. Microscopic examination is also important, to verify the presence or absence of a two-phase morphology (see section VIII).

This section describes the characterization of the resins discussed in section V.

#### a. Crosslink Density:

The degree of cure and crosslink can be analyzed in several ways, the two most common involving determination of swelling (and sol-gel ratio) and modulus in the rubbery state. While, as will be seen, absolute values may not be obtained in densely crosslinked systems, values still give an excellent indication of relative network characteristics.

Thus Whiting and Kline (7) showed that the swelling of epoxy-amine-diluent systems was very sensitive to the nature of the network; the measurements were used to indicate relative values of  $M_c$ . Values of  $M_c$  can also be estimated from swelling using the Flory-Rehner equation

(equation 1). Use of this or modified empirical equations (2) has had some success with epoxy resins (7,47); in any case, the values can be correlated with values derived from mechanical tests. In principle, distribution functions can be estimated for  $M_c$  from measurements of swelling as a function of pressure; in practice, this is difficult (2).

Values of  $M_c$  can also be determined from moduli measured by dynamic mechanical spectroscopy using a Rheovibron or similar unit. Although the kinetic theory of rubber elasticity (equation 2) is not valid for highly crosslinked systems, an approximation (2) may be useful (equation 10):

$$\log G \approx 7.0 + 293 \rho/M_c \quad (10)$$

where  $G$  is the shear modulus,  $\rho$  the density, and  $M_c$  the average molecular weight between crosslinks. For convenience,  $\rho$  was taken to equal unity; true values ranged up to  $\sim 1.2$  so that true  $M_c$  values may be up to 20% higher than estimated below. In our experience (49,50), equation 2 held well for several epoxy resins (cured with polyamides), yielding values of  $M_c$  in excellent agreement with prediction; equation 10 may be better when the rubbery modulus is greater than, say,  $10^8$  dyn/cm<sup>2</sup>. Values of  $M_c$  have also been estimated from the elevation of the glass transition temperature,  $T_g$ , by crosslinking (2,6):

$$M_c = \frac{3.9 \times 10^4}{T_g - T_{g0}} \quad (11)$$

where  $T_{g0}$  is the transition temperature of uncrosslinked polymer (made by incompletely curing an epoxy-amine mixture).

As discussed below, values of  $M_c$  based on measurement of  $G$  were concluded to be most reliable and were, therefore, usually used for comparison.

#### b. Effects of Crosslinking and Network Structure:

Crosslinking profoundly affects the viscoelastic behavior of polymers: the  $T_g$ , the damping (as measured by  $\tan \delta$  or  $E''$ ), and the slope of the glass transition (2,6,7). In addition, crosslinking affects the characteristics of the next loss peak appearing as one lowers the temperature from  $T_g$  - a peak often called the " $\beta$ " peak, as distinct from the " $\alpha$ " peak corresponding to the  $T_g$  (18). Some changes are shown in Fig. 11.

As  $M_c$  decreases (and crosslink density increases)  $T_g$  shifts to higher temperatures, and at very low values (densely crosslinked systems

such as phenolic resins) may disappear altogether. Also the damping peak is broadened and flattened as crosslink density increases, the maximum occurring when stoichiometry is optimum. Effects of stoichiometry and diluents are readily observed (1,6,7). The distribution of crosslinks is believed to be in large part responsible for the noticeable broadening of the glass transition as  $M_c$  decreases (1, chapter 4); this effect is also seen with crystallinity. Presumably a spread in crosslink distribution (or crystallinity) may result in a spread in relaxation times and hence slope of the transition.

Stress relaxation and creep are also sensitive to network characteristics (2) though most scientific work on characterized specimens appears to have been concerned with rubbers. In general, creep of highly crosslinked systems in the glassy state is very slow, probably lower at high loads, long times, and temperatures just below  $T_g$  than for less crosslinked systems (2). The stress relaxation technique (which is essentially equivalent to the inverse of a creep test) can often reveal long-time effects, when coordinated long range molecular motions or disentanglements first become important. Each type of test has been used successfully to predict the modulus of epoxies at long times (63); correlations using time-temperature superposition principles (25) in the form of master curves is feasible.

#### B. Experimental Details, Results, and Discussion

This section updates and revises results reported previously for swelling and dynamic mechanical spectroscopy (51). New results obtained from torsional creep studies are also presented and discussed.

##### a. Swelling:

Details were described in the last report (51); see Figs. 12 and 13. It was found that results for series A agreed with those obtained by Bell (47), and gave a minimum at an amine/epoxy ratio close to the stoichiometric value. However, as noted by Whiting and Kline (7), absolute values were difficult to reproduce. For this reason, further studies were confined to measurement of a simple swelling ration,  $q'$ , measured by immersion in acetone for 15 days and defined by

$$q' = \frac{\text{swollen wt} - \text{dry wt}}{\text{dry wt}} \quad (12)$$

Since the density of specimens changes very little as a function of stoichiometry (7), this relationship should suffice to show up any significant effects of, for example,  $M_c$  distribution.

In the earlier work (51), it was reported that series B (blended) resins exhibited swelling behavior similar to that of controls. In this part of the study (see Tables 8 and 9), values of  $q'$  were obtained for

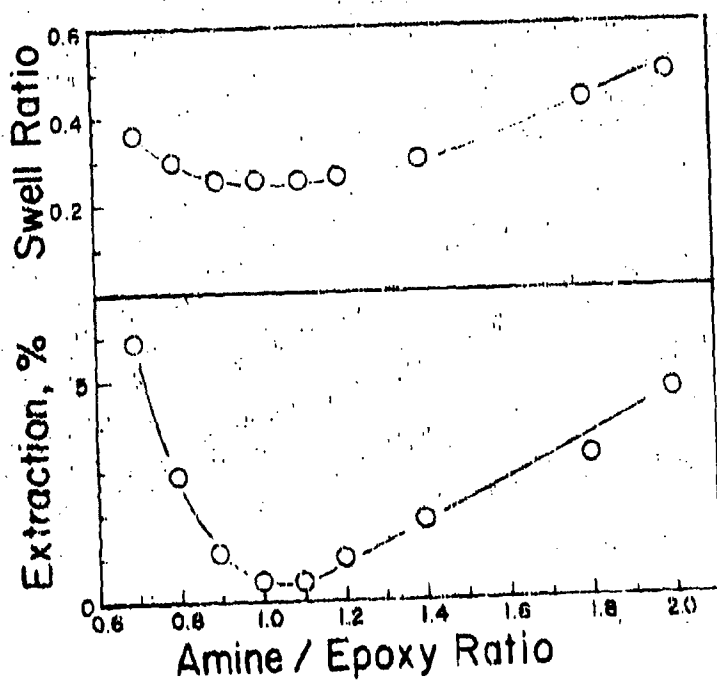


Fig. 12. Swelling data of Series A epoxy resins as function of amine/epoxy ratio.

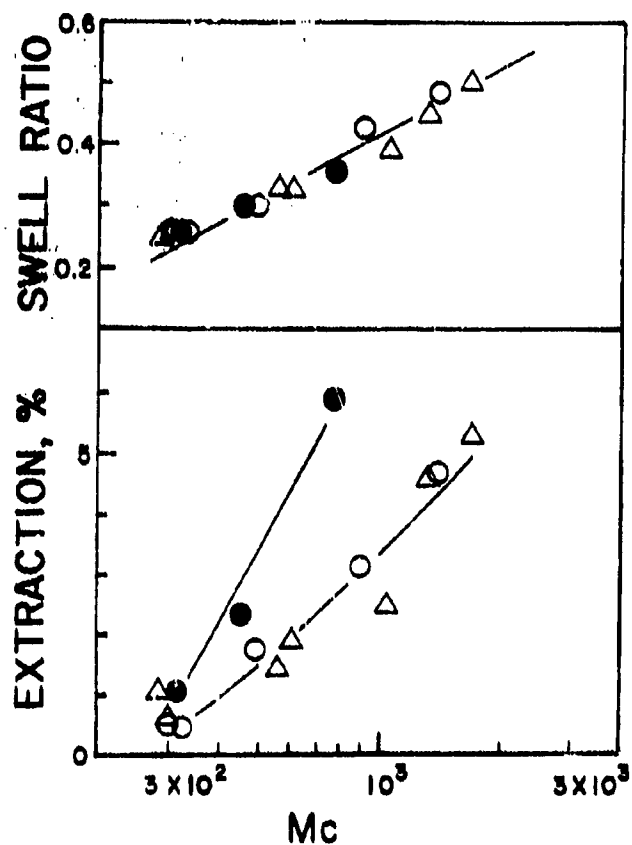


Fig. 13. Swelling data as function of  $M_c$ : closed circle, epoxy excess in Series A; open circle, amine excess in Series A; and triangle, Series E.

Table 8. Swelling and Extraction of Series E Epoxies.

Sample	$M_c^a$	% extraction			swelling ratio, $q'$		
		a	b	avg.	a	b	avg.
E-1	308	0.98?	1.23	1.11	0.25	0.25	0.25
E-2	326	0.67	0.55	0.61	.26	.26	.26
E-3	430	1.96	1.96	1.96	.31	.31	.31
E-4	493	1.49	1.31	1.40	.31	.31	.31
E-5	740	2.51	2.56	2.54	.40	.38	.39
E-6	980	4.56	4.80	4.68	.46	.45	.45
E-7	1400	5.45	5.11	5.28	.49	.51	.50

<sup>a</sup>Theoretical value.

Table 9. Swelling and Extraction of Series F Epoxies (Bimodal Blends).

Sample	$M_c^a$	% extraction			swelling ratio, $q'$		
		a	b	avg.	a	b	avg.
F-1	326	0.46	0.37	0.42	0.26	0.25	0.25
F-2	413	1.48	1.38	1.43	.27	.27	.27
F-3	419	0.46	0.52	0.49	.29	.29	.
F-4	430	2.05	1.81	1.93	.31	.31	.31
F-5	740	2.39	2.72	2.56	.39	.39	.39

<sup>a</sup>Theoretical value.

series E and F resins (epoxies of varying molecular weight and bimodal blends, respectively) and plotted against  $M_c$  calculated theoretically, assuming a 1:1 amine/epoxy ratio and complete reaction. As seen in Fig. 14, the bimodal-blends deviate from the control curve when  $330 < M_c < 430$ . (While the effect is small, similar deviations are found for other properties - see below.) On the other hand, while the % extracted rose steadily with  $M_c$ , the broad-distribution samples behaved like the base resins in this respect.

#### b. Crosslink Density:

In order to correct apparent  $M_c$  values calculated by equations 7 and 9, values of residual primary amine and epoxy groups were determined by titration using the methods described by Bell (46). Results (Table 10), which agreed well with those quoted by Bell (46), confirmed that cure was essentially complete, at least for amine/epoxy ratios between 1/1 and 2/1. However, values for residual epoxy were consistently low and improbably values of  $M_c$  were obtained when correction of  $M_c$  values for incomplete networks was attempted. For A-20, it was impossible to calculate  $M_c$  from Bell's equation (48) and these chemical analysis data. In fact, more reasonable value [ $M_c$  (calc)] was found by using a simpler equation given by Bell (46), which had been printed incorrectly.

Table 10. Residual Functional Groups in Series A Epoxies and Corrected  $M_c$ .

Specimen	Epoxy Content mole/mole of epoxy	Primary Amine Content mole/mole of epoxy	Secondary Amine Content mole/mole of epoxy	$M_c$	
				Uncorrected	Corrected
A-7	0.228	n <sup>a</sup>	n	1523	509
A-8	0.136	n	n	526	411
A-9	0.067	n	n	383	356
A-10	n	n	n	326	326
A-10A	0.037	n	0.037	326	331
A-11	n	n	0.2	370	362
A-14	n	n	0.8	592	526
A-16	n	0.045	1.15	924	829
A-18	n	0.066	1.47	1922	1571
A-20	n	0.099	1.80	∞	b

<sup>a</sup> n = not detected.

<sup>b</sup> Impossible to calculate using Bell's new equation and analysis data.

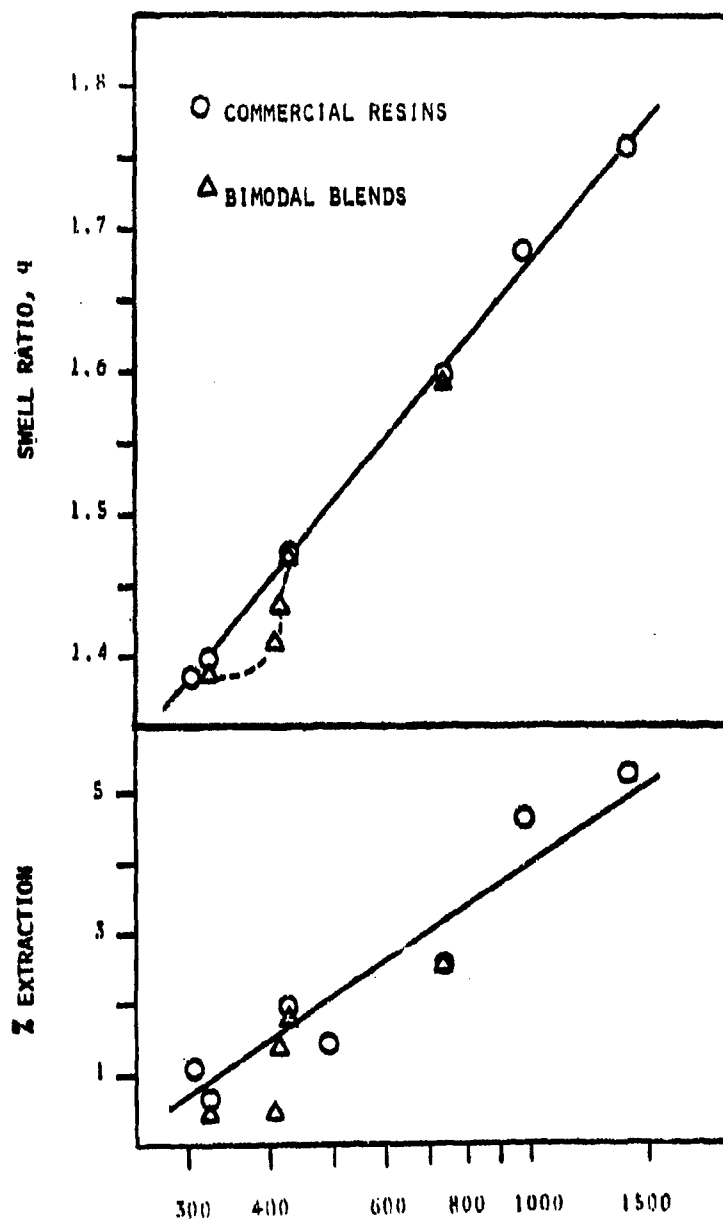


Figure 14. Swelling of series E and series F epoxies (bimodal blends) as a function of  $M_c$  (theor.).

For this reason, it was decided to estimate  $M_c$  from values for rubbery modulus,  $E_r'$  (equation 2). Since values of  $E_r'$  were not greater than 10 MPa, it was thought that equation 2 should be valid. Also, a plot of  $M_c$  (from  $E_r'$ ) against  $M_c$  (calc) gave a smooth curve (Fig. 15). Thus, values of  $M_c$  should reflect reality qualitatively and fairly quantitatively as well.

Values of  $M_c$  estimated from  $E_r'$  are given for series A in Table 11, along with values calculated from equations 2, 10 and 11. Tables 12 and 13 give data for series E and series F. Since in these cases, several values estimated from  $E_r'$  fell off the curves of  $M_c$  (from  $E_r'$ ) vs  $M_c$  (theor), values of  $M_c$  ( $E_r'$ ) were obtained from the appropriate calibration curve.

Table 11. Values of  $M_c$  for Series A Epoxy Resins.

Specimen	from $E_r'^a$		from $T_g$ shift <sup>b</sup>	
	from equation 2	from equation 10	DSC	Vibron
A-7	721 (780) <sup>c</sup>	412	1114	1258
A-8	457	313	650	639
A-9	314	259	453	406
A-10	303	256	411	402
A-10A	305-300	257-255	-	429-402
A-11	328	265	459	438
A-12	-	-	500	-
A-14	496	324	696	619
A-16	821 (620) <sup>c</sup>	442	1026	975
A-18	896	473	1345	1114
A-20	1381	706	1444	2167

<sup>a</sup> Density,  $\rho$ , assumed to be 1.

<sup>b</sup> From equation .  $T_g$ 's from DSC and Rheovibron measurements were plotted against  $M_c$  values of <sup>c</sup>column of this table;  $T_{g0}$ 's were thus estimated to be 340 °K and 374 °K, respectively.

<sup>c</sup> Corrected using calibration curve.

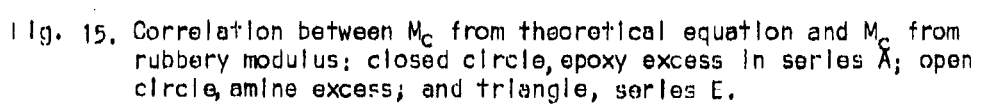


Table 12. Values of  $M_c$  for Series E Epoxy Resins.

Specimen	From $E_r^a$ , equation 2	Theoretical, equation 8
E-1	288 (308) <sup>b</sup>	308
E-2	303 (326) <sup>b</sup>	326
E-3	701 (550) <sup>b</sup>	430
E-4	568 (660) <sup>b</sup>	493
E-5	1140	740
E-6	1310	980
E-7	1680	1400

<sup>a</sup> Density assumed to be 1.

<sup>b</sup> Corrected using calibration curve.

Table 13. Values of  $M_c$  for Series F Epoxy Resins.

Specimen	From $E_r^a$ , equation 2	Theoretical, equation 8
F-1	303 (326) <sup>b</sup>	326
F-2	570 (510) <sup>b</sup>	413
F-3	700 (520) <sup>b</sup>	419
F-4	706 (550) <sup>b</sup>	430
F-5	1146	740

<sup>a</sup> Density assumed to be 1.

<sup>b</sup> Corrected using calibration curve, series E.

c. Dynamic Mechanical Spectroscopy:

Measurements of complex Young's moduli (1) were made using a Rheovibron viscoelastometer, model DDV-11, (Toyo Measuring Instrument Company). The instrument applies a sinusoidal tensile strain to one end of a sample, and measures the stress sensed at the other end. Transducers permit the reading of the absolute dynamic modulus  $|E^*|$  (the ratio of maximum stress to maximum strain) and the phase angle  $\delta$  between the strain and the stress. The storage modulus,  $E'$ , the loss modulus,  $E''$ , and the dissipation factor,  $\tan \delta$ , are given as follows:

$$\begin{aligned} E' &= |E^*| \cos \delta \\ E'' &= |E^*| \sin \delta \\ \tan \delta &= E''/E' \end{aligned} \quad (13)$$

$E''$  and  $\tan \delta$  are measures of the energy dissipated irreversibly, and  $E'$  a measure of the energy stored reversibly.

The experimental procedure was as follows. Thin strips (1x2 mm) were cut out carefully from 0.5mm in sheets and polished well along the edges using fine sandpaper. Heating to above  $T_g$  prior to cutting helped minimize shattering of the more brittle specimens. Measurements were made at 110 Hz and a heating rate of 1°C/min over a temperature range from -80°C to about 40°C above the  $T_g$ . Icing of the specimens at low temperature was avoided by sweeping dry nitrogen through the chamber.

The  $T_g$  and  $\beta$ -transition temperature were taken from the major and lower maxima, respectively, on the loss modulus ( $E''$ ) vs. temperature curves. The slope of  $\log E' (d \log E' / dT)$  at  $T_g$  was obtained in the region of  $T_g \pm 4^\circ\text{C}$ .

Typical original data are reproduced in Fig. 16 in order to show the kind of scatter encountered. Provided that care is taken to frequently recalibrate temperature readings and to allow for variations in the instrumental correction factor (K) as a function of specimen cross-sectional area, it is possible to obtain values of transition temperatures with a precision of about  $\pm 2^\circ\text{C}$ . However, reproducibility of absolute values of  $E$ ,  $E'$ , and  $\tan \delta$  in the glassy region is less good, variations of up to 40% being commonly observed.

1. Series A Epoxy Specimens (Variable Stoichiometry)

Three transitions are often evident in the dynamic spectra of epoxies, as one descends in temperature to about -80°C: one at high temperature, (the  $\alpha$  peak), one at a lower temperature, and one at a still lower temperature, at about -40°C to -50°C. The  $\alpha$ -peak is associated with the glass transition, while the lowest-temperature or  $\beta$ -peak is attributed

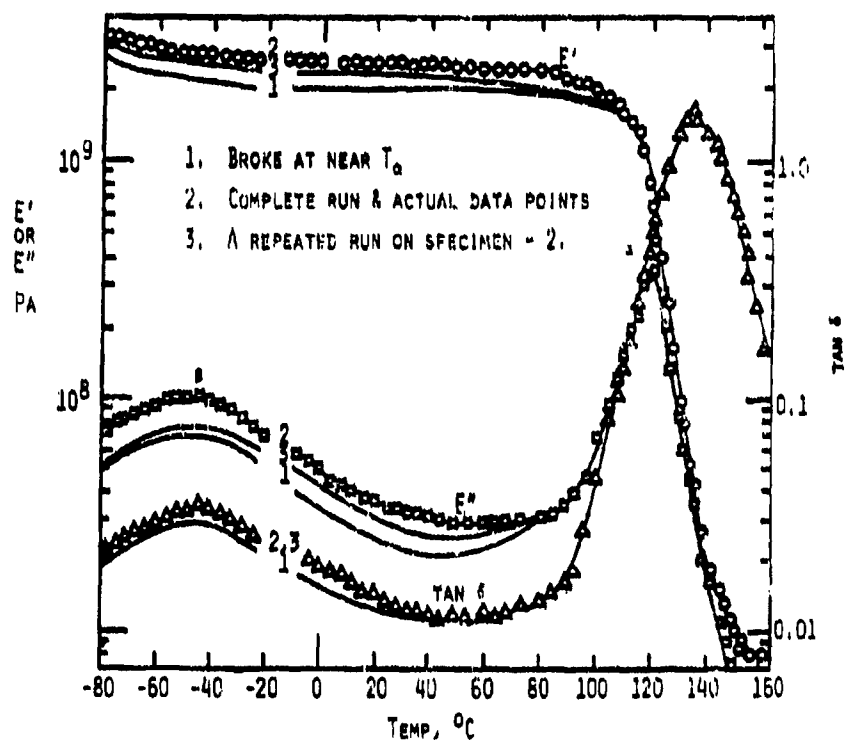


Figure 16. Dynamic mechanical data for A-20 epoxy resins,  
 $f = 110$  Hz.

to motions of the glycidyl group (19). The middle peak is an artefact associated with incomplete curing (8). It may also be noted that with one exception, no evidence for incomplete curing or a gross two-phase morphology is seen in the dynamic spectra, as has been noted in other studies (1,2,8); re-running of a specimen gives essentially the same curve as before.

Data are presented in Tables 14 and 15 and displayed in Figs. 17 to 20. (Note that some values reported previously (51) have been revised after reevaluation.) It may be seen that increased crosslinking raises the temperatures at which the  $\alpha$  and  $\beta$  transitions occur, as reported in other studies (6,7,18). Curiously, values of  $T_g$  are inexplicably high--higher than those noted by Bell (47) (even after allowance for the higher frequency used in this study) and higher than predicted based on the curing temperature (5). At present, no explanation in terms of temperature error or adiabatic heating is tenable.

Increased crosslinking also increases the value of the rubbery modulus,  $E'$  (from which  $M_c$  was estimated using the theory of rubber elasticity, equation 2) and decreases the slope of the  $\alpha$ -transition, in conformity with prediction (2). It is interesting that the slope is a function of stoichiometry only when the amine is in excess; the amine appears to sharpen the transition, perhaps by enhancing mobility of the chain segments. The maximum value of  $\tan \delta$  at the  $\alpha$ -transition is also decreased, as reported by Murayama and Bell (6) but is increased at the  $\beta$ -transition, as reported by Arridge and Speake (18) and Fogany (19).

When the dynamic parameters are plotted as a function of  $M_c$ , it is seen that most parameters are independent of which resin component is in excess. Some parameters (slope at  $T_g$  and  $\tan \delta$  value at  $T_g$ ) show different relationships with  $M_c$  depending on whether the amine or the epoxy is in excess. This behavior suggests that the networks must be different in the two cases. Specifically, since the  $\beta$  transition is attributed to the localized motion of the glycidyl group, it is not expected to be sensitive to network structure details. If the increase in  $T_g$  is due to tightening the network (by approaching stoichiometry), then the increase in  $\tan \delta_{\max}$  value seems inexplicable. However, contrary to our results, Fogany (19) and Arridge and Speake (18) observed  $T_g$  decreasing as more and more excess epoxy was added, and the amine excess did not affect  $T_g$  significantly (both with aliphatic amines).

## 2. Series B Epoxy Resins (Blends)

Data for this series are given in Table 16, see also Fig. 17. It may be seen that the blends comprising this series behave very much like the reference resins of series A.

Table 14. Dynamic Mechanical Data of Series A Epoxy Resins (Variable Stoichiometry).

Specimen	Amine/ Epoxy Ratio	$T_{\alpha}^a$	$T_{\beta}^a$	$d \log E'/dT$ at $T_{\alpha}(n)$ dyn/cm <sup>2</sup> -deg	$\tan \delta_{\max}$ ( $\alpha$ peak)		$E_r' \times 10^{-8}^b$ dyn/cm <sup>2</sup>
		°C	°C		Value	Temp. (°C)	
A-7	0.7	132	-62	0.050	1.10	148	1.54
A-8	0.8	162	-60	0.050	0.91	177	2.59
A-9	0.9	197	-50	0.038	0.72	213	4.05
A-10	1.0	198	-45	0.056	0.70	206	4.20
A-10A	1.0 <sup>c</sup>	192-198	-47	0.043-0.050	0.76-0.68	202-206	4.13-4.25
A-11	1.1	190	-52	0.056	0.82	201	3.82
A-14	1.4	164	-54	0.067	1.08	176	2.40
A-16	1.6	141	-56	0.077	1.25	153	1.38
A-18	1.8	136	-65	0.083	1.30	149	1.25
A-20	2.0	119	-68	0.083	1.60	133	0.78

<sup>a</sup> From maxima in  $E''$  vs. temperature curve.

<sup>b</sup> Storage modulus in rubbery state (at  $\geq T_g + 40$ ).

<sup>c</sup> Epon 828/99% MDA. This specimen was shown to have incomplete curing; first runs on new specimens gave  $T_{\alpha}=192$ ,  $n=0.050$  and repeated runs on the same specimen gave  $T_{\alpha}=198$ ,  $n=0.043$ , i.e., further curing during the test.

Table 15. Characteristics of the  $\beta$  Transition of Series A Epoxy Resins (Variable Stoichiometry).

Specimen	Amine/ Epoxy Ratio	$\tan \delta_{\max}$		Temp. of $E''_{\max}$ , °C
		Temp. °C	Value	
A-7	0.7	-58	0.051	-62
A-8	0.8	-54	0.058	-60
A-9	0.9	-42	0.063	-50
A-10	1.0	-40	0.068	-45
A-10A	1.0	-40	0.068	-47
A-11	1.1	-46	0.068	-52
A-14	1.4	-50	0.066	-54
A-16	1.6	-54	0.063	-56
A-18	1.8	-60	0.063	-65
A-20	2.0	-64	0.056	-68

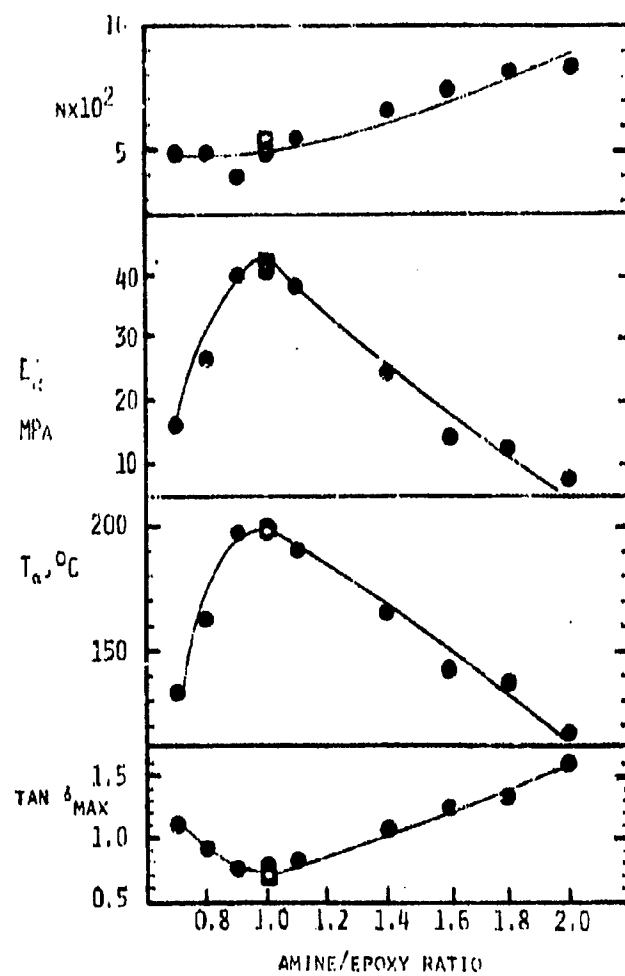


Fig. 17. Dynamic mechanical properties of Series A epoxy resins as functions of stoichiometry. Range of data also shown for Series B,  $\square$ .

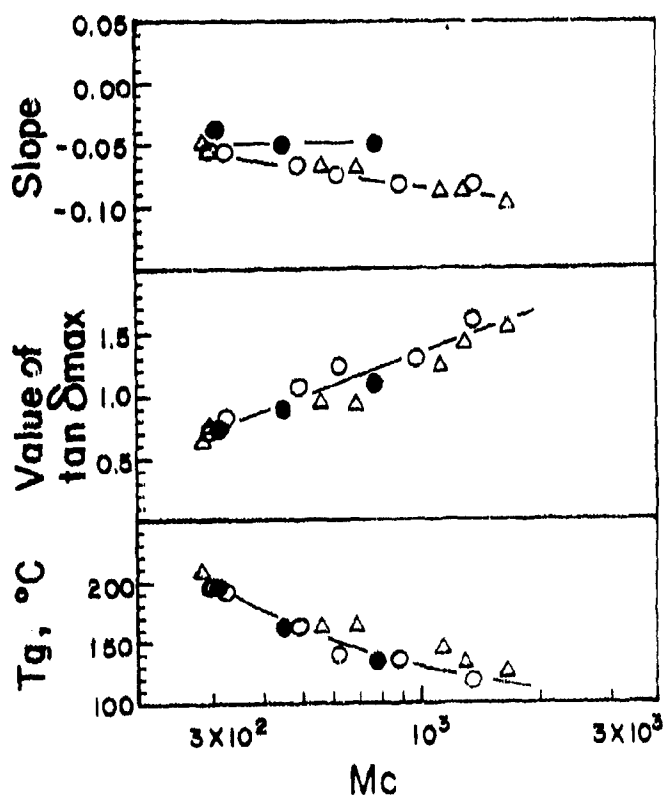


Fig. 18. Dynamic mechanical parameters at  $T_g$  as function of  $M_c$ ; closed circle, epoxy excess in Series A; open circle, amino excess in Series A; and triangle, Series E.

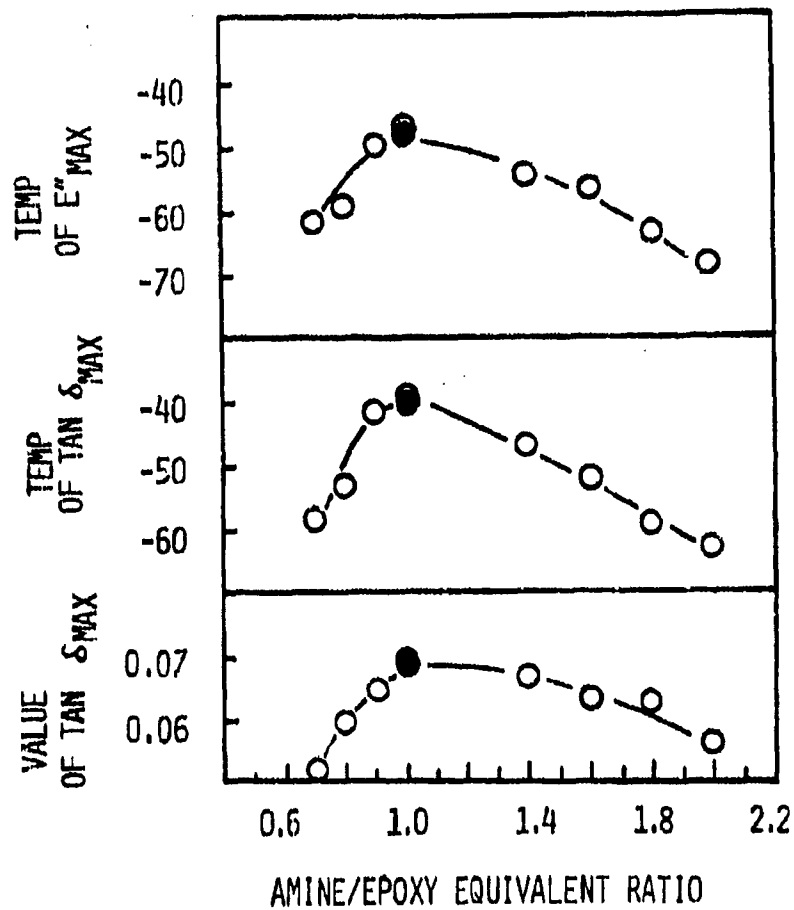


Fig. 19. Dynamic mechanical parameters at  $\beta$  transition vs. amine/epoxy equivalent ratio, Series A epoxy resins at 110 Hz.

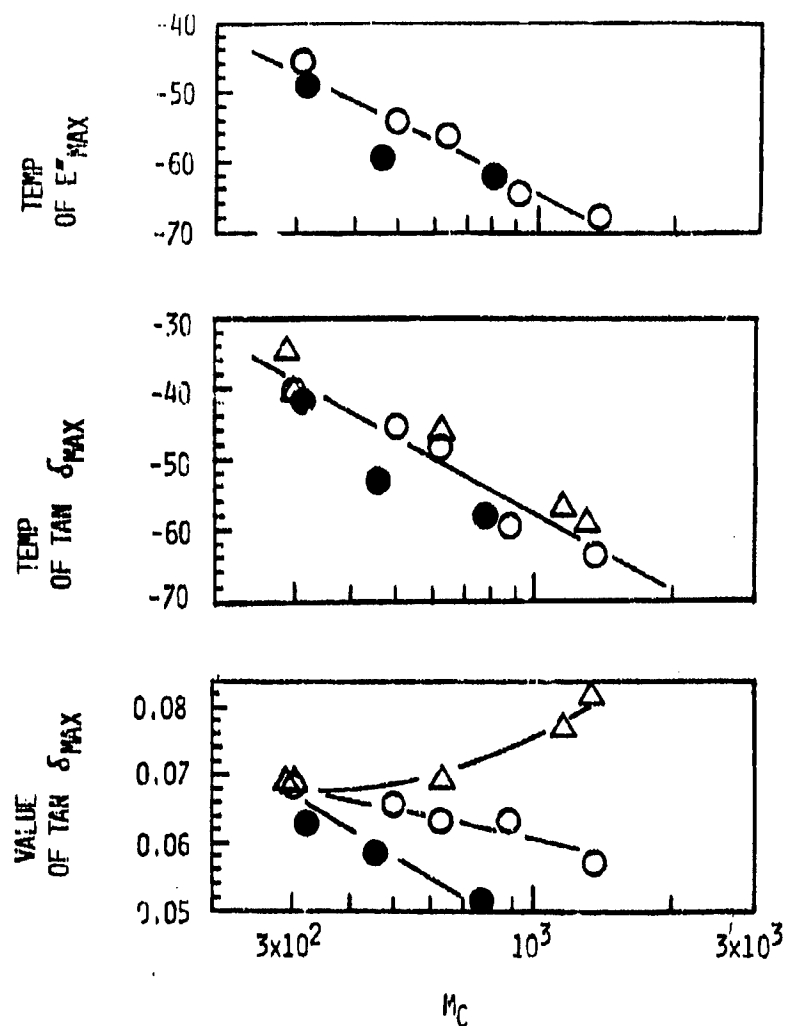


Fig. 20. Dynamic mechanical parameters at  $\beta$  transition as function of  $M_C$ : closed circle, epoxy excess in series A; open circle, amine excess in series A; triangle, series E.

Table 16. Dynamic Mechanical Data of Series B Epoxy Resins (Blends).<sup>a</sup>

Sample No.	$\tan \delta^c$ at $\beta$	$T_\beta$ , °C	$T_g$ , °C	$E_r'$ $\times 10^{-8}$ dyn/cm <sup>2</sup>	Slope ( $\underline{n}$ ) $\frac{d(\log E')}{dT}$
B-1	.048	-40	198	4.0	.050
B-2	.043	-38	198	4.0	.056
B-6	.028	-35	198	4.0	.055
B-5 <sup>b</sup>	.036	-45	198	4.0	.056
B-4	.038	-44	198	4.0	.050
B-3	.038	-41	198	4.0	.054

<sup>a</sup> All specimens blended to give  $M_c = 326$ ; for compositions see Table 3.

<sup>b</sup> Nominal composition for Epon 828 (control specimen).

<sup>c</sup>  $\tan \delta(\max)$ , seen near  $T_g$ , ranges between 0.70 and 0.71 in all cases.

Thus the broadening of the distribution within the limits available in Series B (see Table 4) has no significant effect on viscoelastic behavior. It is true that Epon 828 (75% of epoxy with  $n=0$ ; 25%,  $n=1$ ) behaves differently from Epon 825 ( $n=0$ ), but the difference can be attributed solely to the higher  $M_c$  of the latter.

It should be noted, however, that some viscoelastic parameters change significantly with  $M_c$ , some parameters change relatively little. For a 5-fold decrease in crosslink density,  $E_r'$  must, of course, change 5-fold, and  $T_g$  drops by 80°C - significant changes which will have a profound effect on engineering behavior. On the other hand, parameters characterizing the glass-to-rubber transition itself are insensitive, the slope  $\underline{n}$  and the value of  $\tan \delta_{\max}$  are changed by only +60% and +150%, respectively. Thus, in testing for consistency of behavior in a cured epoxy resin,  $E_r'$  and  $T_g$  would be the best properties to select.

### 3. Series E Epoxy Resins (Unblended Commercial Resins)

Viscoelastic data are summarized in Table 17 and in Fig. 18, 21, and 22. In general, when comparison is made at equal  $M_c$ , trends in viscoelastic behavior is similar to that observed in Series A. Indeed values of  $T_g$  and  $\tan \delta_{\max}$  agree remarkably well with those of Series A, while values of  $\underline{n}$

agree reasonably well. Values of  $T_g$  did, however, appear to vary more strongly with  $M_c$  than was the case with Series A; also, for a given theoretical value of  $M_c$ , values of  $E'_g$  were consistently lower for Series E.

Table 17. Dynamic Mechanical Properties of Series E Epoxy Resins (Commercial Resins).

Specimen	$M_c$ (theor.)	$T_g^a$ , °C	$\tan \delta_{\max}$ (at $\alpha$ )		$T_g$ , °C	$E'$ , GPa <sup>c</sup> × 10		$\eta$ × 10 <sup>-2</sup>
			Value	Temp, °C		$E'_g$	$E'_g$	
E-1	308	-35	0.62	221	207	0.45	22	5.2
E-2	326	-40	0.75	211	197	0.42	21	5.6
E-3	430	-46	0.90	175	165	0.17	20	6.7
E-4	493	-46	0.95	175	165	0.21	20	6.7
E-5	740	-55	1.25	157	145	0.10	19	9.1
E-6	980	-57	1.40	147	135	0.085	18	9.1
E-7	1400	-60	1.52	138	125	0.065	18	10.0

<sup>a</sup> From maximum in  $\tan \delta$ .

<sup>b</sup>  $E'_g$  refers to the glassy state. <sup>c</sup> 1 GPa =  $10^{10}$  dynes/cm<sup>2</sup>.

Thus, to a good approximation, the viscoelastic behavior of the epoxy resins discussed so far is governed by  $M_c$ , and hence by the average crosslink density. This is so whether a given  $M_c$  is attained by varying stoichiometry or by changing the molecular weight of the epoxy prepolymer - a conclusion not noted in previous literature. Several of the viscoelastic parameters will now be discussed in more detail.

$T_g$ : Values of  $T_g$  obtained were checked independently using differential scanning calorimetry (DSC) and the Gehman creep tester. As shown in Table 18, excellent agreement was obtained, after allowance for the differences in effective frequency. The dynamic tests were run at 110 Hz, and the creep experiment had an effective frequency of 0.1 Hz ( $\approx$  10-sec-measuring time), while the effective frequency of the DSC is somewhere in between.  $T_g$ 's from the dynamic and creep tests differed by an average of 24°C, which<sup>g</sup> is in good agreement with the prediction that  $T_g$  should increase by up to about 13°C per decade increase in frequency. Also, values of the temperature at which  $\tan \delta$  was a maximum were consistently about 8°C higher than  $T_g$  (obtained from the peak in  $E''$ ), as expected.

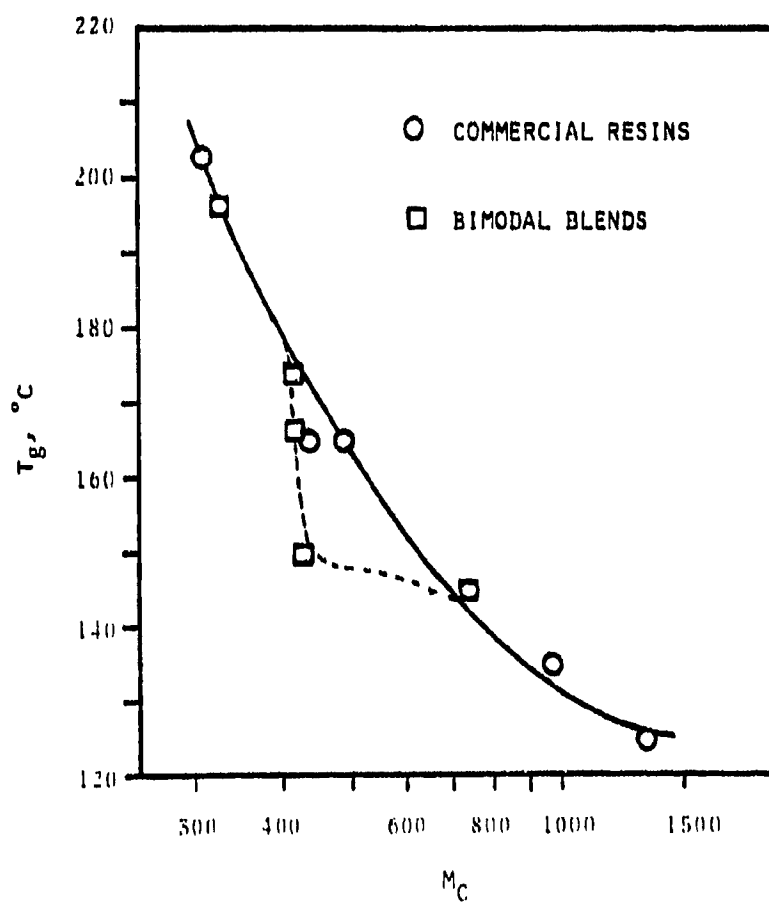


Figure 21.  $T_g$  as function of  $M_c$  (theor.) for series E and F.

Table 18.  $T_g$  Data for Series E Epoxy Resins.

Specimen	$T_g, ^\circ\text{C}$		
	from DSC	from creep <sup>a</sup>	from Rheovibron <sup>a</sup>
E-1	189	174	207
E-2	185	167	197
E-3	157	142	165
E-4	-	-	165
E-5	137	118	145
E-6	124	108	135
E-7	116	101	125

<sup>a</sup> Frequencies: Rheovibron, 110 Hz; Gehman tester, 0.1 Hz  
( $\approx$  measurement of E at 10 sec. after loading).

Because of the consistency of  $T_g$  as a function of  $M_c$ , it seemed reasonable to develop a quantitative relationship between the two parameters. Several relationships are described by Nielsen (1, pp.23-24); the simplest of these, obtained by averaging many data in the literature, may be expressed as follows:

$$T_g - T_{g0} = \frac{K}{M_c} = \frac{3.9 \times 10^4}{M_c} \quad (14)$$

where K is an empirical constant, and  $T_{g0}$  is the  $T_g$  of uncrosslinked polymers having the same composition as the polymer of interest. By extrapolating  $T_g$  (at 110 Hz) to  $M_c = \infty$ , a value of 100°C was found for  $T_{g0}$ . On averaging values of K for all Series E resins, equation 14 becomes

$$T_g - T_{g0} = \frac{3.2 \times 10^4}{M_c} \quad (15)$$

In good quantitative agreement with Nielsen's approximation. Of course, the constant K may vary somewhat for different epoxy systems.

Once established for a given epoxy system, equation 15 could be used as the basis for a simple test to determine  $M_c$  for any resin of the same type. (Of course,  $T_g$  is of interest in its own right.) A major advantage is that  $T_g$  can be measured quickly and precisely by a variety of techniques, e.g., DSC, which are more convenient and less time-consuming than creep or dynamic mechanical spectroscopy.

Young's Modulus: As expected, Young's modulus at room temperature,  $E_g$ , was found to be nearly independent of prepolymer molecular weight (Table 17). All values fall within the range  $2 \pm 0.2$  GPa, compared to an average of 1.3 GPa for obtained from tensile stress-strain curves (section VII). However, the mean values of  $E$  do tend to decrease slightly but consistently as  $M_c$  is increased.

Rubbery Modulus: The rubbery modulus,  $E_r$ , was found to be related to the modulus in the glassy state,  $E_g$ , and to  $E_r$  the modulus of a network having  $M_c = \infty$  by the following expression

$$\frac{E_g - E_r}{E_r - E_{r,\infty}} = K_1 (M_c - M_{o1}) \quad (16)$$

where  $K_1$  is a constant, and  $M_o$  is the value of  $M_c$  corresponding to  $E_g$  (that is a value which corresponds to the case of no glass transition. The following parameters were found to give a good fit to the data (for  $E_g = 2.0$  GPa

$$E_{r,\infty} = 4 \text{ MPa}$$

$$M_{o1} = 190$$

$$K_1 = 0.6$$

Tan  $\delta$ : Since the value of  $\tan \delta_{\max}$  increases with  $M_c$  it is of intent to define the relationship. The following expression was found to hold for Series E:

$$\frac{\tan \delta_o - \tan \delta_{\max}}{\tan \delta_{\max}} = \frac{K_2}{(M_c - M_{o2})} \quad (17)$$

where  $\tan \delta_o$  = the value of  $\tan \delta$  for  $M_c = \infty$ ,  
 $M_{o2}$  = the  $M_c$  at which  $\tan \delta_{\max} = 0$ , and  
 $K_2$  = constant,  $3 \times 10^2$  in this case.

$M_{o2}$  was determined by plotting the ratio of  $\tan \delta_{\max}$  vs.  $M_c$  and extrapolating to  $\tan \delta_{\max} = 0$ . The value thus determined for  $M_{o2}$  was 160 -- in fair agreement with the value of 190 determined in the previous discussion of  $E_r$ .

Slope,  $n$ : As mentioned, the slope  $n$  varies directly with  $M_c$ . The following expression was found to correlate the experimental data well:

$$n = K_3 \log_{10} (M_c / M_{o3}) \quad (18)$$

where  $K_3$  = a constant, and  
 $M_{03}$  = the limiting value of  $M_c$  at which  $n=0$ .

Using the present data,  $n=0$  when  $M_{03}=75$ --a value lower than found from  $E_r$  and  $\tan \delta_{\max}$ .

#### 4. Series F Epoxy Resins (Bimodal Blends)

Viscoelastic data are summarized in Tables 19 and 20 and in Figures 21 and 22.

Table 19. Dynamic Mechanical Properties of Series F Epoxy Resins (Bimodal Blends).

Specimen	$M_c$	$T_g, ^\circ C$	Tan $\delta_{\max}$ (at $\alpha$ )		$T_g, ^\circ C$	$E', GPa \times 10$		Slope $-\frac{n}{x10^2}$
			Value	Temp. $^\circ C$		$E'_r$	$E'_g$	
F-1	326	-40	0.75	211	197	0.42	21	5.6
F-2	413	-45	0.75	185	174	0.21	20	5.6
F-3	419	-45	0.80	175	166	0.17	20	5.9
F-4	430	-46	0.75	168	150	0.17	20	5.6
F-5	740	-55	1.25	157	145	0.10	19	9.1

As was the case with Series B and Series E, most properties at constant  $M_c$  are little affected by the greater breadth of the  $M_c$  distribution. However, two new probable anomalies exist. First, the slope of the glass transition tends to be lower than for F-2, F-3 and F-4, resins with  $M_c$  values between 500 and 600. Second (Fig. 21),  $T_g$  is abnormally low for specimen F-4. This cannot be due to an error in measurement, for the value found is in excellent agreement with values determined from creep and DSC studies.

The conclusion that an anomaly in  $T_g$  exists is supported by Fig. 22, which displays  $T_g$  as a function of nominal composition. Clearly there is a sharp break in the  $T_g$ -composition curve between compositions corresponding to F-3 and F-4. At high Epon 825 contents, the  $T_g$  is dominated by the Epon 825 component; at high Epon 1004 contents, the  $T_g$  is dominated by that component.

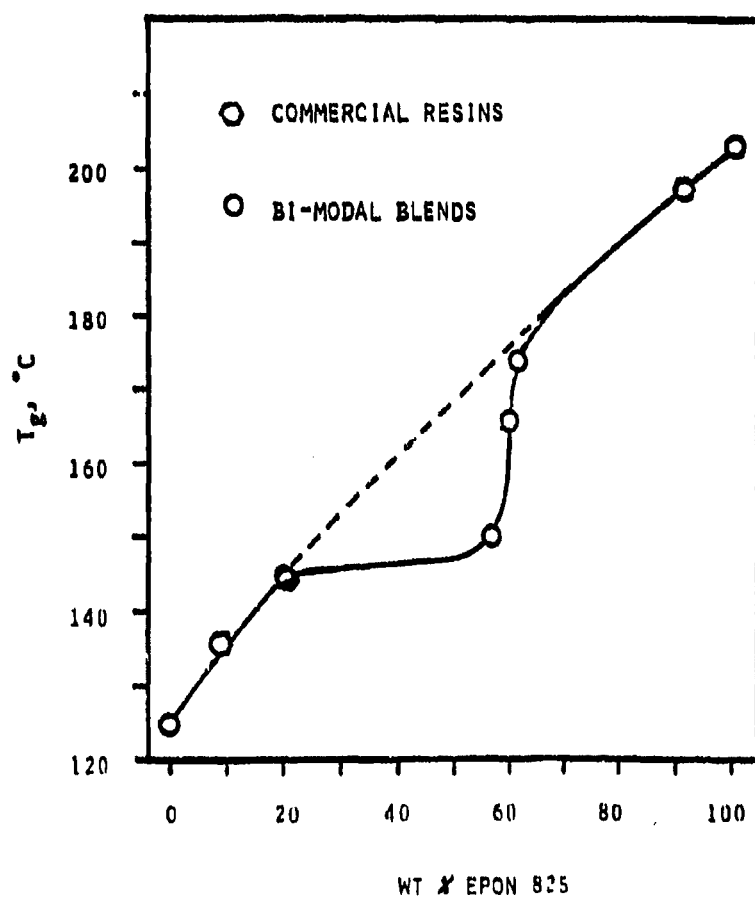


Figure 22.  $T_g$  as function of wt % of Epon 825 in the resin for series E and F.

Table 20.  $T_g$  Data for Series F Epoxy Resins.

Specimen	$T_g$ , °C		
	from DSC	from creep	from Rheovibron
F-1	184	167	197
F-2	163	147	174
F-3	157	139	166
F-4	146	129	150
F-5	136	118	145

d. Creep:

Measurements of creep modulus (10-sec) were made using the Gehman torsional tester, as described in section IV. Data were obtained at times between 10 and 1000 sec., over a temperature range which spanned the glass-to-rubber transition region. Creep or stress relaxation displays the transition region on log-time scale. Since a few degrees in temperature corresponds to a decade in time, creep or stress relaxation provides a convenient window to observe transition behavior with a high degree of sensitivity.

A typical curve is shown in Fig. 23. The data are then shifted to obtain a master curve at 150°C using the time-temperature superposition principle (28). Calculations showed that the experimental and theoretical values for the WLF shift factor,  $a_T$ , agreed well between  $T_g - 10^\circ\text{C}$  and  $T_g + 25^\circ\text{C}$ . The time constant,  $T_0$  (actually, the characteristic retardation time) was measured at the inflection point of the transition in E.

1. Series A Epoxy Resins (Variable Stoichiometry)

As shown in Fig. 23 and Table 21, clearly  $T_g$  changes very significantly--by orders of magnitude--as the amine/epoxy ratio and, hence,  $M_c$  is varied, reflecting the change in  $T_g$  from 114°C to 168°C. These values agree well with values obtained using dynamic mechanical spectroscopy (see Table 12). Curiously, the slope of the transition was constant except for specimen A-20; since the slope of the  $\alpha$  transition in the E-T plots varied significantly with stoichiometry, one might have expected a change in the creep transition slopes as well. Finally, the creep behavior at constant  $M_c$  is independent of which component is in excess.

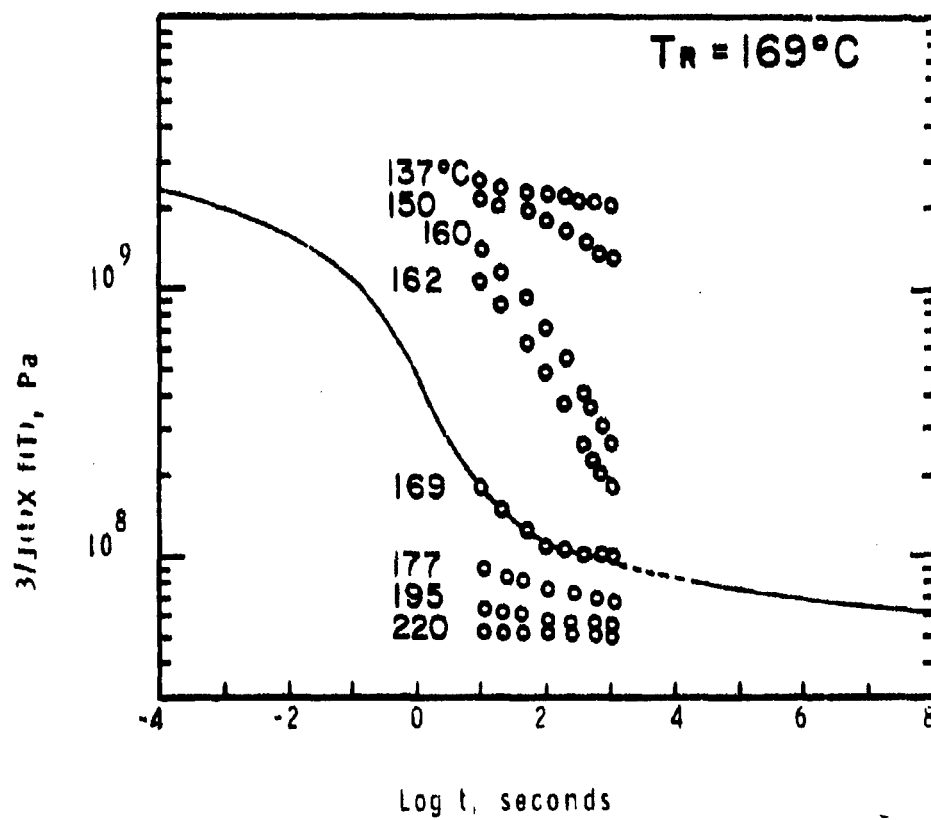


Figure 23. Creep compliance of A-10 epoxy resin.

Table 21. Creep Data for Epoxy Series A.

Specimen	$T_g, ^\circ\text{C}^a$	$E_r, \text{MPa}$	$\log \tau_c, \text{sec}$	$b_n^b$
A-7	114	30	-9.7	-0.36
A-8	140	33	-2.5	-0.38
A-10	168	44	4.0	-0.42
A-12	151	50	0.3	-0.38
A-20	100	10	-13.0	-0.63

<sup>a</sup>determined by finding the temperature at which  $E = 2 \times 10^8 \text{ Pa}$ .

<sup>b</sup> $b_n = d [\log E(t)] / d (\log \tau_c)$ .

## 2. Series E Epoxy Resins (Unblended Commercial Resins)

Results are given in Table 22 and Fig. 25. As with Series A, the creep behavior is very sensitive to crosslink density, with values of  $\log \tau_c$  ranging between -6 and 7.6, depending on the molecular weight of the prepolymer. In contrast to Series A, however, the transition slopes tend to increase steadily as  $M_c$  increases. In a sense, an increase in epoxy molecular weight seems to flexibilize the system, thus sharpening the transition. (It should be noted that values of  $\tau_c$  are greater than for Series A because of the lower reference temperature used with the E series.

Interestingly, the values of  $E_r$  and  $T_g$  agree well with data obtained from other tests (see Tables 47 and 48).

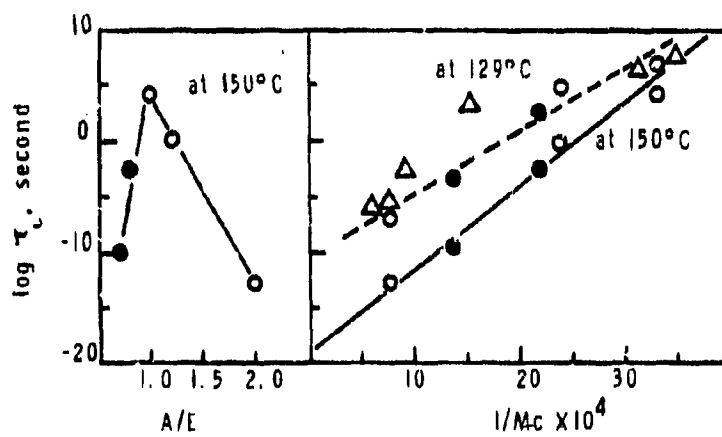
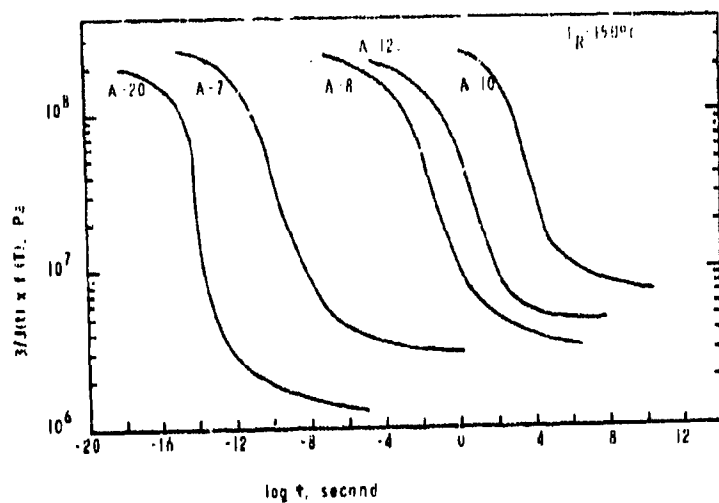


Fig. 24. Creep-compliance behavior of series A epoxy resins. Data reduced to  $150^\circ\text{C}$ .

Table 22. Creep Data for Series E Epoxy Resins  
(Reduced to 129°C).

Specimen	$T_g$ , °C	$E_r'^a$ , MPa	$\log \tau_c$	$\underline{n}$
E-1	174	15	7.6	-0.38
E-2	167	45	6.0	-0.46
E-3	142	30	3.4	-0.63
E-4	-	-	-	-
E-5	118	08	-2.5	-0.59
E-6	108	09	-5.4	-0.71
E-7	101		-6.0	-0.80

<sup>a</sup> At  $T_g + 35^\circ\text{C}$ .

#### 4. Series F Epoxy Resins (Bimodal Blend)

Creep data are summarized in Table 23; see also Fig. 25. In general, at constant  $M_c$ , Series F tends to behave like Series E. There is, however, a possibility that specimens F-2 and F-3 may deviate somewhat from the  $\underline{n}$ - $M_c$  curve, and that specimen F-4 may deviate from the  $\tau_c$ - $M_c$  curve. The slopes for F-2 and F-3 are also low when  $\underline{n}$  is plotted vs. the % Epon 825 in the blend, as in the value of  $\tau_c$  for F-4. Finally, the  $T_g$  for F-4 is, as noted before, significantly lower than expected.

Table 23. Creep Data for Series F Epoxy Resins  
(Reduced to 129°C).

Specimen	$T_g$ , °C	$E_r'$ , MPa <sup>a</sup>	$\log \tau_c$	$\underline{n}$
F-1	167	$45 \pm 10$	7.6	-0.38
F-2	147	$30 \pm 06$	3.6	-0.40
F-3	139	$30 \pm 06$	2.4	-0.39
F-4	129	$30 \pm 06$	0.8	-0.44
F-5	118	$8 \pm 01$	-1.6	-0.71

<sup>a</sup> At  $T_g + 35^\circ\text{C}$ .

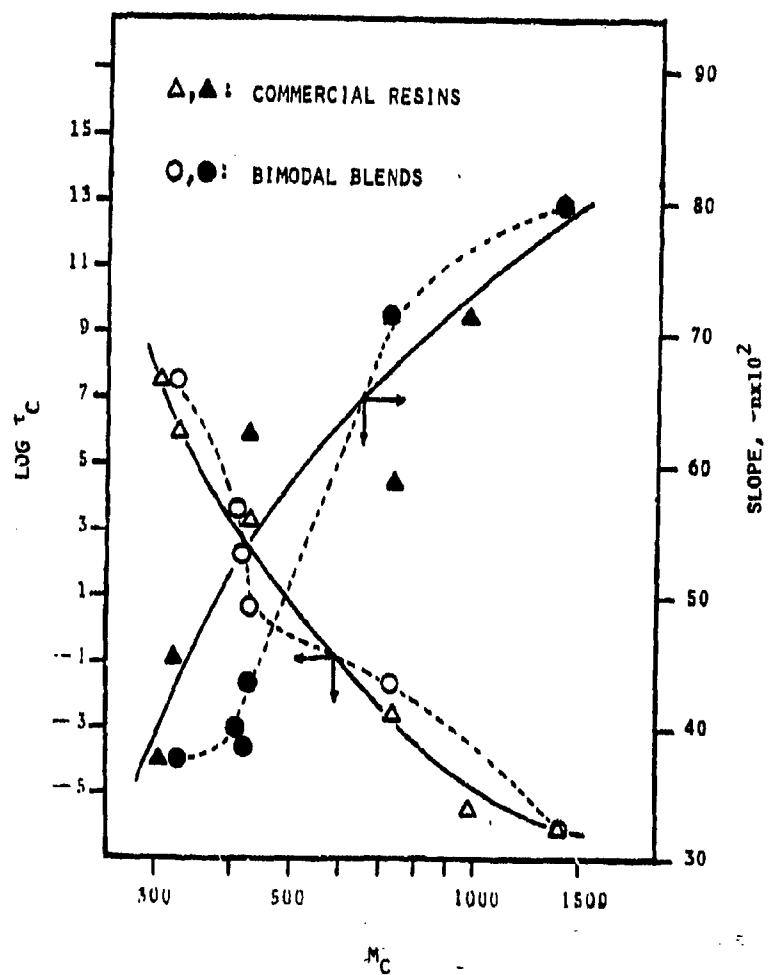


Figure 25. Creep data for series E and series F epoxy resins.

e. Effect of Distribution of  $M_c$  on Viscoelastic Behavior:

In general, for a given average  $M_c$ , variations in the distribution of  $M_c$  may be expected to have little or no effect on properties such as glassy-state or rubbery moduli. This expectation is amply confirmed by this study. Effects on the transition behavior (e.g.,  $T_g$ , or slope of the transition), could be expected in principle, and have indeed been proposed. In fact, this study shows little effect, unless the distribution is made extremely broad. While the deviations in, for example, specimen F-4 are small, they exceed twice the experimental error in some cases, and anomalies are observed in a number of tests. At the same time, no evidence for incomplete curing has been noted for any specimens, and recasting of F-4 gave a resin with essentially the same properties as the first specimen.

## SECTION VII

### FRACTURE TOUGHNESS, FATIGUE CRACK PROPAGATION AND STRENGTH OF EPOXY NETWORKS

#### A. Introduction

This section deals with fracture toughness, fatigue crack propagation (FCP), and stress-strain and impact behavior. Measurements and results are described after the general is discussed.

##### a. Fracture Toughness:

Fracture toughness may be measured using either of two approaches, based on concepts of either a critical energy balance or a critical stress intensity factor (31).

The former concept is due originally to Griffith (60), who showed that crack extension in an ideally brittle solid containing an elliptical crack should occur at a stress,  $\sigma$ , when the following relationship holds (assuming a plane stress condition):

$$\sigma = \sqrt{\frac{2ES}{\pi a}} = \sqrt{\frac{EG}{\pi a}} \quad (19)$$

where E is Young's modulus, S the surface energy of the solid, a the crack length, and G (=2S) the strain energy release rate. Put simply, the release of strain energy must exceed the amount of energy required to break bonds and form new surface.

In fact, values determined for S invariably greatly exceed those calculated on the basis of bond fracture energies (31). Thus, even a brittle epoxy exhibits a value for S the order of  $10^4$  erg/cm<sup>2</sup> - two orders of magnitude greater than calculated; more ductile resins show even greater discrepancies. Thus S should be considered as an "effective" fracture energy that includes a dominant contribution from plastic deformation, evidence for which is seen by electron microscopy.

The second concept is due to Irwin (61), who suggested that crack instability could be expressed in terms of the stress intensity factor K - a measure of the distribution of stress at the crack tip. Since K can be calculated from the applied stress, crack length, and geometry, it is an especially convenient parameter for correlation purposes.

Catastrophic crack propagation will occur when either  $\sigma$  or K reach critical levels ( $\sigma_c$  or  $K_c$ ), corresponding in turn to critical

values of S or G. The two concepts are essentially equivalent, and

$$G_c E = \frac{K_{Ic}^2}{(1 - \nu^2)} \quad (20)$$

for the case of interest here, plane strain, where  $\nu$  is Poisson's ratio.  $K_{Ic}$  is a useful material constant, though it depends on temperature and on the mode of crack opening. (For simplicity, we shall use " $K_c$ " below.)

The fracture energy, S, of the Epon 828/MDA system has been determined by Selby and Miller (17), and found to be dependent on both the method of test and on the MDA content, tending to peak at an amine/epoxy ratio of 1.3. Values ranged between 0.7 MPa and 1.5 MPa, depending on the test. Values reported for other epoxies range between 0.4 MPa and 1.5 MPa (62).

#### b. Fatigue Crack Propagation:

Fatigue failure may occur by two mechanisms: (1) a thermal mode in which failure occurs by melting due to hysteretic heating, and (2) a mechanical mode comprising the initiation and propagation of a crack. The rate of temperature rise,  $\Delta \dot{T}$ , characteristic of thermal failure is a function of stress amplitude,  $\sigma$ , frequency,  $f$ , and the loss modulus,  $G''$  (28):

$$\Delta \dot{T} = C f G'' \sigma^2 \quad (21)$$

where C is a constant, and  $G''$  is itself a function of  $f$  and  $T$ . While temperatures can, indeed, rise in the fatigue of, for example, epoxy resins in composites due to such hysteretic heating of a whole specimen, this study is concerned with low-frequencies and loads well below those which will cause large temperature rises. Of course, there may be hysteretic effects locally, but the volume of polymer affected is small, and any effect will be seen as an effect on the mechanical propagation rate.

Failure of a resin takes place in two stages: Initiation of a crack, and propagation of the crack to catastrophic rupture. While in some cases, the initiation step may be the critical one, frequently in plastics the propagation step is the most important (63). Thus, most polymers contain flaws introduced during processing. Such flaws will begin to grow after a certain number of cycles - the number being lower the higher the stress applied. However, the important point in determining fatigue life is the number of cycles required to grow those flaws to a size which meets the requirements of catastrophic fracture (see equation 19). In fact, frequently most of the fatigue life is in the stage of crack propagation; also, failure may occur at loads well below those

required for static rupture. Hence measurements of fatigue crack propagation are of special interest in the characterization of toughness in an engineering plastic; in addition, approximate values of a quasi-fracture toughness may be obtained as well (see below).

The crack propagation region can be examined exclusively by precracking (notching) the test specimen so that the artificial flaw is essentially ready to propagate. This approach has received increased attention recently (63) and was adopted in this investigation.

A useful parameter to characterize the fatigue crack propagation (FCP) response in notched specimens is the stress intensity factor  $K$  mentioned above (61). Derived from principles of fracture mechanics, the stress intensity factor describes the stress conditions at the tip of the advancing crack and is defined by

$$K = Y\sigma\sqrt{a} \quad (22)$$

where  $K$  is the stress intensity factor,  $Y$  a correction for specimen geometry,  $\sigma$  the stress, and  $a$  the crack length.

Fatigue crack propagation data are generated by cycling notched samples within a constant load range and recording crack growth over the corresponding number of fatigue cycles. Under fatigue conditions  $K$  will also vary over a range defined by  $\Delta K$  (calculated from equation 22). The crack length  $a$  will also increase, enabling the measurement of the rate of crack growth per cycle,  $da/dN$ , over a range of  $\Delta K$ . It has been shown (64), that the relationship between  $da/dN$  and  $\Delta K$  can often be represented by a simple equation of the form:

$$\frac{da}{dN} = A\Delta K^n \quad (23)$$

where  $A$  and  $n$  are constants for a given polymer. Other relationships exist, but offer no special advantage in discerning trends in the effects of chemical structure and composition (63).

In addition, using equation 22, an approximate value of  $K_c$  may be estimated from the value of  $\Delta K_{max}$ , the last value of  $\Delta K$  noted prior to catastrophic failure, and the load range. It has been shown that good agreement can be obtained with values of  $K_c$  measured independently from static fracture tests (63).

Using this relationship between  $da/dN$  and  $\Delta K$ , it is possible to analyze the FCP response of a polymer as a function of external variables such as frequency and temperature (64,65) and structural variables such as molecular weight, composition, and plasticization (65-69). Using equation 23, many correlations between fatigue and structural parameters have been made successfully. The following factors have been shown to

enhance FCP resistance: crystallinity, high molecular weight, linearity vs crosslinking, and presence of a rubbery inclusion. Several specific points in these studies are worth noting in more detail.

First, while studies of controlled crosslinking have not been made until now, earlier work in these laboratories showed that crosslinking tends to increase the slope of the  $da/dN$  curve and, at least at high values of  $\Delta K$ , to decrease  $\Delta K_{max}$  significantly; each of these effects is a measure of decreased toughness. Further, studies with a densely cross-linked epoxy resin showed that stable FCP behavior could be obtained only for a few cycles, and then only by increasing the temperature. (A new possible solution to working with such brittle thermoset resin is described later; see section B-a, below).

Second, there is an unexpectedly large effect of molecular weight in linear polymers such as poly(methyl methacrylate) and poly(vinyl chloride) (67,68); in fact, it was shown that  $da/dN$  varies with the term  $e(\exp)1/M$ . Values of  $K_C$  also depend strongly on  $M$ , rising sharply as  $M$  exceeds the critical value required for chain entanglements to become effective, and levelling off more or less asymptotically at higher values of  $M$  - say, the order of  $10^5$ . However, even though  $M$  is in the nearly asymptotic range, the FCP rate at a given  $\Delta K$  still depends strongly on  $M$ . Hence a strong specific effect of fatigue per se exists - an effect attributed to a disentanglement of chains due to cyclic loading. The higher the average molecular weight, the greater the resistance to fatigue; a high-molecular-weight tail in a broad distribution also gives, for the same average  $M$ , enhanced fatigue resistance (67).

Third, the  $\beta$  transition appears to play a role not only in strength phenomena such as yielding but also in FCP and its sensitivity to frequency. Thus the FCP rate is highest at the temperature and frequency corresponding to the  $\beta$  transition (63); the closer test conditions correspond to the  $\beta$  transition, the greater the sensitivity of FCP rate (at a given  $\Delta K$ ) to frequency--the rate being reduced by an increase in frequency.

Fourth, it has been abundantly clear that crazing in advance of the crack tip is a nearly universal phenomena in fatigue as well as in static crack growth. Under some conditions (69), the craze grows incrementally with each cycle, and the crack then strikes through, yielding one striation per cycle on the fracture surface. Under other conditions, the craze may grow for many cycles before the crack strikes through, yielding one striation for many cycles (so-called "discontinuous growth bands"). While precise explanations of the role of structure in craze formation do not yet exist, it seems likely that stable crazes, and hence a degree of crack growth resistance, require the presence of even a small proportion of high molecular weight material (70). Although crazing has been reported in epoxies (15), nothing is known about crazing and fatigue. It does seem likely that crazing will tend to be suppressed by tightly crosslinked networks. In any case, fracture surface morphology ("fractography") can help in elucidating the micromechanisms of failure (71).

Finally, relatively little has been published on fatigue in monolithic epoxy resins. Schrager (72) has noted increases in the shear modulus and dissipation factor in an epoxy resin; a similar effect has been noted by Outwater and Murphy (73). It was suggested that cycling may have enhanced the degree of cure. Outwater and Murphy also found that  $da/dN$  was a linear function of  $\Delta K$ . Sutton (74) described FCP in a "representative commercial epoxy-resin" cured with tetraethylene pentamine, and also found that equation 23 and a variant which takes account of mean stress held very well. The response was quite sensitive to mean stress; with  $da/dN$  at constant  $\Delta K$  increasing by two orders of magnitude for a 5-fold change in load ratio ( $K_{min}/K_{max}$  from 0.1 to 0.5). Tomkins and Biggs (75) suggested that FCP in a brittle epoxy is dominated by crack branching -- a phenomenon possibly related to crazing.

#### c. Stress-Strain and Impact Behavior:

Several studies describe stress-strain behavior in epoxies; some results being especially relevant to this program. Thus Selby and Miller (17) reported that Young's modulus of the Epon 828/MDA system depended somewhat on stoichiometry, with minima at amine/epoxy ratios of 1:1 (tension) and 1.1/1 (compression) - a finding apparently inconsistent with the expectation that modulus might be highest at equal stoichiometry, if it varied at all. Tensile strengths also tended to exhibit a similar minimum. On the other hand, Bell (46) reported essential independence of tensile strength on stoichiometry. Labana et al. (76) and Whiting and Kline (7) worked with different epoxies, but found slight variations in tensile strength and modulus with stoichiometry. Finally, Kaelble (59) reminds the reader that moduli and strengths in the glassy state should depend more on cohesive energy density and polymer chemistry than on the network structure per se. (Plasticization, however, could change the values significantly.)

Impact strength has been studied by Bell (46) as a function of stoichiometry. He reported essentially no dependence, though his limited data could permit the conclusion that impact strength may peak in the amine-rich region.

### B. Experimental Details, Results and Discussion

#### a. Fatigue Studies

Fatigue test specimens used were cast sheets (see section VI-B) 1/4-in (0.635 cm) x 3-in (7.62 cm) x 3-in (7.62 cm) in dimensions. Such specimens are commonly referred to as "compact tension" specimens. A 1/4-in (0.635 cm) notch was first cut into the edge using a saw; a vee was then cut using a fine jeweller's saw. Specimens were mounted using pin grips.

To start the crack, a sharp razor blade was drawn across the tip of the vee, and cycling was then begun at a low load. The load was gradually increased until the crack was observed to begin growing. This procedure was satisfactory for all specimens except those having 1:1 stoichiometry, though great care was necessary since only a slight increase in load sufficed to induce catastrophic rupture.

For the 1:1-stoichiometry specimens, the above procedure proved to be ineffective, and stable cracks could not be grown. However, it was found that stable crack growth could be induced by rubbing the razor blade to the vee while the specimen was being cycled. In this way, a crack could be initiated with considerable delicacy. Discovery of this procedure constitutes a significant advance in dealing with specimens such as brittle epoxies. The technique also works with other polymers which are prone to fail before a stable crack can be induced, and may well open up the possibility of studying refractory materials which are otherwise most difficult to handle.

For compact tension specimens,  $\Delta K$  is given by

$$\Delta K = \frac{Y\Delta P\sqrt{a}}{BW} \quad (24)$$

where  $\Delta P$  is the load range,  $B$  the specimen thickness,  $W$  the specimen width,  $a$  the crack length, and

$$Y = 29.6 - 185.5(a/w) + 655.7(a/w)^2 - 1017(a/w)^3 + 638.9(a/w)^4 \quad (25)$$

All fatigue tests were performed on an MTS electrohydraulic closed loop testing machine operated at a test frequency range of 10 Hz and with the load ratio  $P_{min}/P_{max} = 0.1$ . Crack growth rates were monitored with the aid of a travelling microscope in increments of approximately 0.25mm.  $K_C$  was determined from the last stable value of  $\Delta K$  rated prior to fracture, after allowing for the load ratio used (63). All fatigue tests were run in laboratory air. Fracture surfaces were examined by scanning electron microscopy.

#### b. Fracture Toughness

Data for series A, series B, and series D are given in Table 24; see also Figures 26 and 27. Clearly, values of  $K_C$  increase smoothly as the amine content is increased. In terms of fracture energy, we have a range from 10 J/m<sup>2</sup> to 440 J/m<sup>2</sup>, in good agreement with values reported by Selby and Miller (17) based on different tests. As expected, series D (cured with Versamid, which confers flexibility) exhibits still higher fracture toughness. Since  $K^2 = ES$  (equation 20), and since  $E$  in fact increases slightly with the amine/epoxy ratio (see Section VI), the principal effect of amine excess is to confer ductility (in the sense of plastic deformation) and hence increase  $S$ .

Table 24. Fracture Toughness and Fatigue Characteristics of Epoxy Resins (Series A, B, D).

Series Type	Specimen	Amine/ Epoxy Ratio	$\Delta K_I^a$	$K_{IC}^b$ , MPa $\sqrt{m}$	Slope of da/dN Curve
Variable Stoichiometry	A-7	0.7	0.50	0.58	9.3
	A-8	0.8	-	-	-
	A-9	0.9	0.49	0.63	19.3
	A-10 <sup>c</sup>	1.0	-	-	-
	A-10A	1.0	0.53	0.73	11.1
	A-11	1.1	0.58	0.78	7.7
	A-14	1.4	0.75	0.93	17.6
	A-16	1.6	0.72	0.93	18.3
	A-18	1.8	0.79	0.98	19.0
	A-20	2.0	0.83	1.0	9.9
Epoxy/Versamid Type	D-2	1.0	0.68	1.00	7.9
	D-3	1.0	0.68	1.22	7.9
Epoxy Blends ( $M_c = 326$ )	B-1	1.0	0.53	0.72	13.6
	B-2	1.0	0.57	0.80	11.6
	B-3	1.0	0.57	0.76	15.8
	B-4	1.0	0.57	0.78	10.8
	B-5 <sup>c</sup>	1.0	0.53	0.72	13.6

<sup>a</sup> At  $da/dN = 3 \times 10^{-4}$  mm/cyc.

<sup>b</sup> Calculated from relationship  $K_{IC} = \Delta K_{max}/0.9$ .

<sup>c</sup> A-10 and B-5 are equivalent; A-10A is similar, but cured with 99% MDA instead of Tonox.

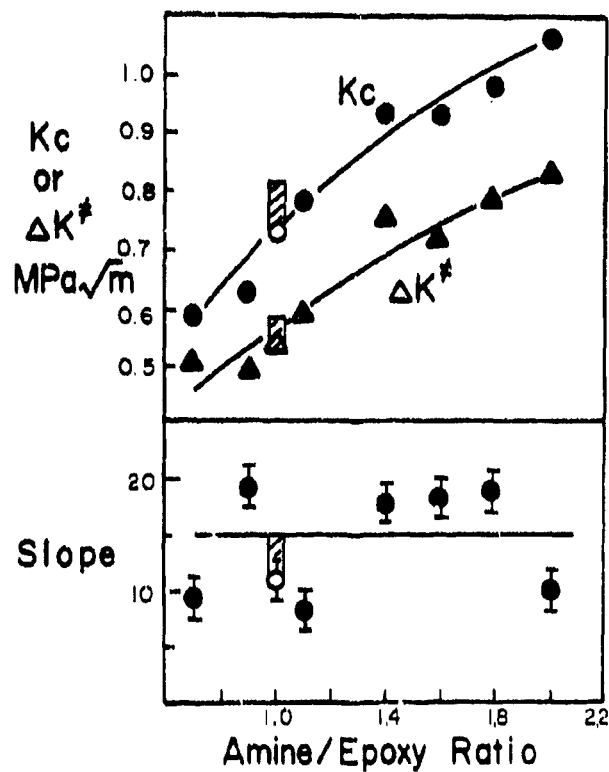


Figure 26. Fracture toughness,  $K_{IC}$ , and FCP parameters  $\Delta K^*$  ( $\Delta K$  at  $da/dN = 3 \times 10^{-4}$  mm/cyc), and slope of the  $da/dN$  curve as a function of the stress intensity factor range,  $\Delta K$ , as function of stoichiometry; circles and triangles for series A, open corresponding to A-10A; shaded area for series B.

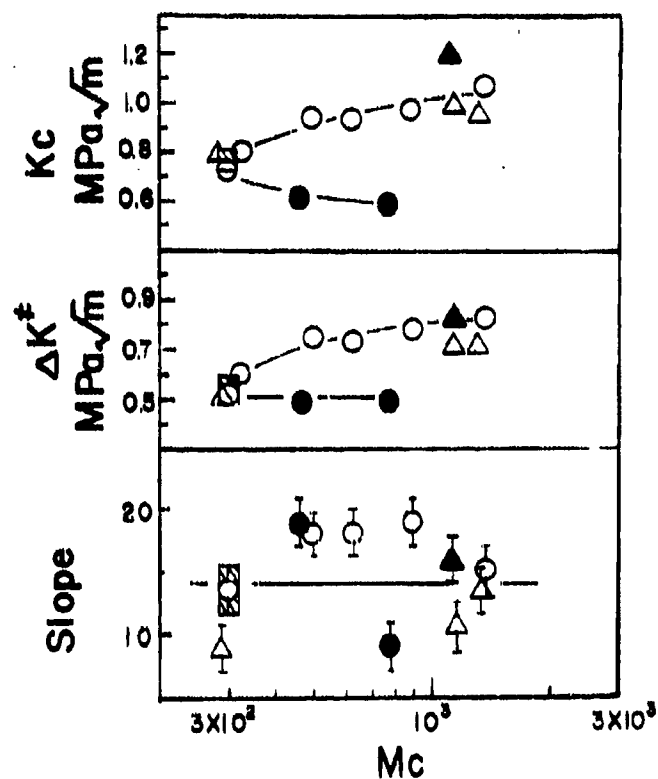


Figure 27. Fracture toughness,  $K_{IC}$ , and FCP parameters  $\Delta K^*$  ( $\Delta K$  at  $da/dN$   $3 \times 10^{-4}$  mm/cyc), and slope of the  $da/dN$  curve as a function of the stress intensity factor range,  $\Delta K$ , as function of  $M_c$ : open circle, amine excess in series A; closed circle, epoxy excess; shaded area, series B; open triangle, series E; closed triangle, series F.

On the other hand, an excess of epoxy resin decreases  $K_C$ . Since  $E$  is increased by such excess, the value of  $S$  must be significantly lowered by the presence of branched epoxy structures. (For discussion of the contradictory trends in  $K_C$ , tensile strength, impact strength, and tensile energy-to-break, see section e).

Although series B blends appear to be slightly tougher than series A controls, the effect does not seem to be statistically significant. Hence, a moderate distribution in  $M_C$  does not appear to influence  $K_C$  appreciably.

All series E resins (Table 25, Figure 27) exhibited values of  $K_C$  close to those of series A. Although data for series E resins appear to scatter more than those for series A, specimen F-5 still seems to exhibit a high value of  $K_C$  in comparison with its counterpart, E-5--a value higher than those of its constituent resins, E-1 and E-7. This point is worth further investigation.

So far then, fracture toughness is increased by increasing the amine/epoxy ratio or by increasing the molecular weight of the epoxy prepolymer. On the other hand, contradictory effects of distribution in  $M_C$  are observed in the limited number of systems studied, the direction of the effect differing in Versamid and MDA systems.

Table 25. Fracture Toughness and Fatigue Characteristics Of Epoxy Resins. (Series E and F)

Series Type	Specimen	$\Delta K_I^a$	$K_C \text{ MPa}\sqrt{\text{m}}^b$	$n^c$
Unblended Commercial	E-1	0.51	0.87	9.2
	E-2 <sup>d</sup>	0.53	0.72	13.6
	E-3	--	--	--
	E-4	--	--	--
	E-5	0.72	1.07	10.5
	E-6	0.70	1.02	13.4
	E-7	--	--	--
Bimodal Blends	F-1	--	--	--
	F-2	--	--	--
	F-3	--	--	--
	F-4	--	--	--
	F-5	0.78	1.56	11.9

<sup>a</sup>At  $da/dN = 3 \times 10^{-4}$  mm/cyc. <sup>b</sup>Calculated from relationship  $K_C = \Delta K_{\text{max}}/0.9$

<sup>c</sup>Slope of  $da/dN$  curve.

<sup>d</sup>E-2, B-5, and A-10 are equivalent; see Tables 3, 4, and 6.

#### c. Fatigue Crack Propagation (FCP)

Several FCP parameters are presented in Tables 24 and 25, and in Figures 26 and 27. The behavior itself is illustrated in Figures 28 to 32, inclusive.

First, for Series A, the data show that, just as  $K_{IC}$  did, values of  $\Delta K^*$  (a measure of the energy to drive a crack at a given velocity) increase as the amine content increases. Data for Series B fall, within experimental error, on the same curve. In contrast, the Series D resins are identical in their behavior, except for their  $K_{IC}$  values. This finding is in contrast with the results of Selby and Miller (17) and Bell (46), who found maxima in static  $K_{IC}$  and impact strength, respectively, as a function of amine/epoxy ratio, see also the contrast with tensile data obtained in this study (Section e).

In any case, the results are quite self-consistent, and should serve as a standard of reference for future work. Indeed,  $\Delta K^*$  correlates well with  $K_{IC}$  (Figure 33) - a relationship suggested earlier by Manson and Hertzberg (64). Thus, in contrast to metals, it was shown that the higher the static fracture toughness,  $K_{IC}$ , the greater the value of  $\Delta K^*$  required to drive a fatigue crack. Interest here exhibit a similar phenomenon.

Further work will be required to clarify the role of distribution in  $M_c$  on FCP rates. However, so far, modest changes in distribution do not affect FCP behavior significantly.

#### d. Fracture Surface Morphology

Fracture surfaces of all resins examined resembled those of other glassy polymers (71), with a classic combination of smooth and rough regions and river-like features running in the direction of the crack. As with other crosslinked polymers, there was thus evidence for considerable plastic deformation.

In view of current findings that fatigue cracks often grow discontinuously -- that is, many cycles being required before the crack jumps to a new position -- surfaces were examined for evidence of fatigue striations corresponding to crack jumps. Although striations could be seen, they were too faint to photograph. However, their spacings were measured at various locations (corresponding to particular values of  $\Delta K$  and crack length  $a$ ). As shown in Figure 34,  $da/dN$  curves constructed using values of  $da/dN$  thus derived were plotted against  $\Delta K$ , along with data for specimen A-20. Clearly, the cracks grow incrementally -- one jump per fatigue cycle.

With other polymers discontinuous growth has been shown to reflect the growth of stable crazes ahead of the growing crack. If crazes do grow ahead of the crack in these epoxies (and no direct evidence has yet been

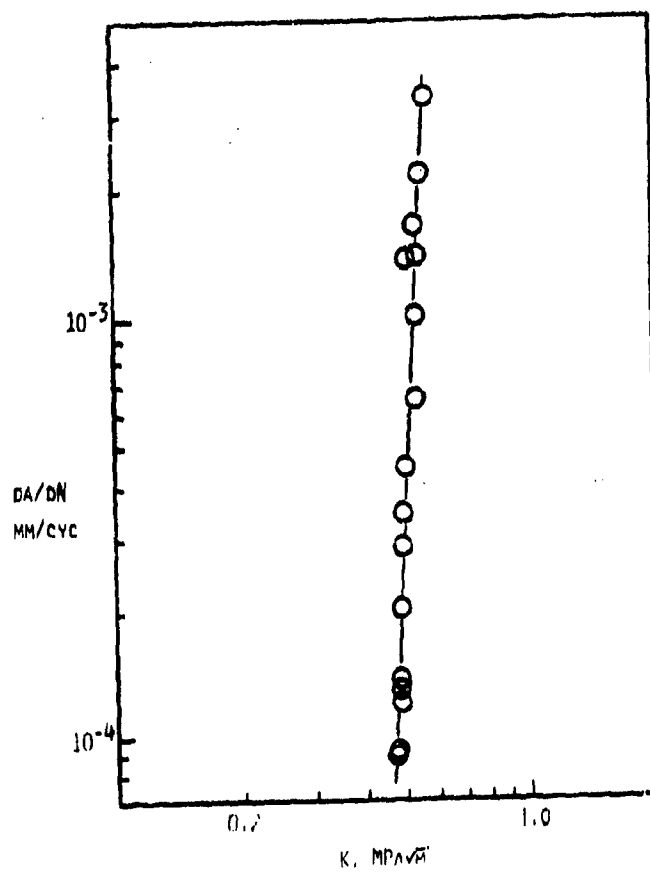


Figure 28. Typical FCP behavior as a function of  $\Delta K$ . Specimen, A-18;  $f=10\text{Hz}$ .

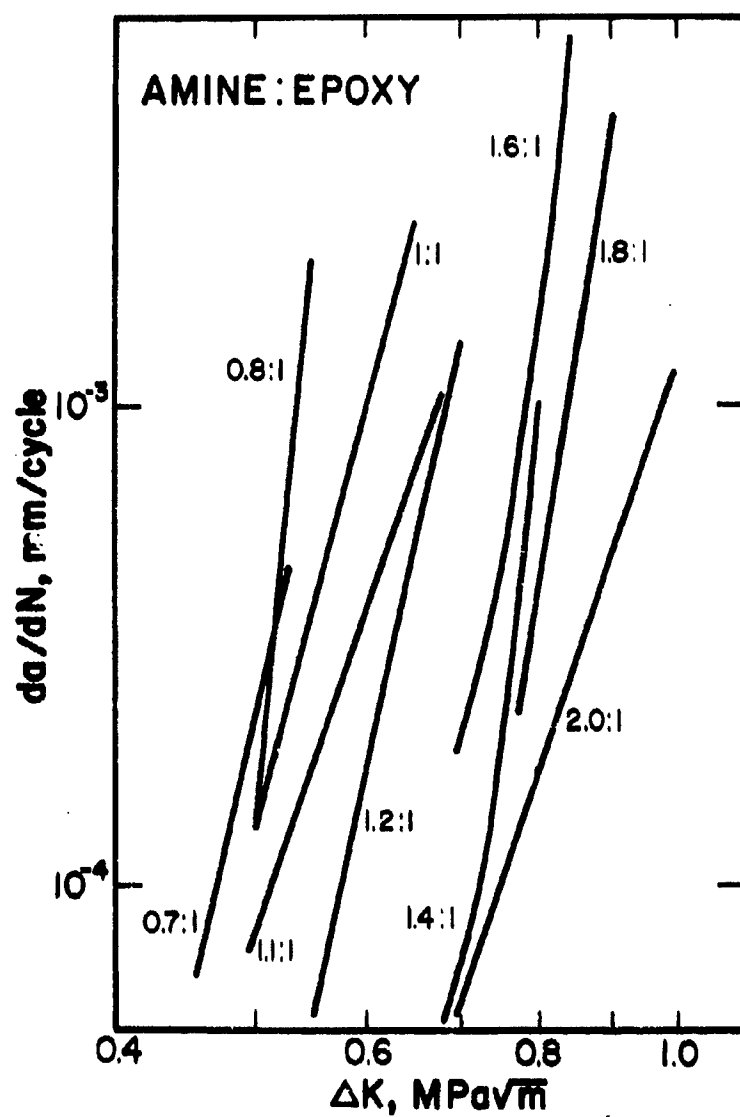


Fig. 29. FCP behavior of Series A epoxy resins;  $f = 10 \text{ Hz}$ .

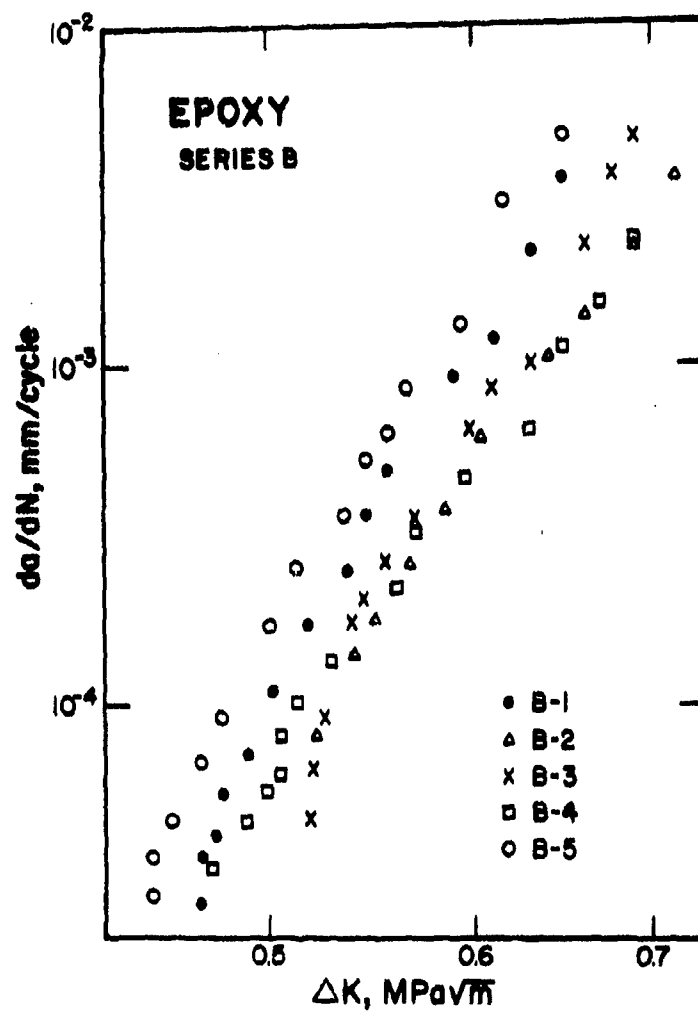


Fig. 30. FCP behavior of Series B (broad distribution) epoxy resins:  
 rate of crack growth per cycle as a function of  $\Delta K$ ;  
 $f = 10 \text{ Hz}$ .

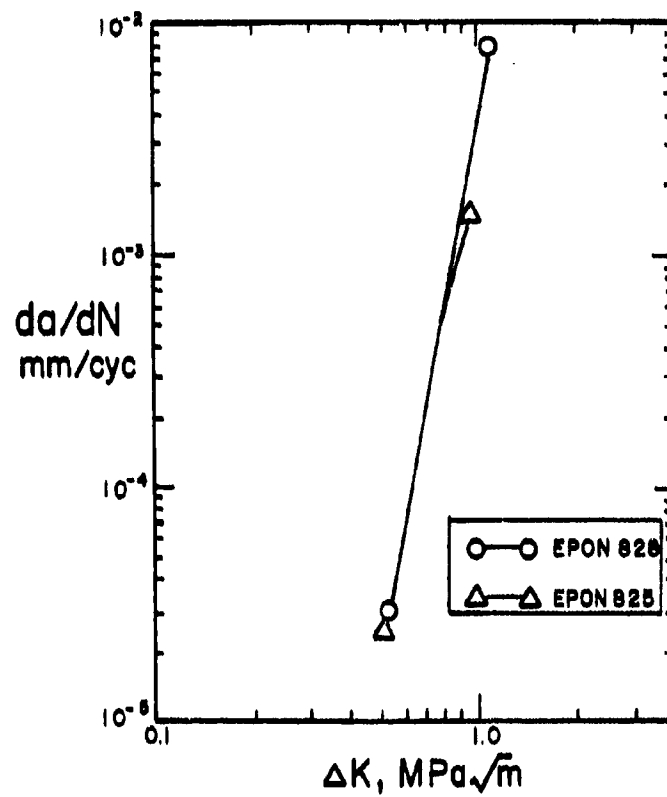


Fig. 31. FCP behavior of Series D (polyamide-cured) epoxy resins: only the first and last points shown;  $f = 10$  Hz.

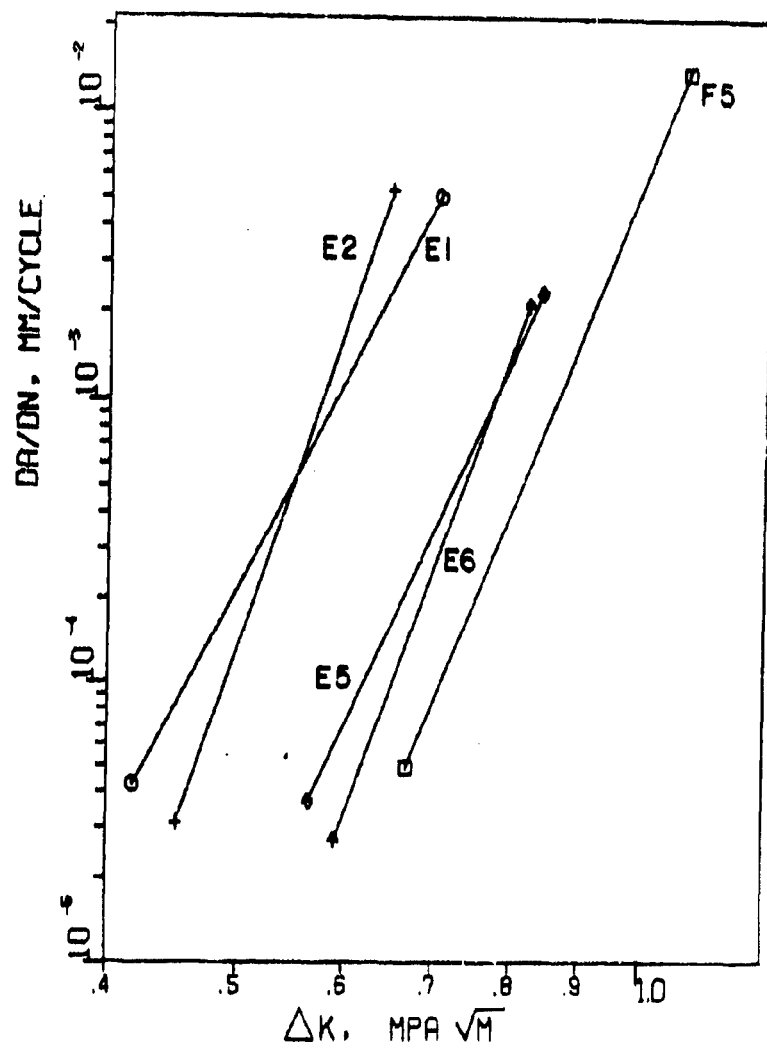


Figure 32. FCP behavior of series E and series F epoxies;  $f=10\text{Hz}$ .

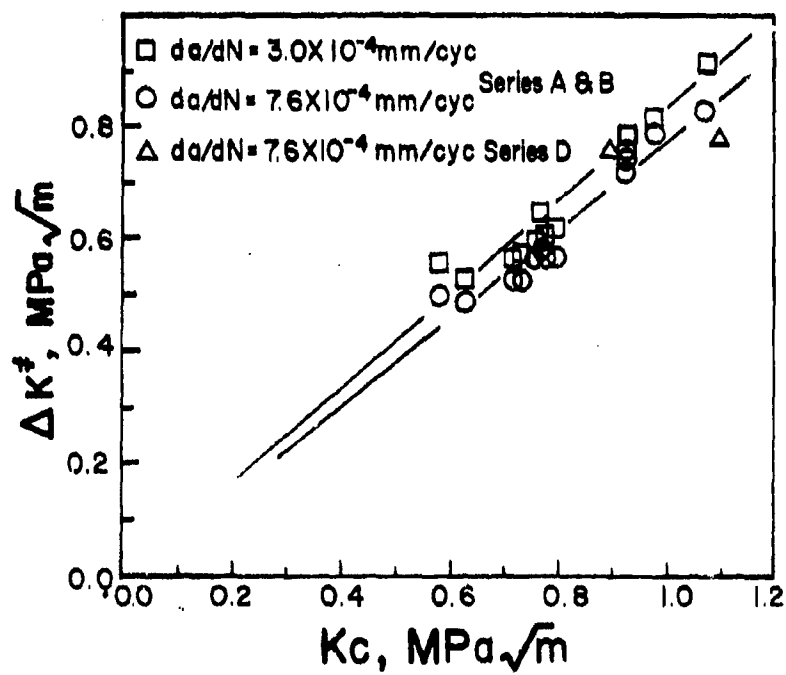
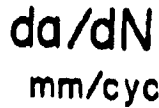


Fig. 33. Correlation of  $\Delta K_I$  ( $\Delta K$  at an arbitrary crack growth rate) and  $K_{IC}$  in epoxy resins.



88

found), the crazes must be able to resist only one load cycle -- a phenomenon found with other polymers only at very high loads or high molecular weight.

Finally, no evidence was found for the existence of large aggregates of microgel (see section VIII. This observation does not, however, exclude the possibility that such aggregates exist, for the crack could pass right through them, as is the case with poly vinyl chloride. The use of selective etching, as reported in Section VIII, should be helpful in settling this question.

#### e. Stress-Strain and Impact Behavior

Tensile tests were made using an Instron tester at room temperature according to ASTM test D-638-68, type IV, with a crosshead speed of 1.27 mm/sec. Young's modulus, ( $E$ ), ultimate tensile strength ( $\sigma_u$ ), yield strength ( $\sigma_y$ ), ultimate elongation ( $\epsilon_u$ ), and energy-to-break ( $T$ ) were determined.

Impact tests were conducted according to ASTM test D-256-70, method B (Charpy type, notched).

Results for the various series of resins are presented and discussed below.

##### 1. Series A Epoxy Resins (Variable Stoichiometry)

Tensile data are presented in Figures 35 to 38, as a function of both amine/epoxy ratio and  $M_c$ . In general, results are similar to those reported by Bell (46), Selby and Miller (17), and Whiting and Kline (7). Values of  $E$  and  $\epsilon_u$  do tend to be lower and higher, respectively, probably due to the use of the thinner specimens in this case, with consequently greater plastic deformation at the edges. As noted by others (7,17,46), the absolute magnitudes of  $\sigma_u$ ,  $E$ , and  $\epsilon_u$  vary little ( $\pm 20\%$  at most) over the whole range of stoichiometry. On the other hand, the toughness or energy-to-break,  $T$  (corresponding to the area under the stress-strain curve), shows a 2-fold variation (consistent with systematic variations in  $\sigma_u$  and  $\epsilon_u$ .)

This general relative insensitivity is as predicted for tests in the glassy state (59); glassy-state properties should be more closely related to cohesive energy density (that is, to the specific polymer chemistry of the system) than to the network structure. In other words, if the polymer behaves as an elastic, brittle solid, one would not expect major differences in glassy behavior. Nevertheless, as may be seen from Figures 36 to 39, small but consistent second-order variations in  $E$ ,  $\sigma_u$ , and  $\epsilon_u$  can be seen, with maxima or minima noted, usually when the amine is slightly in excess. Interestingly, values of  $E$  and  $\sigma_u$  are more than 50% of the values predicted theoretically for a brittle glass (59), confirming that the specimens are reasonably well-behaved.

In some cases, for a given  $M_c$ , the tensile behavior depends on which component is in excess. A similar observation was made for some visco-elastic behavior (see Section VI).

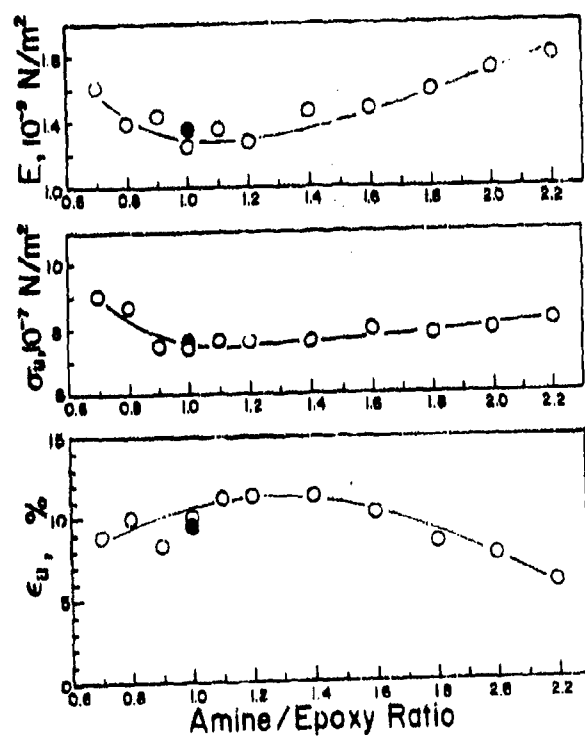


Fig. 35. Tensile parameters for Series A epoxy resins as function of amine/epoxy ratio.

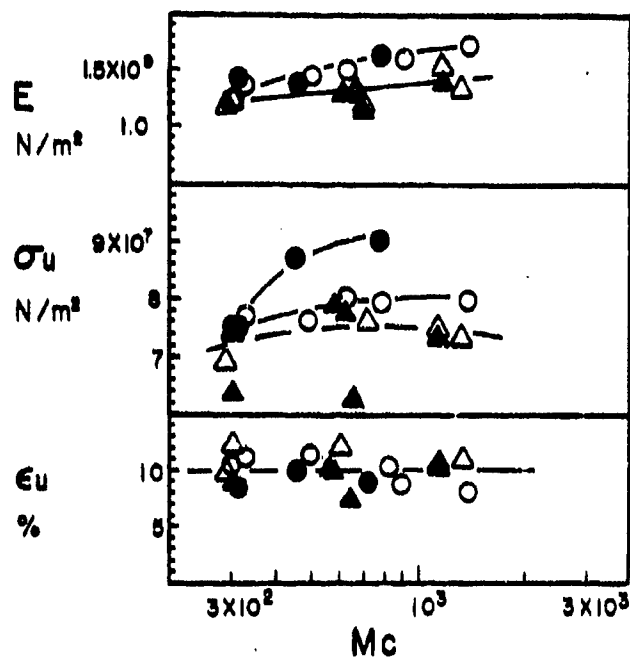


Fig. 36. Tensile parameters as function of  $M_c$ : closed circle, epoxy excess in Series A; open circle, amine excess in Series A; open triangle for Series E; and closed triangle for Series F.

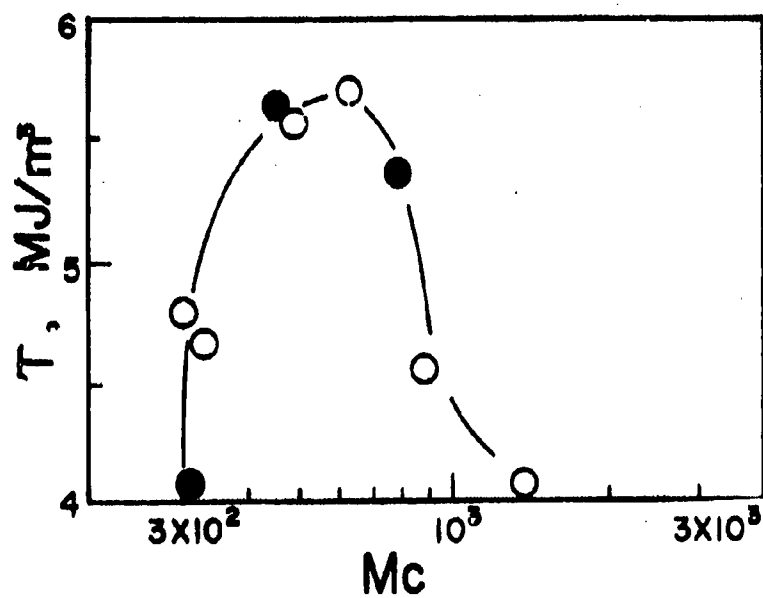


Fig. 37. Tensile toughness,  $T$ , of series A as function of  $M_c$ : closed circle, epoxy excess and open circle, amine excess.

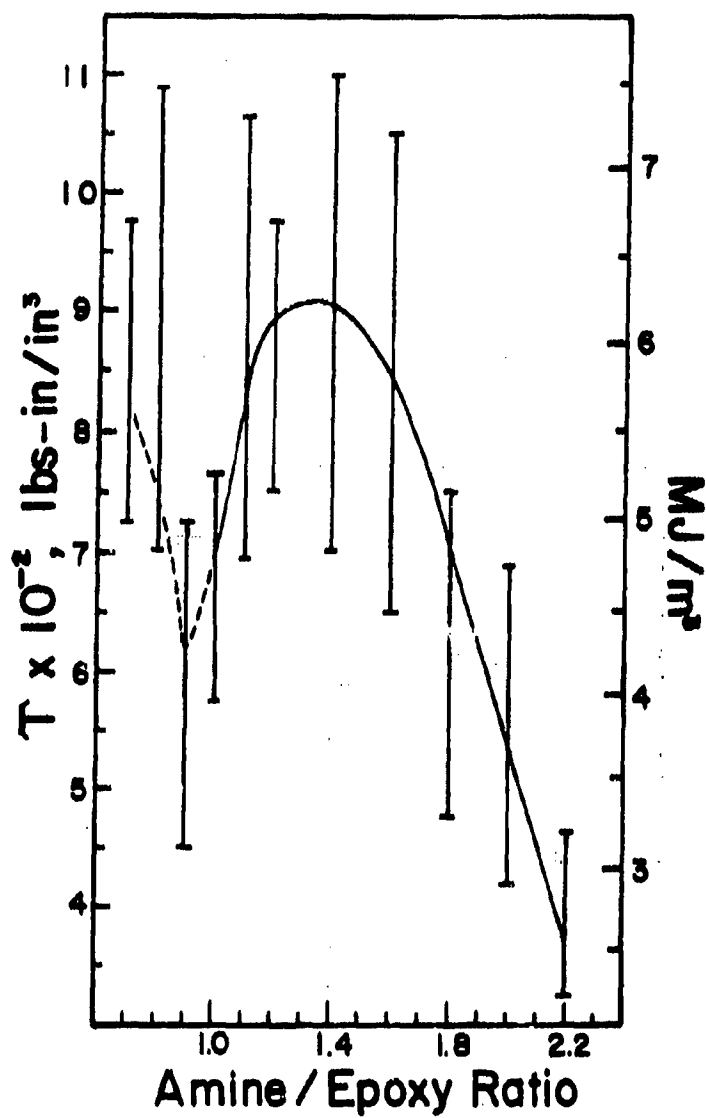


Fig. 38. Tensile toughness,  $T$ , of Series A epoxy resins vs. amine/epoxy ratio.

Values of impact strength (Figures 39 and 40) agree reasonably well with Bell's (46), though the peak with Series A is shifted slightly and flattened. As with T, impact strength is more sensitive to stoichiometry than are E,  $\sigma_u$ , and  $\epsilon_u$ .

In summary, modulus and strength tend to be higher when amine or epoxy is significantly in excess, while impact strength tends to be lower. For further discussion of the interplay between tensile and impact properties, fracture toughness, and morphology, see sections VIII--3.4 and IX.

## 2. Series E Epoxy Resins (Unblended Commercial Resins)

Tensile data for Series E are given in Table 26 and Figure 36. Results are in reasonable agreement with those of Series A, when plotted as a function of  $M_c$ , though the data are somewhat more scattered, with results at the highest  $M_c$  tending to fall below the trend for Series A. In general, however, as with viscoelastic behavior, tensile behavior tends to follow  $M_c$  regardless of whether a particular  $M_c$  is obtained by changing stoichiometry or by changing prepolymer molecular weight.

Table 26. Tensile Data for Series E Epoxy Resins

Sample	% Elongation	$E_g$ , GPa	$\sigma_u$ , MPa	$\sigma_y^a$ , MPa
E-1	9.9±1.0	1.12±.12	69±3	-
E-2	12.7±1.2	1.15±.11	75±2	-
E-3	12.3±2.2	1.13±.10	76±3	-
E-4	9.0±0.5	1.34±.10	74±3	-
E-5	10.5±0.7	1.52±.13	69±3	75±2 <sup>b</sup>
E-6	10.8±1.7	1.23±.05	64±7	74±1 <sup>b</sup>
E-7	-	-	-	-

<sup>a</sup>Yield Strength (where observable).

<sup>b</sup>Actual stress at fracture.

Impact strengths (Figure 40) do not agree as well with those of Series A as did other properties (perhaps due to differences in operator technique, impact tests being very sensitive to this factor). However, the results are internally consistent, and show, in contrast to the case of Series A, a tendency to decrease as  $M_c$  increases (that is, as the prepolymer molecular weight increases).<sup>c</sup>

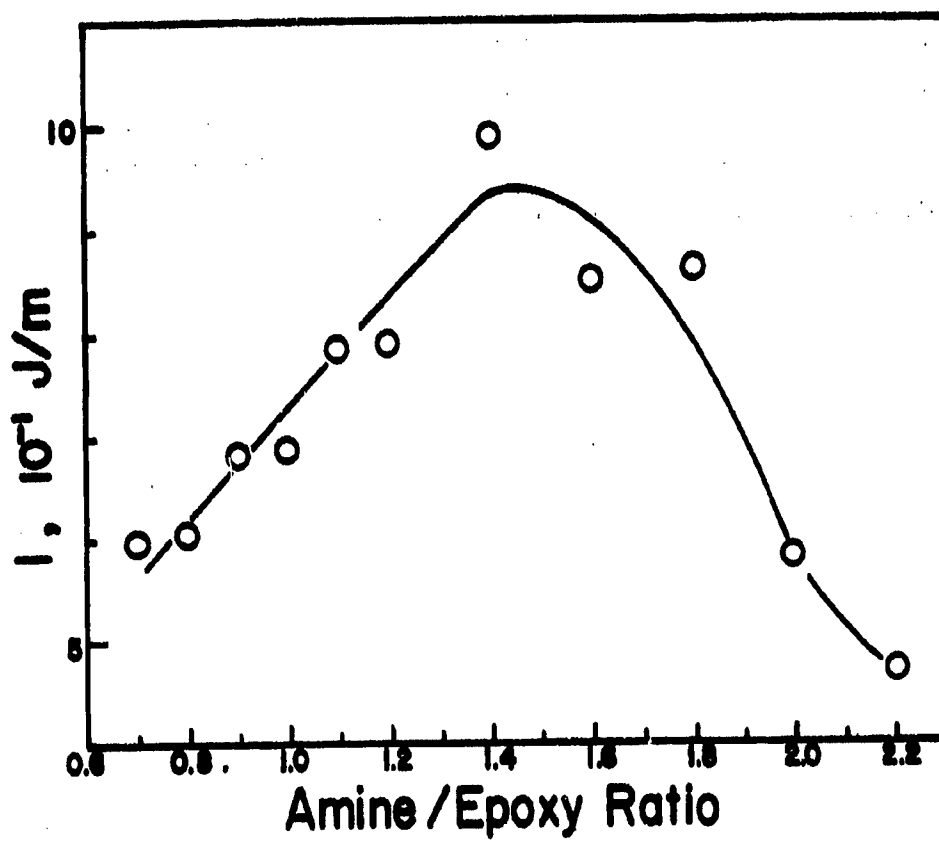


Fig. 39. Charpy Impact strength,  $I$ , of Series A epoxy resins as function of amine/epoxy ratio.

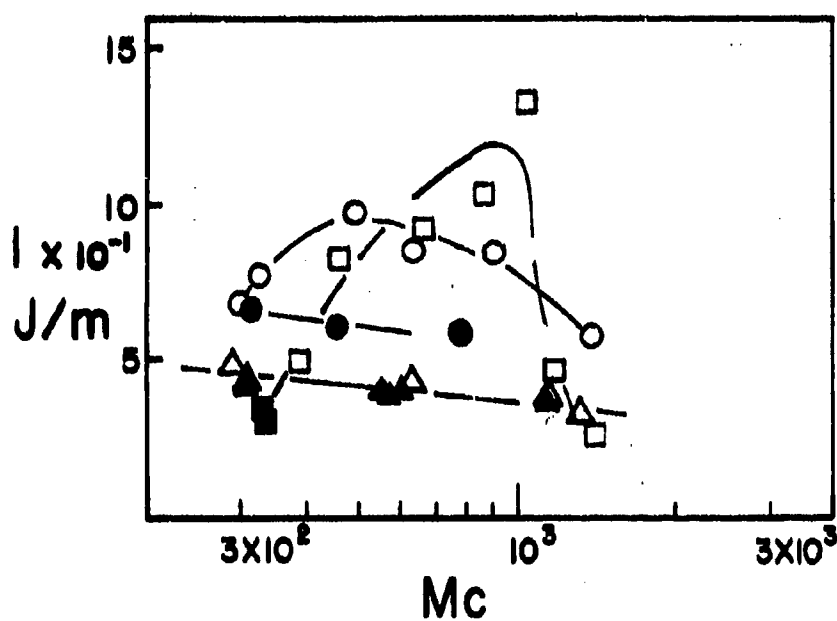


Fig. 40. Charpy impact strength,  $I$ , as function of  $M_c$ : closed circle, epoxy excess in Series A; open circle, amine excess in Series A; open triangle for Series E; closed triangle for Series F; and squares are Bell's data (ref. 46).

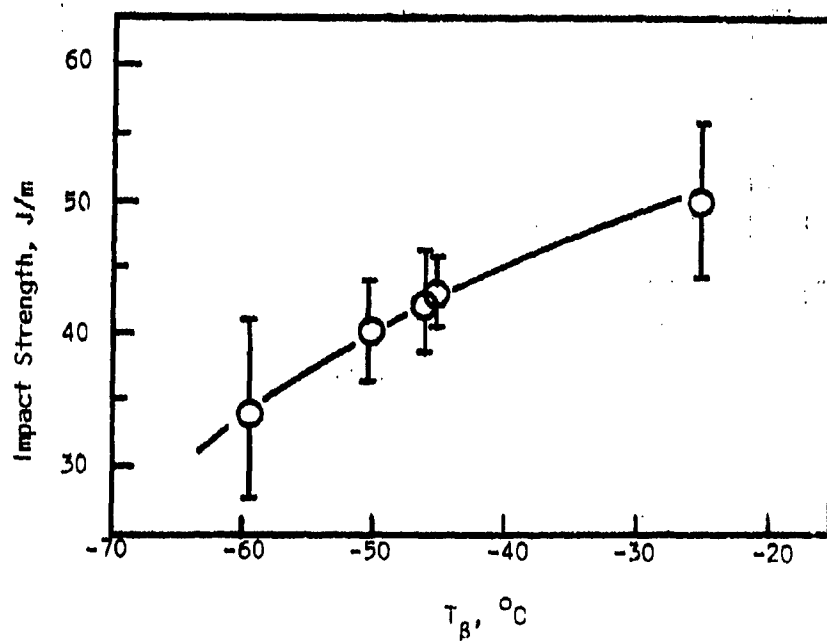


Figure 41. Impact strength and  $\beta$ -transition temperature for series E epoxy resins.

Table 27. Impact Data for Series E and Series F Epoxy Resins

Sample	Impact Strength, J/m	Sample	Impact Strength, J/m
E-1	50±6	F-1	42±2
E-2	43±3	F-2	41±3
E-3	42±4	F-3	38±2
E-4	-	F-4	41±3
E-5	40±4	F-5	37±4
E-6	34±7		
E-7	-		

In view of the fact that impact strengths may be related to the  $\beta$ -transition behavior (77), the relationship was examined with Series E. It was found that the higher  $T_g$ , the greater the impact strength (Fig. 41). This behavior was not noted with series A. Conceivably this relationship, which agrees with some results reported by Vincent (78) but which disagrees with other results in the literature, may be due to a role of  $\tan \delta$ , which would be higher, the closer the test temperature to  $T_g$ .

### 3. Series F Epoxy Resins (Bimodal Blends)

Tensile data are summarized in Table 28 and Figure 36. In general, values of  $E_g$  and  $\sigma_y$  tend to fall below the values reported for Series E (and Series 9A).

Table 28. Tensile Data for Series F Epoxy Resins

Sample	% Elongation	$E_g$ , GPa	$\sigma_y$ , MPa	$\sigma_u$ , MPa
F-1	8.5±2.0	1.20±.11	63±9	-
F-2	10.1±1.6	1.23±.10	75±5	-
F-3	9.6±1.4	1.24±.13	77±6	-
F-4	7.2±1.8	1.10±.10	62±10	-
F-5	10.5±0.7	1.30±.31	64±2	73±5

Impact strengths, on the other hand (Table 27), agree well with those found for Series E, though they too lie below the range found for Series A.

In short, the bimodal blends may indeed show some deviations from the behavior for other epoxy resins, but the differences are small. The greatest deviation noted was for specimen F-4, which, as noted above, appears to be anomalous in other respects.

f. Correlation of Tensile, Impact, and Fatigue Data

In any attempt to correlate mechanical data, the basic differences in tests must be kept in mind. Thus, tensile tests are run at low rates using unnotched specimens, impact tests are run at high rates using, in this case, bluntly notched specimens, and  $K_{IC}$  tests are fast using sharp notches. It must also be kept in mind that various parameters may act in opposing ways; for example, plasticization tends to enhance elongation but to weaken the material as well.

An example of the competitive effects may be seen in the case of series A. As discussed above,  $K_{IC}$  increases monotonically by a factor of 2 as the amine/epoxy ratio is increased, while  $\sigma_u$  first decreases and then increases. The question of Griffith's (60) critical flaw size,  $a$ , was also of interest. To evaluate relative changes in  $a$  as stoichiometry was varied, values of  $a$  were estimated from the following equation:

$$K_{IC} = \frac{2}{\sqrt{\pi}} \sigma_u \sqrt{a} \quad (26)$$

where  $a$  = the radius of a hypothetical disc-shaped flaw embedded in a tensile specimen, with the plane of the disc perpendicular to the tensile axis. In this simple example,  $\sigma_u$  is taken to be the smooth-bar tensile strength and  $K_{IC}$ , the fracture toughness. While an actual flaw may not correspond to this model, the trend of the calculated values will not be affected.

Calculations with series A show that  $a$  increases monotonically from 32 $\mu$ m to 141 $\mu$ m as the amine/epoxy ratio is increased from 0.7 to 2.0. Values of  $a$  for series E range between 72 $\mu$ m and 337 $\mu$ m, depending on the epoxy molecular weight. These values are in the range of sizes of heterogeneities observed by the SEM (see section VIII).

Several correlations do, however, pose special problems. Why in series A does impact strength rise and then fall as the amine/epoxy ratio is increased? It is difficult to see why the decrease would occur when  $K_{IC}$  (and hence the resistance to growth of a crack) is increasing. Also, why should the modulus increase in amine and epoxy-rich compositions? No clear answer is evident.

## SECTION VIII

### MORPHOLOGY AND NETWORK MODELS

#### A. Introduction

Since the properties of thermosetting polymers depend on their network structures, the morphology of such polymers has long been a subject of considerable theoretical and practical interest [for a recent review, see Morgan and O'Neal (15)]. Thus, it is well known that the tensile strength of thermoset resins is less than predicted theoretically on the basis of the breakage of primary or van der Waals' bonds (59), and it was proposed long ago (78) that the discrepancy was due to the rupture of weak regions created during network formation. Indeed, it has been shown (23) that high internal stresses can be developed during curing, especially when the curing rate is low. This view of the role of structural defects is also given credence by modern theories of fracture mechanics (31), which emphasize the concept of the concentration of stress at a flaw (see section VII).

Other investigators [9,22,23,59,76,79,80; see also other references cited by Morgan and O'Neal (15)] have emphasized a view of the network as essentially a composite, with a high-crosslink-density (essentially spherical) phase (often considered as a microgel) embedded in a less-crosslinked matrix. In fact, it is probably generally accepted that, regardless of specific details, the curing of thermosets results in an inhomogeneous, two-phase network. Inhomogeneity has been attributed to compatibility problems or non-optimum curing conditions (59), but has also been proposed to be inherently characteristic of gelling systems (76).

The existence of inhomogeneities has been inferred from results of diverse investigations using many techniques, including electron and optical microscopy, thermomechanical measurements, differential swelling, and differential scanning calorimetry. Dispersed phases have been referred to by such terms as "micelles," "globules," "flocules," "nodules," and "microgels." In this study, the term "microgel" will be used.

In general, two levels of sizes have been reported in the literature--one (type A) ranging from 10nm to 40nm, and the other (type B) from 20 $\mu$ m to 200 $\mu$ m. It has also been shown (23) that slow curing rates result in larger microgels (type B) which result in a network having higher  $T_g$ , density, and resistance to etching. The surface properties of the network depend on the surface energy of the mold material and on the atmospheric environment (22, 25). The size and density of these microgels have also been related to the presence of plasticizer (81), radiation damage (82), prolonged exposure to heat (83) and aging of the resin (84).

Studies (25) have also shown that certain substrates such as teflon and silicone mold release agent give featureless surfaces, but subsequent etching of the surface show the two-phase structure (25). Microtomed thin sections and small-angle X-ray scattering fail to indicate two-phase structures (17), probably because the electron density of the dispersed phase and the matrix are not sufficiently different.

Both low tensile strengths and nodular morphology in thermosets have been theoretically related to differences in crosslink density (22, 76,80). At the same time, the fact that the yield strength of some epoxies is fairly independent of stoichiometry, has been attributed to the role of microgels as primary flow particles (15).

In this study, morphology was examined as a function of stoichiometry, molecular weight of the epoxy prepolymer and distribution of  $M_c$  in blends. Results are discussed below and implications proposed with respect to model behavior.

## B. Experimental Details, Results and Discussion

### a. Morphological Studies.

Various etching techniques were tried to study the micro- or macro-structure of epoxy networks ("macro-" implying a morphological feature on a scale of  $\mu\text{m}$  or larger). Surfaces (not fracture surfaces) of sample E-2 were etched with HF acid for 30 minutes, with acetone for 15 days, with argon at high voltage under vacuum for 10 hrs, and with a molal aqueous solution of  $\text{Cr}_2\text{O}_3$  (17) at  $80^\circ\text{C}$  for 7 hrs. The etched samples were examined under the SEM. Of all the methods  $\text{Cr}_2\text{O}_3$  etching proved to be the most effective. Argon-milling did produce some effects but not as extensively as  $\text{Cr}_2\text{O}_3$  etching. Then the effect of etching time was studied on sample E-7 with a molal aqueous solution of  $\text{Cr}_2\text{O}_3$  at  $80^\circ\text{C}$ . The specimens were examined after soaking for 1/2 hr, 1 hr, 2 hrs, 4 hrs, and 7 hrs, respectively. It was observed that 1 hour was not sufficient to etch the surface. As shown in Figure 42, progressive etching revealed a very interesting macrostructure with feature sizes of  $\sim 10\text{-}40\ \mu\text{m}$ . Chemical etching renders the less coherent polymer constituents more soluble in water without appreciably affecting the solubility of the high molecular weight material. If the high molecular weight material is connected by weak bonds to the matrix then these weak bonds would be attacked first thus etching out the unattached high molecular material first, before etching the low molecular weight matrix. To study the microstructure of the cured resins, using a two-stage replication technique, an etching time of 4 hrs. was found more convenient. Replicas made from 7-hr-etched surfaces caused experimental difficulty on the microscope.

Samples of Series A, E and F were etched for 4 hrs. at  $80^\circ\text{C}$  in a molal aqueous solution of  $\text{Cr}_2\text{O}_3$ , and two stage replicas were made to study the fine structure. Similar samples were also etched for 7 hr in the same medium to be scanned under the scanning electron microscope (SEM) to determine the gross morphology. Details are discussed below.

## 1. Series A (Varying Stoichiometry)

Examination under the SEM (Figures 43 and 44) revealed a two-phase structure. Dimples were observed on the surface, the dimple size increasing with the amount of MDA in the amine-excess region. Samples having an epoxy excess appeared to be smoother than samples which have similar M but an excess of amine. The sizes of these phases varied from 10 $\mu$ m to 70 $\mu$ m depending on the percent excess of reactants, in agreement with sizes reported by Cuthrell (22). It was also observed that above an amine/epoxy ratio of 1.6/1 the morphological difference was negligible.

The two-stage replicas examined with the transmission electron microscope (TEM) also revealed the existence on a much finer scale of two phases (Figure 45). It should be noted that dimples on a two-stage replica represent elevations or nodules on the actual surface and vice-versa. The replicas showed nodules on the surfaces, corresponding to dimples on the polymer surface, as described by Racich and Koutsky (25).

(One must be very careful in interpreting statements about features seen in replicas. A nodule in a two-stage replica arises from a dimple on the polymer surface; in turn, the dimple may reflect the popping out of a polymer nodule.) The phase sizes were found to be in the range of 20nm to 200nm. It was also observed that as the amount of amine was increased from equal stoichiometry the phases increased in average size. The epoxy-excess samples had smaller-size domains, in any case.

## 2. Series E (Commercial Resins, Varying Prepolymer)

In these cases also (Figures 42, 46, 47), a two-phase-structure was found. A marked difference in morphology was also observed to exist in the specimens from liquid resins as compared to those from solid and semi-solid resins. In the samples from solid and semi-solid resins, highly crosslinked shells were observed encapsulating less-crosslinked material.

It was also observed that the morphology was similar throughout the thickness of the samples (Figure 48). Also, the inhomogeneity did not arise from poor mixing for casting from acetone solutions yielded similar behavior. (In this case, using a fraction of Epon 1001 obtained by precipitation from solution by adding nonsolvent.) The discontinuous phase size was found to increase with increasing molecular weight of the prepolymer. The volume of the continuous phase was found to decrease with increasing molecular weight of the prepolymer. The domain sizes of the large discontinuous phase were found to be in the range of 10 $\mu$ m to 70 $\mu$ m depending on the type of prepolymer used.

It was observed that all the samples made from the solid prepolymers had nearly the same fine structure having the discontinuous phase in the range of 10nm to 20nm.

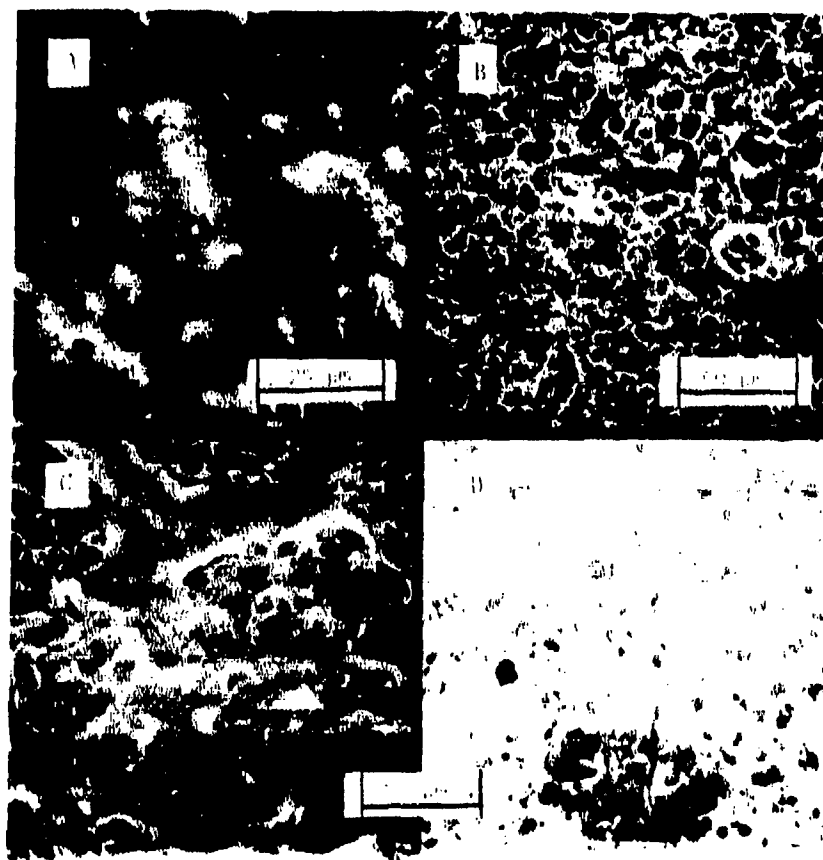


Figure 42. Scanning electron micrographs of epoxy (E-7) surface etched with aq. Cr<sub>2</sub>O<sub>3</sub> for various periods of time: A=2 hr, B=4 hr, C=7 hr, and D=11 hr.

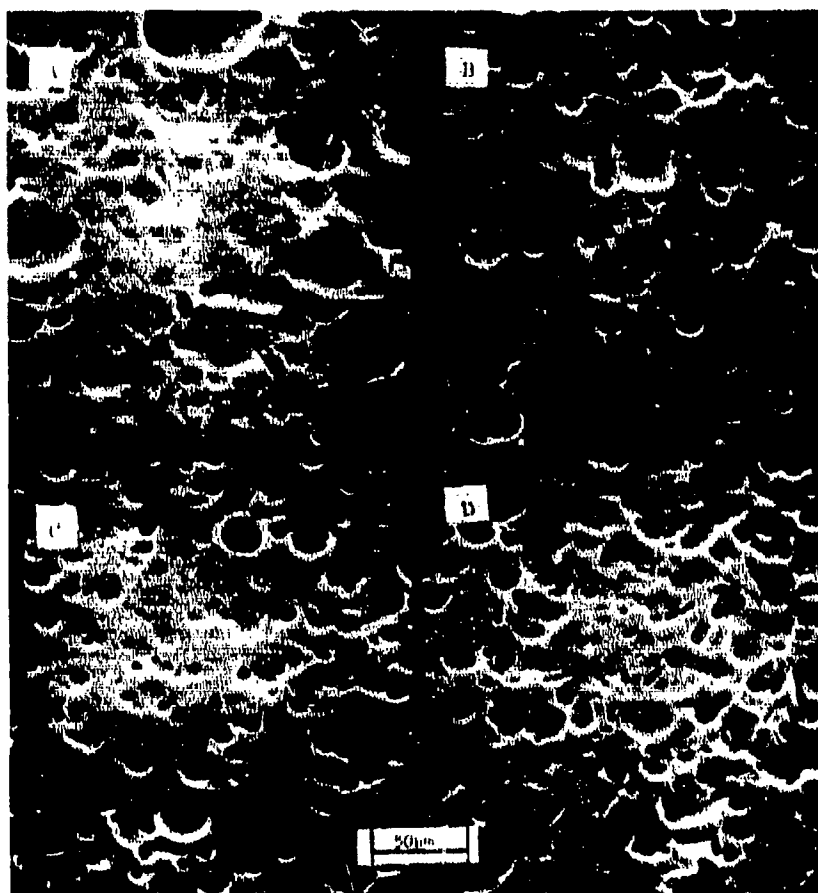


Figure 43. Scanning electron micrographs of series A epoxy resins (etched 7 hr in  $\text{Cr}_2\text{O}_3$ ): A=A-7, B=A-8, C=A-10, and D=A-11.

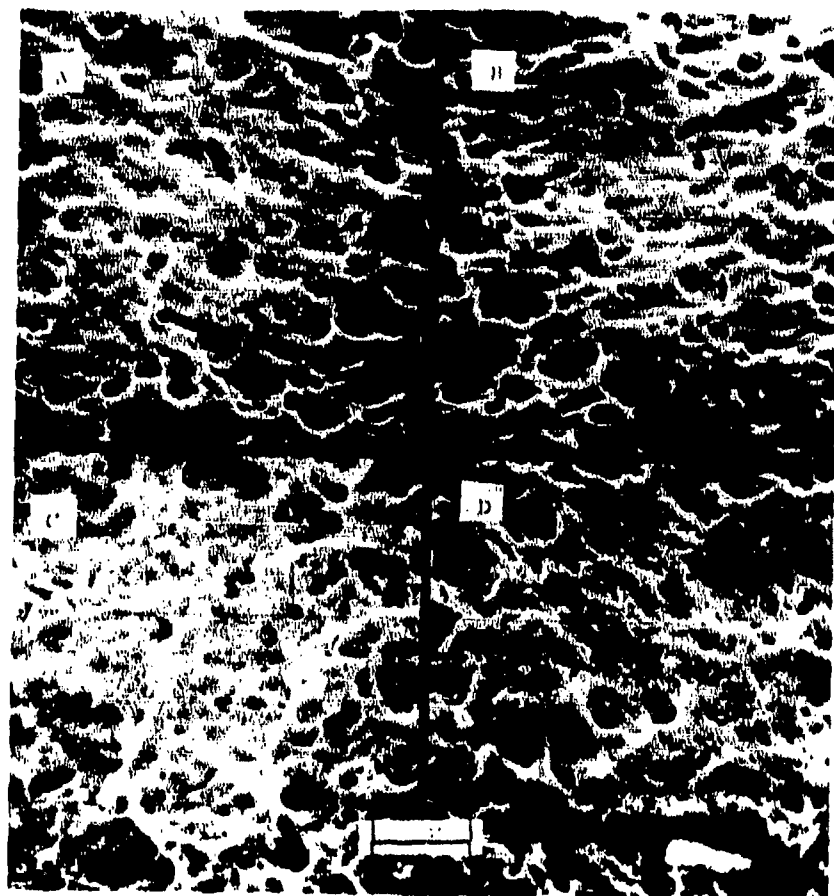


Figure 44. Scanning electron micrographs of series A epoxy resins (etched 7 hr in  $\text{Cr}_2\text{O}_3$ ): A=A-14, B=A-16, C=A-18, D=A-20.

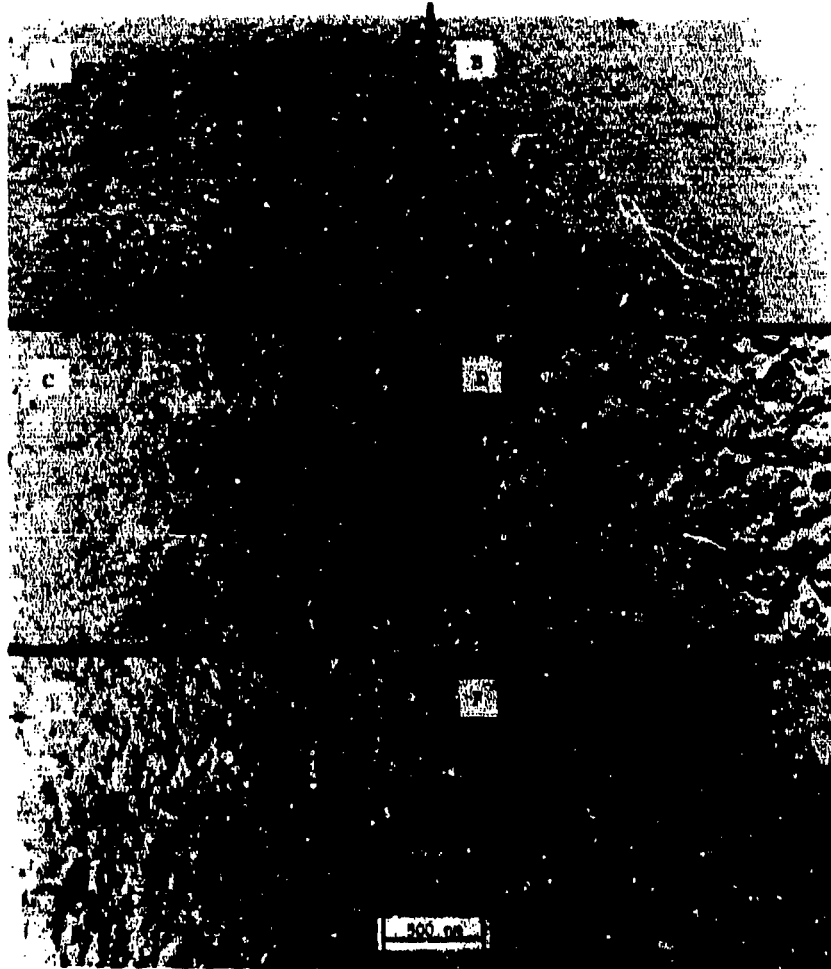


Figure 45. Electron micrographs of replicas made after etching samples of series A for 4 hr. in aq.  $\text{Cr}_2\text{O}_3$ : A-A-7, B-A-8, C-A-11, D-A-14, E-A-16, F-A-20.

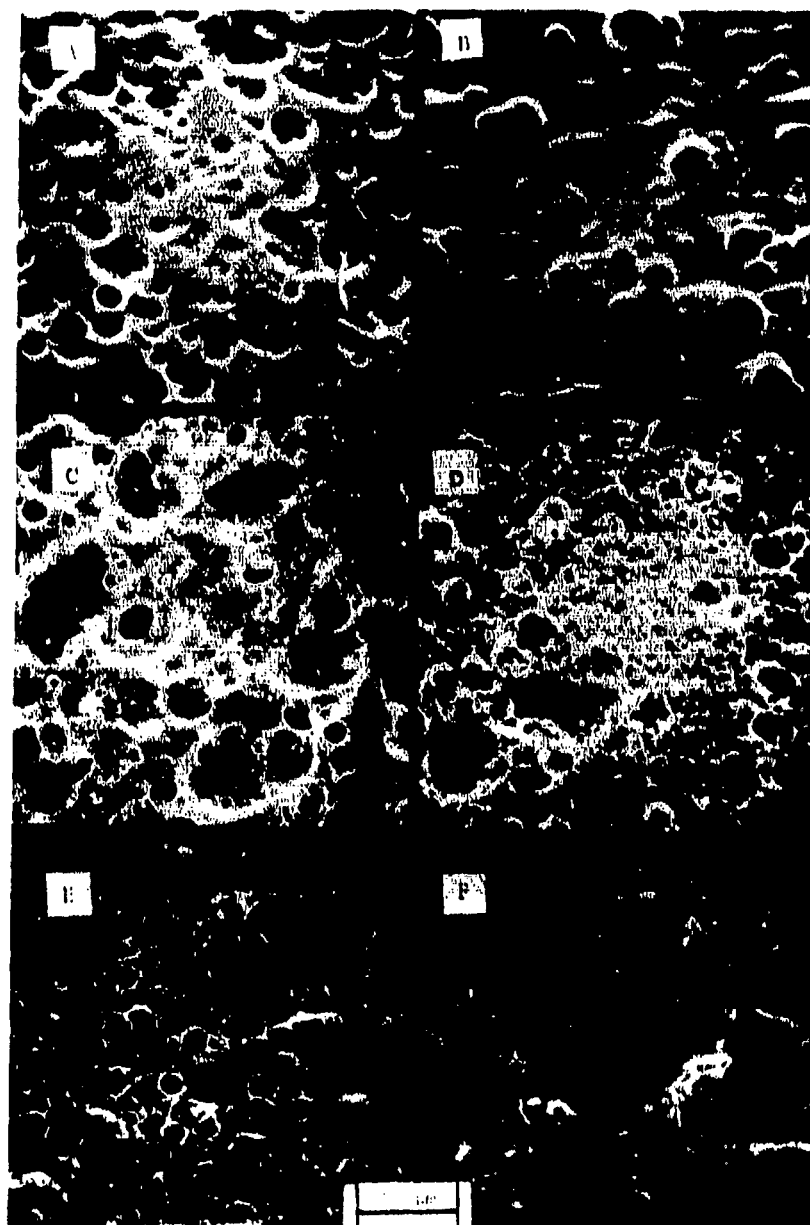


Figure 46. Scanning electron micrographs of series E epoxies etched with aq. Cr<sub>2</sub>O<sub>3</sub> for 7 hr: A=E-1, B=E-2, C=E-3, D=E-5, E=E-6, F=E-7.

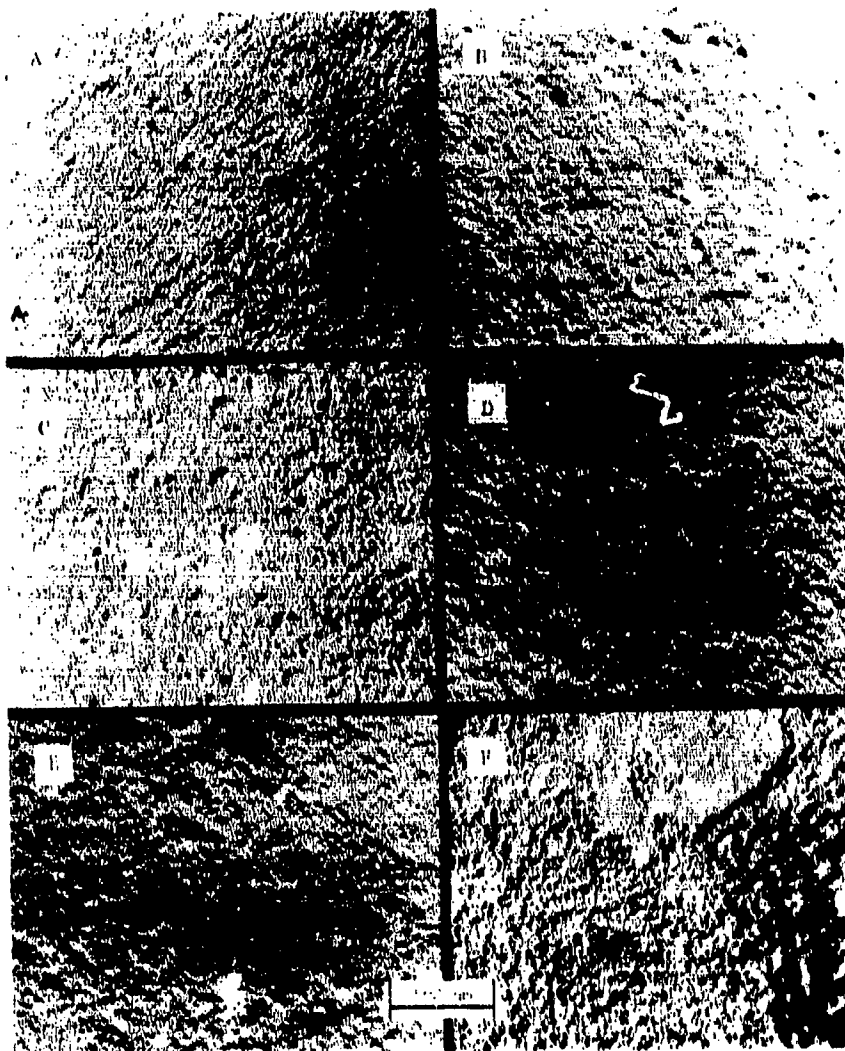


Figure 47. Electron micrographs of 2-stage replicas of series E samples etched for 4 hr in aq.  $\text{Cr}_2\text{O}_3$ : A=E-1, B=E-2, C=E-3, D=E-5, E=E-6, F=E-7.

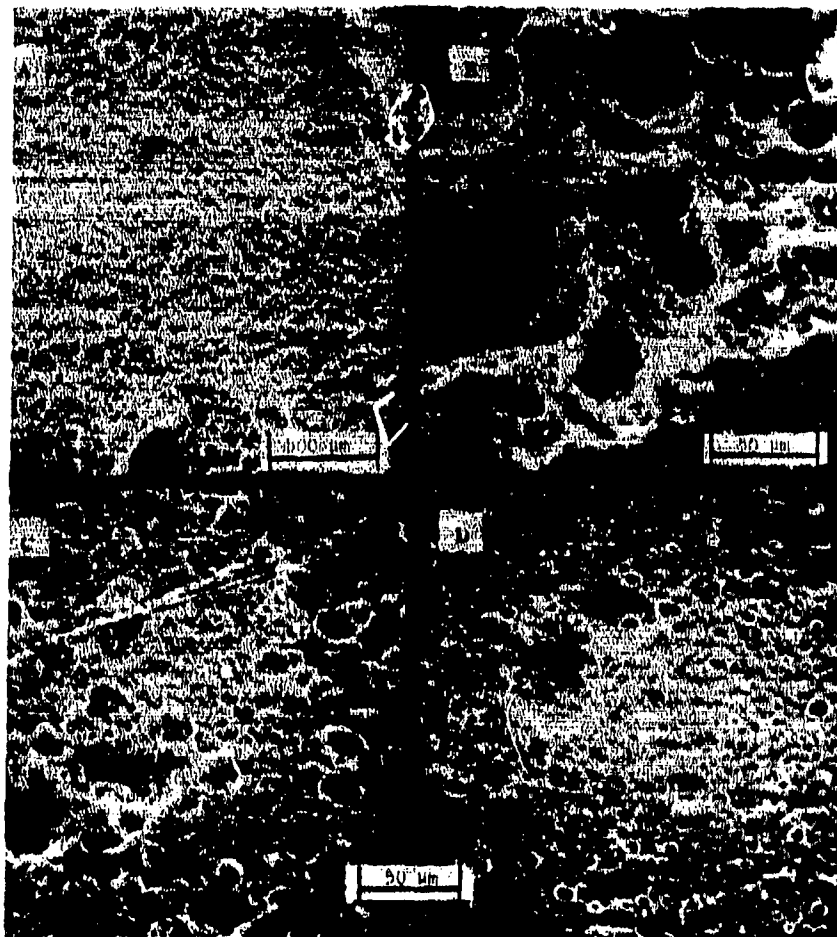


Figure 48. Electron micrograph of Epon 1001/MDA epoxy (E-5) etched for 7 hr in aq.  $\text{Cr}_2\text{O}_3$ . A and B, cross-section area; C, surface; D, resin cast using an acetone solution of a fraction of Epon 1001.

### 3. Series D (Cured with Versamid 40).

These samples also appeared to have a morphology similar to the samples mentioned above (Figure 49). The size of the discontinuous phase was much larger because it had a higher  $M_c$  and lower glass transition temperature ( $\sim 80^\circ\text{C}$ ), and hence was etched out much more.

### 4. Series F (Bimodal Blends)

In these cases (Figs. 50-52), the gross morphology appeared smoother and different from their equivalent counterparts of series E. However, the fine structure did not look much different from that for the equivalent counterparts of series E.

### 5. Isolation of Microgel

To determine whether the dimples observed in SEM & TEM were due to the extraction of higher molecular weight material (i.e., clumps of microgels) or of lower molecular weight phases, the following experiments were done.

Samples of E-2 and E-5 were dissolved before gelation in acetone. Since E-2 has a much longer gelation time than E-5 it was dissolved in acetone after curing at  $60^\circ\text{C}$  for 30 minutes and at  $80^\circ\text{C}$  for another 15 minutes. On the other hand, sample E-5 was dissolved in acetone after curing at  $100^\circ\text{C}$  for only 10 minutes. The solution was diluted to 100 ppm and electron microscope grids were made. Similarly the cured films of these resins were cut into small pieces and etched in a 1-molar solution of  $\text{Cr}_2\text{O}_3$  at  $70^\circ\text{C}$ . The etching solutions were then diluted and electron microscope grids were prepared. Electron micrographs are shown in Fig. 53.

In both cases microgels were observed, indicating that microgel formation takes place before gelation and that the microgels are dispersed and loosely connected to a weaker continuous phase and creating the holes on the surface observed earlier. This experiment also made it clear that the discontinuous phase (though etched out first as clumps) is composed of microgels which are stronger than the continuous phase. It is the connections between the aggregates that are weak. The size and number of these gels keep on increasing till the viscosity becomes high enough for gelation to take place.

### 6. Conclusions

Clearly small microgels ( $\sim 100$  nm) are formed, even before gelation. The particles appear to be embedded in a matrix of lower crosslink density, though they may also aggregate together. In the case of solid prepolymers, an additional phase is present: shells of highly crosslinked resins in a matrix of lower crosslink density, but containing material of still lower crosslink density.

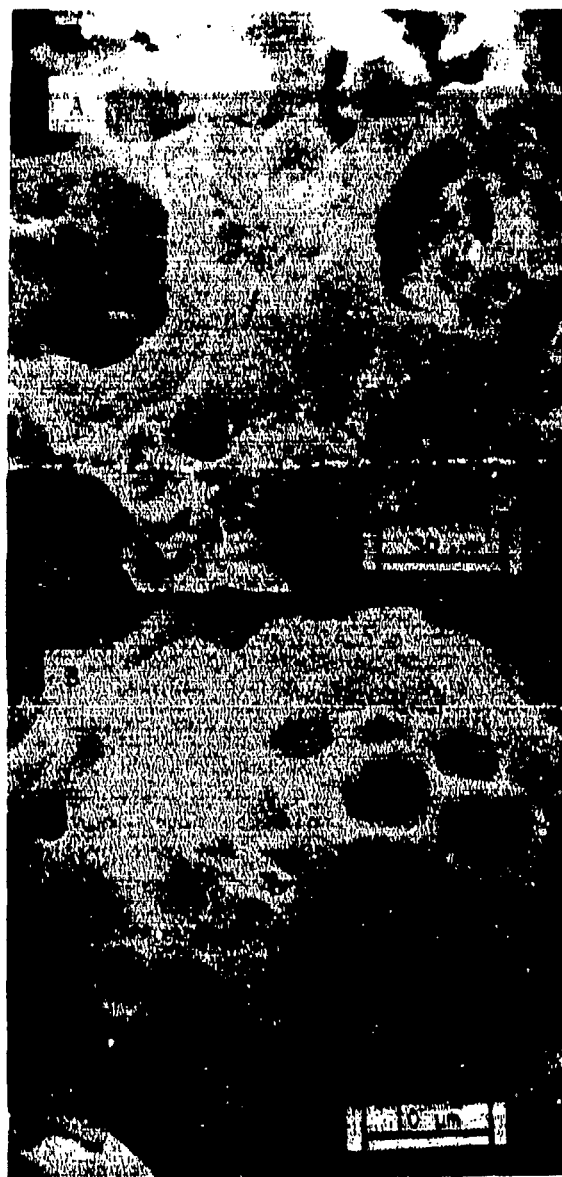


Figure 49. Scanning electron micrographs of Epon 828/Versamid 40 epoxy (described in reference 49; contained glass beads).

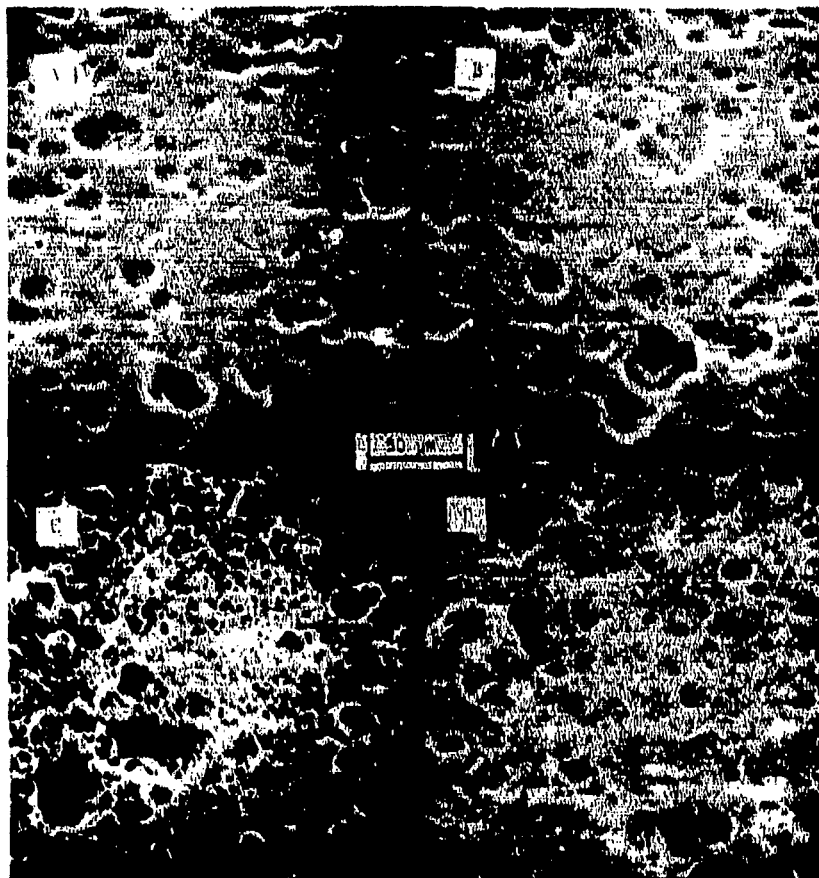


Figure 50. Scanning electron micrographs of series F epoxies, etched 7 hr with aq.  $\text{Cr}_2\text{O}_3$  and their counterparts in series E: A=E-2, B=F-1, C=E-5, and D=F-5. Specimens F-1 and F-5 were blended to match E-2 and E-5, respectively.

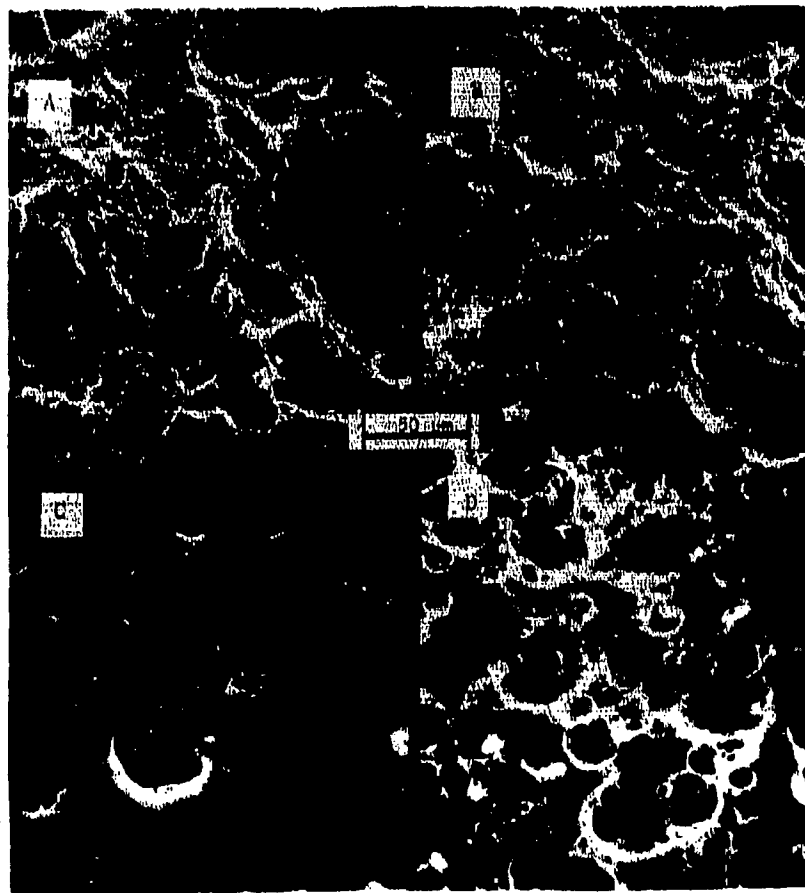


Figure 51. Scanning electron micrograph of series F epoxies etched 7 hr in aq.  $\text{Cr}_2\text{O}_3$ : A=F-2, B=F-3, C=F-4, D=E-3; specimen F-4 is the counterpart of specimen E-3.



Figure 52. Electron micrographs of 2-stage replicas of series F epoxies, etched 4 hr in aq.  $\text{Cr}_2\text{O}_3$ : A=F-1, B=F-4, and C=F-5.

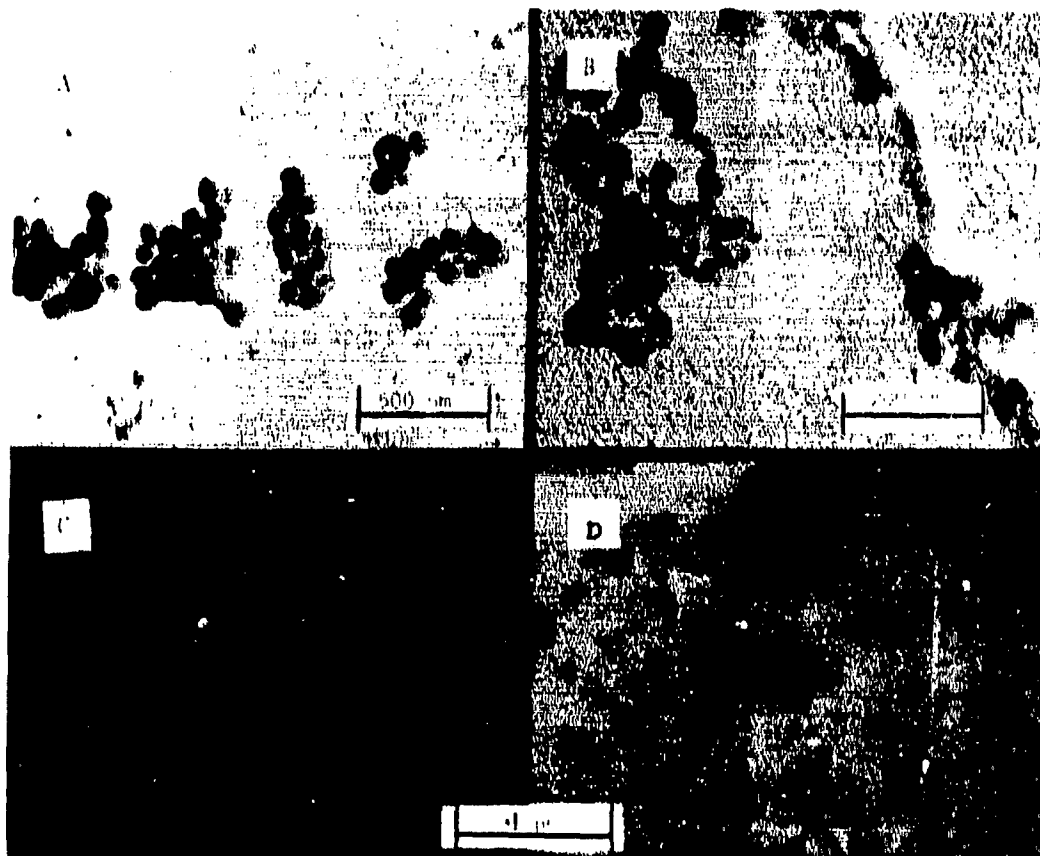


Figure 53. Electron micrographs showing microgel particles from epoxies (using formulations for E-2 and E-5). A and B show gel particles etched out from cured epoxy by aq.  $\text{Cr}_2\text{O}_3$  after 4 hr at 70°C. C and D show microgel isolated prior to gelation.

b. Model for Network Formation:

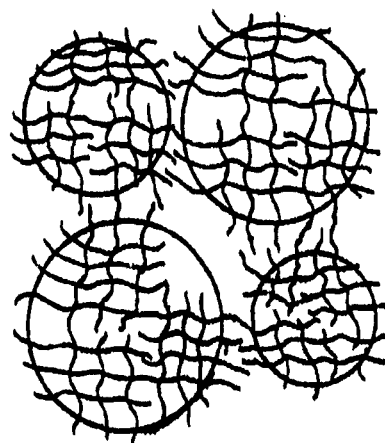
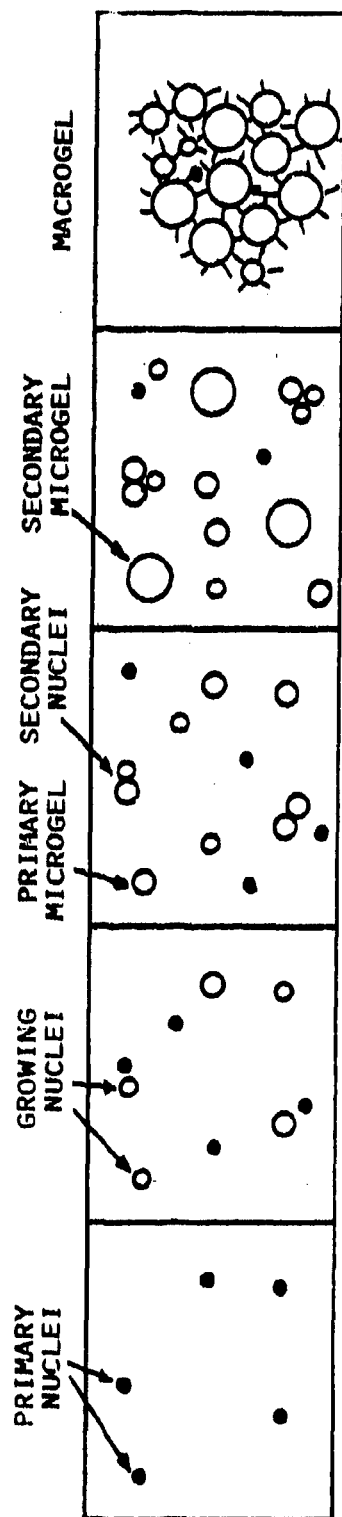
Even though paradoxical behavior still exists, it is interesting to speculate on what kind of model network would be reasonably consistent with the morphological and property data at hand. The principal points to consider include the following questions: the basic morphological unit or units, the phase continuity, and the crosslink density and other properties of the various entities.

First, electron microscopic evidence shows that microgel particles from prior to gelation (Fig. 53), both with low and high-molecular-weight epoxies, and with epoxy and amine-rich systems. [Even with an excess of amine, insoluble and crosslinked polymer is formed, presumably because of reaction of some secondary amine groups (46).] This conclusion is in accord with the suggestion of, for example, Bobalek et al. (80). These particles should have sizes of the same order of magnitude, though they may tend to be somewhat larger, the higher the prepolymer molecular weight, as predicted theoretically (76). As curing proceeds, the number of particles increases until they begin to impinge on one another. Then, in part due to capillary forces which will encourage physical sintering, and in part due to the reaction of unreacted functional groups, the particles first agglomerate in clumps and then fuse together with concomitant phase inversion. In effect this model adds an agglomeration step to the model proposed by Bobalek et al. (76) (see Fig. 54). The formation of large aggregates is compatible with the critical flaw size found in section VII.

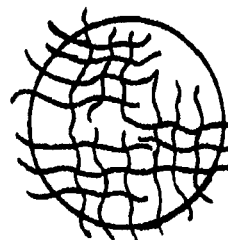
Now we propose that, at least in some cases (such as when one component is in excess), a separate phase may collect in the interstices and ultimately undergo polymerization (with second-stage microgel formation) giving in effect an interpenetrating network. When co-solubility is especially low, as with the solid epoxy resins, the first continuous network formed may actually establish a skin within which curing proceeds again, with secondary microgel formation.

In any case, the network which reacts first will (if analogous to the case of interpenetrating networks - see section V) should dominate properties, even for the same average  $M_c$ . Also this network will have more time to coalesce and enhance its continuity.

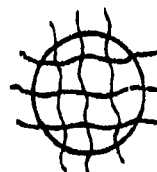
With a high-molecular weight epoxy, microgel formation should be completed early. Large aggregates may be formed, but the connections may be inherently weak. With an excess of amine, microgel should again be formed early, but the plasticizing effect of the amine may enhance the development of enhanced continuity.



MACROGEL



SECONDARY MICROGEL



PRIMARY MICROGEL

Figure 54. Proposed mechanism for morphology development.

Whether the critical flaw size corresponds to the aggregates first formed prior to phase inversion, or whether it corresponds to the inclusions is, of course, not known. Indeed, the reality of a flaw corresponding to the calculated value of  $a$  is not proven. Nevertheless, the close agreement between microscopic evidence and the computed flaw size is strongly suggestive of a correlation.

Now as the amine content is increased, the overall plastic deformation will be increased due to the plasticizing character of the amine, while the modulus  $E$  is not decreased (in fact, increased). Hence  $S$  and  $K_C$  increase.  $E$  itself may well increase due to enhanced continuity of the network. At the same time the flaw size increases, but not as fast as  $S$  so that tensile strength actually increases a little. But with an epoxy excess, the decreased flaw size (corresponding to smaller aggregates) more than balances out the lower value of  $S$  so that strength again increases. However, the toughness otherwise seen at high amine contents is vastly reduced by the high loading rate in impact, while with epoxy excess, the smaller flaw size is able to delay fracture.

When the molecular weight of the epoxy is increased, different behavior occurs. The inherent  $S$  of epoxy components is low compared to that of amine, and hence tensile strength does not increase and impact strength decreases.

With broad distributions such as in the bimodal blends, the properties will be determined by the dominant component. If it is a high-molecular-weight resin (which is more reactive) this network will dominate,  $T_g$  will be low, perhaps because the initial fast reaction yields a rather weak network. At intermediate concentrations, a judicious balancing may occur, and properties may be governed by the low-molecular-weight component.

Although this discussion is clearly speculative, it does explain some of the behavior noted, and suggests ideas capable of testing in the laboratory.

## SECTION IX

### CONCLUSIONS AND RECOMMENDATIONS

#### A. Model Networks

##### a. Conclusions:

Based on research to date, the following conclusions may be made:

(1) The Millar IPN networks exhibit a distinct segregation from each other. The first synthesized network is more continuous in space than the second synthesized network. Electron microscopy shows that the domains are 60-100Å in size.

(2) The results of the poly(styrene)/polystyrene Millar IPN's study bear strongly upon many types of ordinary single networks, such as the thermoset plastics. The results suggest that the first portions of any polymer to reach the gelation stage (when polymerized and cross-linked simultaneously) may be more continuous in space than (accidentally) later portions. If the kinetics of polymerization and crosslinking differ slightly, the drift in composition will have significant effects on mechanical properties such as creep.

##### b. Recommendations for Further Work:

(1) The findings for the PS/PS Millar IPN's should be verified by other experiments, and broadened in scope. Careful experiments, such as interruption of a single network synthesis, altering the crosslinker concentration, and completion of the polymerization ought to be carried out, as such experiments will elucidate the nature and extent of domain separation.

(2) The relationship between Millar IPN's and their respective homopolymers needs exploration. Exactly what is the extent of segregation between early and late polymerized polymer in a single network (or thermoset plastic) synthesis?

#### B. Epoxy Networks

##### a. Conclusions:

Based on research so far, the following conclusions may be made:

(1) Satisfactory experimental techniques have been developed for the synthesis of bisphenol-A-epoxy/MDA and bisphenol-A-epoxy/polyamide resins with the following variations in crosslinking: variable  $M_c$  (by changing stoichiometry or molecular weight of the epoxy); and variable

distribution of  $M_c$  (by blending epoxies of different molecular weights). Attainment of essentially complete curing has been demonstrated.

(2) Standard techniques have been used to determine the following: stress-strain behavior; viscoelastic response (using the Rheovibron elastoviscometer); stress relaxation; swelling; response to differential scanning calorimetry; and morphology (using high-resolution electron microscopy by replica and transmission techniques, and scanning electron microscopy). Also, a standard fatigue fracture technique was successfully modified to conveniently determine the quasi-static fracture toughness and fatigue crack propagation rates as a function of stress intensity factor range and any other fatigue variables of interest.

(3) Thus a precise baseline of viscoelastic and fracture response has been established for use in comparing the effects of any desired variation in composition or network structure.

(4) Viscoelastic responses are usually well-behaved functions of  $M_c$  in typical epoxy systems. Various viscoelastic parameters depend in a quite regular fashion on  $M_c$  whether a given value of  $M_c$  is achieved by changing stoichiometry or by changing the molecular weight of the epoxy - the latter correlation being apparently new. As the degree of crosslinking is increased the following parameters are increased in conformity with expectation:  $T_g$  (or  $T_{\alpha}$ )  $T_g$ , the rubbery modulus, the  $\alpha$  and  $\beta$  transitions, and the creep retardation time. However, the absolute values of  $T_g$  are higher than reported by others using similar curing conditions. The following parameters are decreased by increasing crosslinking: the magnitude of  $\tan \delta$  at its maximum value near  $T_g$ ; and the slope of the modulus-temperature curve at  $T_g$ . In the case of the transition slope, the relationship depends on whether or not the amine or epoxy is in excess. Quantitative correlations were made for series E resins between  $M_c$  and  $T_g$ , Young's modulus, rubbery modulus, and  $\tan \delta_{\max}$ ; these correlations should be of interest for the convenient characterization of  $M_c$ .

(5) The swelling ratio and the soluble fraction are systematically decreased by increased crosslinking, as expected, though results are more variable than the viscoelastic results. Swelling tests were also more difficult to perform than viscoelastic or mechanical tests.

(6) In general, broadening the distribution of  $M_c$  at constant average  $M_c$  had no significant effect on swelling or viscoelastic response. However, possibly significant variations were noted in swelling and in the slope of the modulus-temperature curve for blends of epoxies with widely differing molecular weights. In one particular blend,  $T_g$  and the retardation time were significantly lower than for control specimens, even though no evidence for incomplete curing was found.

(7) Thus, unless a distribution of  $M_c$  is very broad, viscoelastic behavior is determined by  $M_c$ , whether a given  $M_c$  is obtained by changing

stoichiometry or prepolymer molecular weight. Thus testing for  $M_c$  should characterize viscoelastic responses rather well. Indeed, excellent correlations were obtained commercial resins between  $M_c$  and  $T_g$ , Young's modulus, rubbery modulus,  $\tan \delta_{\max}$ , and creep retardation time  $\tau$ . Since  $T_g$  can be obtained very quickly by a variety of tests, and since both  $T_g$  and  $\tau$  are very sensitive to  $M_c$ , use of these parameters in routine testing for consistency of epoxy viscoelastic behavior is recommended.

(8) In contrast to results reported by others, fracture toughness,  $K_{Ic}$ , is a smooth, linear function of the amine/epoxy ratio from less-than-to greater-than-stoichiometric amine contents. All specimens are quite brittle, with values of  $K_{Ic}$  ranging from about 1.1 (excess of amine) to 0.6 (excess of epoxy) MPa $\sqrt{m}$ . The stress intensity factor range,  $\Delta K$ , required to drive a crack at constant velocity under cyclic loading behaves in a generally similar fashion, while the slope of the curves of crack growth rate per cycle vs  $\Delta K$  also appears to be independent of the stoichiometry range of excess amine. (Until this study FCP behavior does not appear to have been described as a function of composition.) Fracture toughness is also increased by increasing the prepolymer molecular weight. Increasing the breadth of distribution in  $M_c$  has little or no effect, except in one case of an exceptionally broad (presumably bimodal) distribution, which showed an exceptionally high  $K_{Ic}$  - 1.5 (but an anomalously low  $T_g$ ).

(9) Curiously, Young's moduli, tensile strength, and elongations (at break) increased as stoichiometry deviated from an equality of functional groups, while impact strength and energy-to-break tended to decrease. Modulus, impact and tensile strengths were decreased by increasing prepolymer molecular weight. Again an anomaly was noted with very broad-distribution specimens, whose tensile strengths tended to be lower than those of the controls.

(10) Scanning and transmission electron microscopy (of etched surfaces) revealed a variety of morphological features, including microgel particles ( $\sim 100$  nm in size), aggregates ( $\sim 40$   $\mu m$  in size), and, in the case of solid epoxy prepolymers, high-crosslink-density skins around the aggregates. The sizes of the large aggregates varied with  $M_c$ ; an effect of  $M_c$  on microgel size was not established. Primary tests showed that these features did not arise from poor mixing, but must have come about during curing. It was also shown that the microgel particles are formed prior to the gel point.

(11) Based on the electron microscopic, viscoelastic, and ultimate mechanical property data, a model may be proposed (similar in some respects to models previously suggested by others, and different in others) to represent the curing of the resins. The model assumes that microgels form, agglomerate, and undergo phase inversion - with inclusion of material crosslinked after the gel point to give in effect a type of interpenetrating network. This model could be used to explain

tentatively at least some of the experimental facts, though further testing and refinement is certainly called for. Interestingly, it was possible to rationalize the conflicting trends in tensile strength and fracture toughness by considering conflicting trends in modulus, fracture energy, and critical flaw size - calculated values for the latter corresponding (perhaps fortuitously well) to the order-of-magnitude sizes of the microgel aggregates. Again, this point requires further study.

b. Recommendations for Further Work:

(1) The relative independence of most behavior on the distribution of crosslinks per se should be tested using a new epoxy system which is free from some of the experimental difficulties associated with conventional epoxy prepolymers. This system, already used by Labana et al. in some preliminary studies, consists of a copolymer of methyl methacrylate with glycidyl methacrylate. By changing the copolymer composition and polymerization conditions we can vary the average spacing of epoxy groups and the prepolymer molecular weight independently. Blends can readily be made for curing with an amine. Emphasis should be placed on the more sensitive properties such as fracture toughness, creep, and  $T_g$ .

(2) Gradients in actual epoxy, and in characteristics should be simulated by providing a gradient of temperature or composition during curing. This may be done by techniques such as quenching surfaces or casting layers of various stoichiometries together.

(3) The effect of cure temperature and diluents should be examined in more detail in both 1 and 2. Also, the kinetics of curing should be studied in detail because of its relationship to eventual morphology. Emphases should be on a statistical approach to functional group reactivity.

(4) In all cases, the detailed morphology should be studied using SEM and replica EM, and variable-time (and more selective) etching. The size, composition, distribution, phase continuity, and volume fraction of various components should be determined, and correlated with kinetics of curing.

(5) The model proposed herein should then be tested and refined by developing a more complete picture of the curing process and by learning more about the relationships between the microgel particles and their aggregates, and phase continuity. Ultimately, the application of quantitative composite relationships involving modulus, strength, and phase continuity should be attempted.

(6) In all cases, torsional creep relaxation should be compared with tensile creep to determine which is more sensitive to variations in network structure per se, and to variations in composition or cure within a specimen.

Results should be useful in (1) confirming what basic network factors are important to the behavior of a crosslinked matrix or adhesive, and (2) developing tests for uniformity within a given resin specimen.

## REFERENCES

1. L. E. Nielsen, "Mechanical Properties of Polymers and Composites", Vol. 1, Marcel Dekker, Inc., New York, 1974.
2. L. E. Nielsen, "Crosslinking-Effect on Physical Properties of Polymers", Monsanto/Washington University/ONR/ARPA Association, Report HPC-68-57, May 1968; J. Macromol. Sci.-Rev. Macromol. Chem., C3 (1), 69 (1969).
3. "Aerospace Structural Adhesives", report of the National Materials Advisory Board, Publication NMAB 300, National Academy of Sciences/National Academy of Engineering, DOD contract no. MDA-903-74-C-0167, July 1974.
4. C. H. Bamford and G. C. Eastmond, "Synthesis, Morphology and Properties of AB Crosslinked Copolymers", In "Recent Advances in Polymer Blends, Blocks and Grafts", L. H. Sperling, ed., Plenum, 1974.
5. J. K. Gillham, J. A. Benci, and A. Noshay, "Isothermal Transitions of a Thermosetting System", J. Appl. Polym. Sci., 18, 951 (1974).
6. T. Murayama and J. P. Bell, "Relation Between the Network Structure and Dynamic Mechanical Properties of a Typical Amine-cured Epoxy Polymer", J. Polym. Sci.-A2, 8, 437 (1970).
7. D. A. Whiting and D. E. Kline, "Effect of Stoichiometric Concentration of Hardener and Percentage Styrene Oxide on the Crosslinking and Mechanical Properties of an Epoxy Resin Cured with DEAPA", J. Appl. Polym. Sci. 18, 1043-52 (1974).
8. A. S. Kenyon and L. E. Nielsen, "Characterization of Network Structure of Epoxy Resins by Dynamic Mechanical and Liquid Swelling Tests", J. Macromol. Sci.-Chem., A3 (2), 275 (1969).
9. D. H. Solomon and J. J. Hopwood, "Molecular Weight Distribution in Alkyd Resins, III. Presence of Microgel in Alkyd Resins", J. Appl. Polym. Sci., 10, 1893 (1966).
10. O. Delatycki, J. C. Shaw, and J. G. Williams, "Viscoelastic Properties of Epoxy - Diamine Network", J. Polym. Sci.-A2, 7, 753-762 (1969).
11. J. P. Bell and W. T. McCarvill, "Surface Interaction Between Aluminum and Epoxy Resin", J. Appl. Polym. Sci., 18, 2243-47 (1974).

12. F. R. Dammont and T. K. Kwei, "Dynamic Mechanical Properties of Aromatic, Aliphatic, and Partially Fluorinated Epoxy Resins", *Polymer Prepr.*, 8, 920 (1967).
13. J. L. Kardos, "Interface Modification in Reinforced Plastics", lecture, U. of Utah Conference Series on Adhesion, June, 1974.
14. T. Hiral and D. E. Kline, "Dynamic Mechanical Properties of Non-stoichiometric, Amine-cured Epoxy Resin", *J. Appl. Poly. Sci.*, 16, 3145-3157 (1972).
15. R. J. Morgan and J. E. O'Neal, "The Mechanical Properties of Polymeric Glasses", *Polymer-Plast. Technol. Eng.*, 5, 173 (1975).
16. N. Hata, "Viscoelastic Properties of Epoxy Resins. I. Effect of Prepolymer Structure on Viscoelastic Properties", *J. Appl. Polym. Sci.*, 15, 2371 (1971).
17. K. Selby and L. E. Miller, "Fracture Toughness and Mechanical Behavior of an Epoxy", *J. Mater. Sci.*, 10, 12-24 (1975).
18. R. G. C. Arridge and J. H. Speake, "Mechanical Relaxation Studies of the Cure of Epoxy Resins: I. Measurement of Cure", *Polymer*, 13 (9), 443 (1972).
19. G. A. Pogany, "Gamma Relaxation in Epoxy Resins and Related Polymers", *Polymer*, 11, 66 (1970).
20. J. N. Sultan and F. J. McGarry, "Effect of Rubber Particle Size on Deformation Mechanisms in Glassy Epoxy", *Polym. Eng. Sci.*, 13, 1 (1973).
21. K. Shibayama, T. Tanaka, and D. H. Solomon, "The Effect of Glyceride Composition on the Mechanical Properties of Alkyd Resin Films", *J. Macromol. Sci.*, A-1, 1531 (1967).
22. R. E. Cuthrell, "Epoxy Polymers II. Macrostructure", *J. Appl. Polym. Sci.*, 12, 1263 (1968).
23. R. E. Cuthrell, "Macrostructure and Environment-Influenced Surface Layer in Epoxy Polymers", *J. Appl. Polym. Sci.*, 11, 949 (1967).
24. R. J. Morgan and J. E. O'Neal, "The Structure-Property Relationships of Epoxy-Amine Systems", *In press*, *J. Appl. Polym. Sci.*
25. J. L. Racich and J. A. Koutsky, "Nodular Structure in Epoxy Resins", *J. Appl. Polym. Sci.*, 20, 2111 (1976).
26. K. Selby and M. O. W. Richardson, "Deformation in an Epoxy Resin Revealed by an Etching Technique", *J. Mater. Sci.*, 11, 787 (1976).

27. P. J. Flory, "Principles of Polymer Chemistry", Cornell University Press, 1953.
28. J. D. Ferry, "Viscoelastic Properties of Polymers", 2nd edition, Wiley, 1970.
29. T. L. Smith, "Relations Between Ultimate Tensile Properties of Elastomers and Their Structures", Proc. Roy. Soc. (London), 282, 102 (1964).
30. F. Bueche and J. C. Halpin, "Fracture of Amorphous Polymeric Solids: Reinforcement", J. Appl. Phys., 35, 3142 (1964).
31. E. H. Andrews, "Fracture in Polymers", American Elsevier, 1968.
32. A. T. DiBenedetto and A. D. Wambach, "The Fracture Toughness of Epoxy-Glass Bead Composites", Int. J. Polym. Mater., 1, 159 (1972).
33. L. H. Sperling, T. C. P. Lee, and A. V. Tobolsky, "Thermodynamic Stability of Elastomeric Networks at High Temperatures", J. Appl. Polym. Sci., 10, 1831 (1966).
34. L. H. Sperling and A. V. Tobolsky, "Thermoelastic Properties of Poly(dimethyl siloxane) and Poly(ethyl acrylate) As a Function of Temperature", J. Macromol. Chem., 1, 799 (1966).
35. L. H. Sperling, E. J. Zaganlaris and A. V. Tobolsky, "Elastomeric and Mechanical Properties of Poly-m-carboranylene siloxanes", J. Macromol. Sci.-Chem., A1, 1111 (1967).
36. L. H. Sperling and A. V. Tobolsky, "Network Relaxation Properties of Crosslinked Poly(ethyl acrylate) and Polydimethylsiloxane", J. Polym. Sci., Part A-2: 6, 259 (1968).
37. K. Shibayama, "Temperature Dependence of the Physical Properties of Crosslinked Networks", Progr. In Org. Coatings, 3, 245 (1975).
38. W. W. Graessley, "Elasticity and Chain Dimensions in Gaussian Networks", Macromolecules, 8, 865 (1975).
39. W. R. Krigbaum and R. G. Goodwin, "Direct Measurement of Molecular Dimensions in Bulk Polymers", J. Chem. Phys., 43, 4523 (1965).
40. A. Guinier and G. Fournet, "Small Angle Scattering of X-rays," Wiley, 1955.
41. F. Rietsch, D. Daveloose, and D. Froelich, "Glass Transition Temperature of Ideal Polymeric Networks," Polymer, 17, 859 (1976).

42. J. R. Millar, "Interpenetrating Polymer Networks. Styrene-Divinylbenzene Copolymers with Two and Three Interpenetrating Networks, and Their Sulphonates", J. Chem. Soc., 1311 (1960).
43. J. R. Millar, D. G. Smith, and W. E. Marr, "Interpenetrating Polymer Networks. Part II. Kinetics and Equilibria in a Sulphonated Secondary Intermeshed Copolymer", J. Chem. Soc., 1789 (1962).
44. J. R. Millar, D. G. Smith, W. E. Marr, and T. R. E. Kressman, "Solvent-Modified Polymer Networks. Part I.", J. Chem. Soc., 218 (1963).
45. J. R. Millar, D. G. Smith, W. E. Marr, and T. R. E. Kressman, "Solvent-Modified Polymer Networks. Part II.", J. Chem. Soc., 2779 (1963).
46. J. P. Bell, "Mechanical Properties of a Glassy Epoxide Polymer: Effect of Molecular Weight Between Crosslinks", J. Appl. Polym. Sci., 14, 1901 (1970).
47. J. P. Bell, "Structure of a Typical Amine-Cured Epoxy Resin", J. Polym. Sci.-A2, 8, 417-437 (1970).
48. C. J. Lin and J. P. Bell, "The Effect of Polymer Network Structure Upon the Bond Strength of Epoxy-Aluminum Joints", J. Appl. Polym. Sci., 16, 1721 (1972).
49. J. A. Manson and E. H. Chiu, "Permeation of Liquid Water in a Filled Epoxy Resin", J. Polym. Sci.-Symp. No. 41, 95-108 (1973).
50. J. A. Manson and E. H. Chiu, "Effect of Water on the Behavior of Glass-Bead-Filled Epoxy Resin", Polym. Prepr., 14, 469 (1973).
51. J. A. Manson, L. H. Sperling, and S. L. Kim, "Influence of Crosslinking on the Mechanical Properties of High- $T_g$  Polymers", Technical Report AFML-TR-76-124, (May 1975 to April 1976), July, 1976.
52. Volker Huelck, D. A. Thomas, and L. H. Sperling, "Interpenetrating Polymer Networks of Poly(ethyl acrylate) and Poly(styrene-co-methyl methacrylate). I. Morphology via Electron Microscopy", Macromolecules, 5, 340 (1972).
53. P. J. Flory and J. Rehner, "Statistical Mechanics of Crosslinked Polymer Networks. I. Rubberlike Elasticity", J. Chem. Phys., 11, 512 (1943).
54. ASTM D-1043, American Society for Testing Materials, Philadelphia, PA., 1974.

55. M. C. Shen and A. V. Tobolsky, "Rubber Elasticity of Preswollen Polymer Networks: Lightly Crosslinked Vinyl-Divinyl Systems", J. Polym. Sci., A2, 2513 (1964).
56. M. C. Shen and A. V. Tobolsky, "Rubber Elasticity of Preswollen Polymer Networks: Highly Crosslinked Vinyl-Divinyl Systems", J. Polym. Sci., A3, 629 (1964).
57. A. A. Donatelli, L. H. Sperling, and D. A. Thomas, "A Semi-Empirical Derivation of Phase Domain Size in Interpenetrating Polymer Networks", J. Appl. Polym. Sci., 21, 1189 (1977).
58. J. Brandrup and E. H. Immergut, "Polymer Handbook", 2nd ed., Interscience, New York, 1975, pp.
59. D. H. Kaelble, in "Epoxy Resins, Chemistry and Technology", ed. by C. A. May and Y. Tanaka, Marcel Dekker, New York, 1973, chapter 5.
60. A. A. Griffith, "The Phenomena of Rupture and Flow in Solids," Phil. Trans. Roy. Soc. (London), 221, 163 (1921).
61. G. R. Irwin, "Fracture," in Handbuch der Physik, V1, 551 (1958).
62. G. Pritchard and G. V. Rhoades, Mater. Sci. Eng., 26, 1 (1976).
63. J. A. Manson and R. W. Hertzberg, "Fatigue Failure in Polymers," Crit. Rev. Macromol. Sci., 1, 433 (1973).
64. R. W. Hertzberg, J. A. Manson, and M. Skibo, "Frequency Sensitivity of Fatigue Processes in Polymeric Solids," Polym Eng. Sci., 15, 252 (1975).
65. G. C. Martin and W. W. Gerberich, "Temperature Effects on Fatigue Crack Growth in Polycarbonate," J. Mater. Sci., 11, 231 (1976).
66. R. W. Hertzberg, J. A. Manson, and W. C. Wu, "Structure of Polymers and Fatigue Crack Propagation," ASTM STP 536, 391 (1973).
67. S. L. Kim, M. Skibo, J. A. Manson, and R. W. Hertzberg, "Fatigue Crack Propagation in Poly (methyl methacrylate): Effect of Molecular Weight and Internal Plasticization," Poly. Eng. Sci., 17 (3), 194 (1977).
68. J. A. Manson, M. Skibo, and R. W. Hertzberg, "Effects of Molecular Weight and Plasticizer on FCP in PVC," Proceedings, Second IUPAC Conference on Poly(Vinyl Chloride), Lyon, France, July 1976.
69. M. Skibo, R. W. Hertzberg, J. A. Manson, and S. L. Kim, "On the Generality of Discontinuous Nature of Fatigue Crack Propagation in Polymers," J. Mater. Sci., 12, 531 (1977).

## Best Available Copy

70. S. Wellenghoff and E. Baer, "The Mechanism of Crazing in Polystyrene," J. Macromol. Sci.-Phys., B-11 (3), 367 (1975).
71. M. Skibo, R. W. Hertzberg, and J. A. Manson, "Fatigue Fracture Processes in Polystyrene," J. Mater. Sci., 11, 479 (1976).
72. M. Schrage, "Fatigue as Monitored by the Torsion Pendulum," J. Polym. Sci., Part A-2, 8, 1999-2014 (1970).
73. J. O. Outwater and M. C. Murphy, "On the Fatigue of Epoxy Resin," 26th Annual Tech. Conf., 1971, Reinforced Plastics/Composite Div., The Society of the Plastics Industry, Inc., Section 10A, p. 1.
74. S. A. Sutton, "Fatigue Crack Propagation in an Epoxy Polymer," Eng. Frac. Mech., 6, 587 (1974).
75. B. Tomkins and W. D. Biggs, "Low Endurance Fatigue in Metals and Polymers, Part 3," J. Mater. Sci., 4, 544 (1969).
76. S. S. Labana, S. Newman, and A. J. Chomppf, "Chemical Effects on the Ultimate Properties of Polymer Networks in the Glassy State," in Polymer Networks, ed. by A. J. Chomppf and S. Newman, Plenum, 1971, p. 453.
77. R. F. Boyer, "Mechanical Motions in Amorphous and Semi-Crystalline Polymers," Polymer, 17, 996 (1976).
78. R. Houwink, "Synthetic Resins, Their Formation, Their Elastic and Plastic Properties, and Their Possibilities," J. Soc. Chem. Ind. (London), 55, 247T (1936).
79. E. H. Erath and R. A. Spurr, "Occurrence of Globular Formations in Thermosetting Resins," J. Polym. Sci., 35, 391 (1959).
80. E. G. Bobalek, E. R. Moore, S. S. Levy, and C. C. Lee, "Some Implications of the Gel Point Concept to the Chemistry of Alkyd Resins," J. Appl. Polym. Sci., 11, 1593 (1967).
81. R. M. Kessenikh, L. A. Korshunova, and A. V. Petrov, Polym. Sci., USSR, 14, 466 (1972).
82. A. N. Neverov, N. A. Birkina, V. Zherdev, and V. A. Kozlov, Vysokomol. Soedin., A10, 463 (1968).
83. R. A. Spurr, E. H. Erath, H. Myers, and D. C. Pease, Ind. Eng. Chem., 49, 1839 (1957).
84. V. Y. Baisin, L. M. Korsunskii, O. Y. Shokniskaya, and N. V. Aleksandrov, Polym. Sci., USSR, 14, 2339 (1972).